A new class of uniformly stable time-domain Foldy-Lax models for scattering by small particles. Acoustic sound-soft scattering by circles

Maryna Kachanovska

A NEW CLASS OF UNIFORMLY STABLE TIME-DOMAIN FOLDY-LAX MODELS FOR SCATTERING BY SMALL PARTICLES. ACOUSTIC SOUND-SOFT SCATTERING BY CIRCLES

MARYNA KACHANOVSKA*

Abstract. In this work we study time-domain sound-soft scattering by small particles. Our goal is to derive an asymptotic model for this problem valid when the size of the particles tends to zero. We present a systematic approach to constructing such models, based on a well-chosen Galerkin discretization of a boundary integral equation. The convergence of the method is achieved by decreasing the asymptotic parameter rather than increasing the number of basis functions. For the case of circular obstacles, we prove the second-order convergence of the field error with respect to the particle size. Our findings are illustrated with numerical experiments.

Key words. Wave equation, asymptotic model, time-domain boundary integral equations

1. Introduction. The problem of wave scattering by many particles has been a subject of active research since more than a century, cf. the monograph by Martin [31] for an overview of the various approaches to multiple scattering, as well as various multiple scattering problem settings, or the monograph by Mishchenko [35] for studies of electromagnetic multiple scattering. This type of wave propagation problems often appears in applications, for example in non-destructive testing (elastic or sound wave scattering by small defects) and atmospheric optics (scattering of light by atmospheric particles). Depending on the nature of the phenomena, such multiple wave scattering can be studied either from deterministic or probabilistic viewpoint, see [40]. E.g. the original seminal articles by Foldy [15] and Lax [24] were concerned with scattering by randomly positioned obstacles. In this work we will concentrate on the time-domain sound scattering by small particles in a deterministic regime.

In the asymptotic regime when the size of the particles tends to zero, and the distance between them is fixed (or decreases 'slowly'), it is possible to obtain simpler (and, in particular, easier for the computational treatment) models. To our knowledge, there exist two principal approaches to do so: either by using matching (near-field and far-field) asymptotic expansions, where one usually works with the original PDE, or by deriving asymptotics from the integral equation representations. Somewhat apart stands the original method of Foldy [15], developed further by Lax [24] (Foldy-Lax methods), cf. [31, Chapter 8.3] for its detailed description.

The literature on the frequency-domain asymptotic models for various types of wave propagation problems is quite rich; a non-exhaustive list of works exploiting either of the above approaches includes [6, 7, 23, 10, 37, 11, 9, 25, 26]. It seems that there exist fewer results in the time domain (see the recent monograph by Martin [32]). Asymptotic models for acoustic and electromagnetic wave propagation were obtained in [33, 4] (3D scattering by a single obstacle), [30], [19] and in [20] (transmission problems) by using matched expansion method. The integral equation approach was applied to the 3D wave scattering by multiple obstacles in the very recent work [39]. However, the stability of the model of [39] was proven under some geometric conditions relating an asymptotic parameter, the number of particles and the minimal distance between them. In general, time-domain asymptotic models may exhibit instabilities, unlike the original model. We will prove that this is the case for the time-domain counterpart of the Foldy-Lax model for the acoustic scattering by circles of [9].

The goal of this work is to derive an asymptotic Foldy-Lax model for the time domain scattering by small particles, which would be stable for arbitrary geometries (i.e. provided that particles do not touch each other). One of the novelties is the way such a model will be obtained: we start with a well-chosen boundary integral formulation, which possesses some coercivity properties, and semi-discretize it in space with the help of a very coarse Galerkin method. The resulting model is then stable due to the coercivity of the underlying boundary integral formulation. The convergence of the method does not rely on increasing the number of the basis functions, but on decreasing the asymptotic parameter.

We proceed as follows. Section 2 is an introduction: we present the problem, introduce the notation,

*POEMS, CNRS, ENSTA Paris, INRIA, Institut Polytechnique de Paris, Palaiseau, France maryna.kachanovska@inria.fr

and discuss whether the scattered field can be approximated by zero. We finish Section 2 by a motivation to the present work: we examine the time-domain counterpart of the Foldy-Lax model for the acoustic scattering by circles [9] and prove that it is unstable for some geometric configurations. Section 3 is dedicated to the introduction of the new Galerkin Foldy-Lax model. In Section 4 we present convergence analysis of the new model. A short Section 5 extends the results of the article to the case when particles densify. In Section 6 we present numerical experiments, and conclude with a discussion of open questions in Section 7.

2. Problem setting and motivation.

2.1. Problem setting. Let Ω_j, $j \in \mathcal{N} := \{1, \dots, N\}$, be a collection of $N > 0$ circular domains (particles), with the jth particle being centered at $\boldsymbol{c}_j \in \mathbb{R}^2$ and having a radius $R_j > 0$, i.e. $\Omega_j = B(\boldsymbol{c}_j, R_j)$. We assume that $\Omega_j \cap \Omega_i = \emptyset$ if $i \neq j$. For $0 < \varepsilon \leq 1$, we introduce the rescaled domains $\Omega_j^\varepsilon = B(\boldsymbol{c}_j, r_j^\varepsilon)$, where $r_j^\varepsilon = \varepsilon R_j$. Their interior, exterior and the boundary are denoted by

$$\Omega^\varepsilon = \cup_j \Omega_j^\varepsilon, \quad \Omega^{\varepsilon,c} = \mathbb{R}^2 \setminus \overline{\Omega}^\varepsilon, \quad \Gamma_j^\varepsilon = \partial\Omega_j^\varepsilon, \quad \Gamma^\varepsilon = \cup_j \Gamma_j^\varepsilon = \partial\Omega^\varepsilon.$$

For the particular case $\varepsilon = 1$, we use a simplified notation $\Omega = \Omega^1$, $\Omega^c = \Omega^{1,c}$ and $\Gamma = \Gamma^1$. The trace operator on Γ^ε is denoted by γ_0. Additionally, we define

$$d_*^\varepsilon = \min_{i \neq j} \operatorname{dist}(\Omega_i^\varepsilon, \Omega_j^\varepsilon), \quad d_* = d_*^1, \quad R_* = \min_j R_j, \quad R^* = \max_j R_j.$$

Evidently, $d_* > d_*^\varepsilon$ for all $0 < \varepsilon < 1$.

We look for the solution of the sound-soft scattering problem. Provided $(u_0, u_1) \in H^2(\mathbb{R}^2) \times H^1(\mathbb{R}^2)$, s.t. $\operatorname{supp} u_0 \cap \overline{\Omega} = \operatorname{supp} u_1 \cap \overline{\Omega} = \emptyset$, we are given the solution $u^{inc} \in C^2(\mathbb{R}_+^*; L^2(\mathbb{R}^2)) \cap C^1(\mathbb{R}_+; H^1(\mathbb{R}^2))$ of the free-space wave equation:

$$\begin{aligned} &\partial_t^2 u^{inc}(t, \boldsymbol{x}) - \Delta u^{inc}(t, \boldsymbol{x}) = 0, \quad (t, \boldsymbol{x}) \in \mathbb{R}_+^* \times \mathbb{R}^2, \\ &u^{inc}(0, \boldsymbol{x}) = u_0(\boldsymbol{x}), \quad \partial_t u^{inc}(0, \boldsymbol{x}) = u_1(\boldsymbol{x}). \end{aligned} \tag{2.1}$$

Presence of the obstacles Ω^ε alters the field; the new field $u_{tot}^\varepsilon \in C^2(\mathbb{R}_+^*; L^2(\Omega^{\varepsilon,c})) \cap C^1(\mathbb{R}_+; H^1(\Omega^{\varepsilon,c}))$ satisfies the following boundary-value problem (BVP):

$$\begin{aligned} &\partial_t^2 u_{tot}^\varepsilon - \Delta u_{tot}^\varepsilon = 0 \quad \text{in} \quad \mathbb{R}_+^* \times \Omega^{\varepsilon,c}, \\ &\gamma_0 u_{tot}^\varepsilon(t) = 0, \quad t \geq 0, \\ &u_{tot}^\varepsilon(0) = u_0, \quad \partial_t u_{tot}^\varepsilon(0) = u_1, \quad \text{in} \quad \Omega^{\varepsilon,c}. \end{aligned}$$

The auxiliary scattered field $u^\varepsilon := u_{tot}^\varepsilon - u^{inc}$ solves the inhomogeneous exterior BVP

$$\begin{aligned} &\partial_t^2 u^\varepsilon - \Delta u^\varepsilon = 0, \quad \text{in} \quad \mathbb{R}_+^* \times \Omega^{\varepsilon,c}, \\ &\gamma_0 u^\varepsilon(t) = g^\varepsilon(t), \quad t \geq 0, \quad \text{where } g^\varepsilon(t) := -\gamma_0 u^{inc}(t), \\ &u^\varepsilon(0) = \partial_t u^\varepsilon(0) = 0 \quad \text{in} \quad \Omega^{\varepsilon,c}. \end{aligned} \tag{2.2}$$

We are interested in solving the above problem efficiently in the asymptotic regime, when the data g^ε is approximately frequency-bandlimited to the frequency ω_{max}, and ε is small compared to the smallest wavelength present in the system, i.e. $\varepsilon\omega_{max} \ll 1$.

For each fixed $t > 0$, for a compact $K \subset \Omega^c$, $\lim_{\varepsilon \to 0} \|u^\varepsilon(t)\|_{L^2(K)} = 0$. In 2D, we can expect that (cf. Section 2.3), $\|u^\varepsilon\|_{L^\infty(\mathbb{R}_+; L^2(K))} \geq c|\log^{-1}\varepsilon|$, with some $c > 0$. Our goal is to find an approximation $\tilde{u}^\varepsilon$ of u^ε which would satisfy the following properties:

- (*convergence*) this approximation is more accurate than approximating u^ε by zero, i.e., for all $t > 0$, compact $K \subset \Omega^c$ and regular initial data u_0, u_1,

$$\|u^\varepsilon(t) - \tilde{u}^\varepsilon(t)\|_{L^2(K)} = o(\log^{-1}\varepsilon). \tag{2.3}$$

- (*uniform w.r.t. ε stability*) the approximation is uniformly stable, i.e. there exist $C > 0$, $\ell_0, \ell_1 \in \mathbb{N}$, $p \in \mathbb{N}$, s.t., for all $0 < \varepsilon \leq 1$, and all $T > 0$,

$$\|\widetilde{u}^\varepsilon\|_{L^\infty(0,T;L^2(\Omega^{\varepsilon,c}))} \leq C(1+T)^p(\|u_0\|_{H^{\ell_0}(\mathbb{R}^2)} + \|u_1\|_{H^{\ell_1}(\mathbb{R}^2)}). \tag{2.4}$$

The uniform stability requirement may seem too strong: indeed, in general it is not necessary for the convergence. One could have authorized a super-polynomial growth (e.g. e^{aT}, with $a > 0$ potentially depending on ε) of the solution. Such a model would likely be unsuitable for long time simulations. Alternatively, one could think of a CFL like condition on ε which would be dependent on the geometry and which would guarantee the bound (2.4) (for example, this is the case for the model [39]). However, in practical situations such a condition may be difficult to ensure. Thus we prefer to have models possessing a uniform stability property.

2.2. Notation. *Fourier-Laplace transform.* We will use the following convention of the Fourier-Laplace transform; for $v \in L^1(\mathbb{R}; X)$ (with X being a Banach space), s.t. $v = 0$ on $\mathbb{R}_-$ (i.e. a causal function), we define

$$\hat{v}(\omega) := \int_0^{+\infty} \mathrm{e}^{i\omega t} v(t)dt, \quad \omega \in \mathbb{C}.$$

The above integral converges in particular for $\omega \in \mathbb{C}^+ := \{\omega \in \mathbb{C} : \operatorname{Im}\omega > 0\}$.

In the frequency domain (2.2) reads, for $\omega \in \mathbb{C}^+$,

$$\begin{aligned} -\omega^2\hat{u}^\varepsilon - \Delta\hat{u}^\varepsilon = 0 \quad \text{in} \quad \Omega^{\varepsilon,c}, \\ \gamma_0\hat{u}^\varepsilon = \hat{g}^\varepsilon, \text{ where } \hat{g}^\varepsilon := -\gamma_0\hat{u}^{inc}. \end{aligned} \tag{2.5}$$

Let us introduce the fundamental solution for $-\Delta - \omega^2$:

$$G_\omega(r) = \frac{i}{4}H_0^{(1)}(\omega r), \quad r > 0.$$

It is a Fourier-Laplace transform of the Green function for the 2D wave equation

$$\mathcal{G}(t,r) = \frac{\mathbb{1}_{t>r}}{2\pi\sqrt{t^2 - r^2}}.$$

Sobolev spaces on the boundary of a circle. Let $r > 0$, and let $\mathcal{C}_r := \partial B(0,r)$. Given a function $u \in L^2(\mathcal{C}_r)$, we define its Fourier decomposition (with $\hat{s}_\theta = (\cos\theta, \sin\theta)$):

$$u(\hat{s}_\theta) = \sum_{m\in\mathbb{Z}} u_m \mathrm{e}^{im\theta}, \quad u_m = \frac{1}{2\pi}\int_0^{2\pi} \mathrm{e}^{-im\theta}u(\hat{s}_\theta)d\theta.$$

The fractional Sobolev spaces on the boundary of the circle are defined as follows: $u \in H^s(\mathcal{C}_r)$, $s \geq 0$, iff the following norm is finite:

$$\|u\|^2_{H^s(\mathcal{C}_r)} = 2\pi r \sum_{m\in\mathbb{Z}} \left(1 + \frac{m^2}{r^2}\right)^s |u_m|^2. \tag{2.6}$$

For $s < 0$, we define $H^s(\mathcal{C}_r)$ as a completion of $L^2(\mathcal{C}_r)$ for the norm (2.6).

We will further make use of the following observation: by [18, proof of Lemma 4.2.5], the Sobolev-Slobodeckij seminorm

$$|v|^2_{\mathcal{H}^{1/2}(\mathcal{C}_r)} = \iint_{\mathcal{C}_r\times\mathcal{C}_r} \frac{|v(x) - v(y)|^2}{|x-y|^2} dx\, dy \tag{2.7}$$

is equivalent to $\sum_{m\neq 0} m|v_m|^2$, with the equivalence constants independent of r.
Sobolev spaces on Γ^ε. We define

$$H^s(\Gamma^\varepsilon) := \prod_{k\in\mathcal{N}} H^s(\Gamma_k^\varepsilon), \quad s\in\mathbb{R}.$$

For a function $\boldsymbol{v}\in H^s(\Gamma^\varepsilon)$, let us set $v_m := \boldsymbol{v}|_{\Gamma_m^\varepsilon}$. We equip $H^s(\Gamma^\varepsilon)$ with the norm

$$\|\boldsymbol{v}\|^2_{H^s(\Gamma^\varepsilon)} := \sum_{k\in\mathcal{N}} \|v_k\|^2_{H^s(\Gamma_k^\varepsilon)}.$$

Sometimes we will use a shortened notation $\|\boldsymbol{v}\|_s$ for $\|\boldsymbol{v}\|_{H^s(\Gamma^\varepsilon)}$.

By (ρ_j,θ_j) we will denote the polar coordinates centered in $\boldsymbol{c}_j$. The coefficients of the Fourier expansion of v_j on Γ_j^ε will be denoted by $v_{j,m}$, $m\in\mathbb{Z}$.

The (real) duality bracket in $H^{-1/2}(\Gamma^\varepsilon), H^{1/2}(\Gamma^\varepsilon)$ will be denoted by $\langle .,.\rangle$. More precisely, for $\boldsymbol{u}$, $\boldsymbol{v}\in L^2(\Gamma^\varepsilon)$, $\langle \boldsymbol{u},\boldsymbol{v}\rangle = \displaystyle\int_{\Gamma^\varepsilon} \boldsymbol{u}\,\boldsymbol{v}\,d\Gamma$.
An energy norm. Given $a>0$ and a domain $\mathcal{O}$, we denote

$$\|v\|^2_{a,\mathcal{O}} = a^2\|v\|^2_{L^2(\mathcal{O})} + \|\nabla v\|^2_{L^2(\mathcal{O})}.$$

A notation for a complement domain. Given a domain $\mathcal{O}$, we denote by $\mathcal{O}^c = \mathbb{R}^3\setminus\overline{\mathcal{O}}$.
Inequality notation. We will use $a\lesssim b$ (resp., $a\gtrsim b$) to indicate that $a\leq Cb$ (resp., $a\geq Cb$), for a generic constant C independent of ε, N, geometry, final time, data (i.e. any parameters of the problem).
Notation for constants. We will denote by $C_i(R^*,R_*)>0$, $i\in\mathbb{N}\setminus\{0\}$, generic constants appearing in proofs, which depend on R^*, R_*.
Notation for $\min(1,a)$. Where convenient, we will use the notation $\underline{a} = \min(1,a)$.

2.3. On the accuracy of approximating u^ε by zero. The goal of this section is to argue that in general we cannot expect approximating u^ε by zero with an error smaller than $O(\log^{-1}\varepsilon)$. This is illustrated in the one-particle case, where the argument is fairly straightforward in the frequency domain, but requires more technicalities in the time domain. Instead of presenting such a technical proof, we decided to explain the corresponding argument in the frequency domain, and next illustrate its time-domain counterpart with numerical experiments. Let us finally remark that a related (but more general) question was studied in [4].

2.3.1. Frequency domain. Let $\omega>0$, $N=1$, $\boldsymbol{c}_1=0$, $R_1=1$. Then the outgoing solution to (2.5) is given by (we write $\hat g_n^\varepsilon$ for $\hat g_{1,n}^\varepsilon$):

$$\hat u^\varepsilon(\omega,\rho\hat s_\theta) = \sum_{n\in\mathbb{Z}} \frac{H_n^{(1)}(\omega\rho)}{H_n^{(1)}(\omega\varepsilon)}\hat g_n^\varepsilon \mathrm{e}^{in\theta}, \quad \hat s_\theta=(\cos\theta,\sin\theta), \quad \rho>\varepsilon.$$

We fix ρ and split $\hat u^\varepsilon$ into two terms $\hat u^\varepsilon = \hat u_0^\varepsilon(\omega,\rho\hat s_\theta) + \hat u_\perp^\varepsilon(\omega,\rho\hat s_\theta)$ defined below. As $\varepsilon\to 0$, one of the terms dominates over the other one.

$$\hat u_0^\varepsilon(\omega,\rho\hat s_\theta) = \frac{H_0^{(1)}(\omega\rho)}{H_0^{(1)}(\omega\varepsilon)}\hat g_0^\varepsilon, \quad \hat u_\perp^\varepsilon(\omega,\rho\hat s_\theta) = \sum_{n\in\mathbb{Z}\setminus\{0\}} \frac{H_n^{(1)}(\omega\rho)}{H_n^{(1)}(\omega\varepsilon)}\hat g_n^\varepsilon \mathrm{e}^{in\theta}.$$

Based on the asymptotic behaviour of Hankel functions, for a fixed frequency ω, we can show that when $\varepsilon\to 0$, by [14, 10.8], one has that

$$\hat u_0^\varepsilon(\omega,\rho\hat s_\theta) = -\frac{i\pi}{2} H_0^{(1)}(\omega\rho)\hat g_0^\varepsilon \log^{-1}\varepsilon + o(\log^{-1}\varepsilon).$$

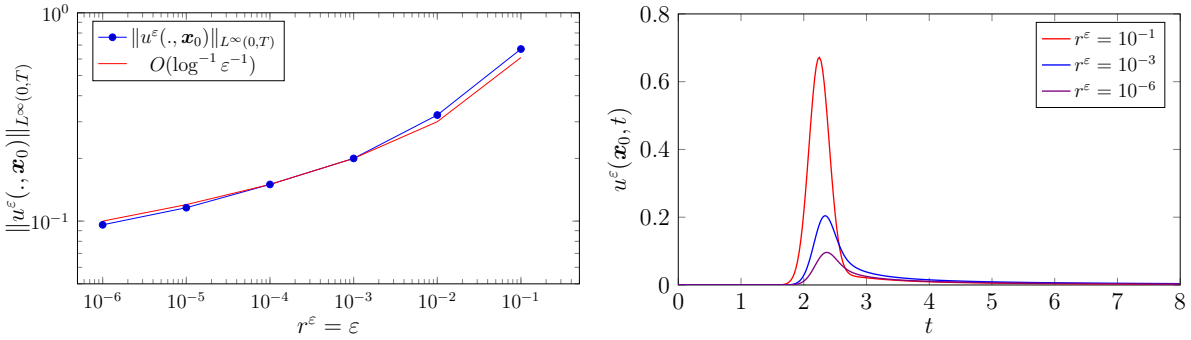

FIG. 1. *Illustration to the numerical experiment of Section 2.3.2. Left: the dependence of the magnitude* $\|u^\varepsilon(.,\boldsymbol{x}_0)\|_{L^\infty(0,T)}$ *measured in the point* $\boldsymbol{x}_0 = (0.2, 0.2)$*, for* $T = 8$*, on* ε*. Right: the dependence of* $u^\varepsilon(t,\boldsymbol{x}_0)$ *on time for different values of* ε*.*

As for the term $\hat{u}^\varepsilon_\perp(\omega,\rho\hat{s}_\theta)$, we bound it

$$|\hat{u}^\varepsilon_\perp(\omega,\rho\hat{s}_\theta)|^2 \le \sum_{n\in\mathbb{Z}\setminus\{0\}} \left|\frac{H_n^{(1)}(\omega\rho)}{H_n^{(1)}(\omega\varepsilon)}\right|^2 \sum_{n\in\mathbb{Z}\setminus\{0\}} |\hat{g}^\varepsilon_n|^2 \le C\varepsilon^2 \sum_{n\in\mathbb{Z}\setminus\{0\}} |\hat{g}^\varepsilon_n|^2,$$

where the last bound follows from Lemma C.1.
Let us now estimate the quantities related to the data. For sufficiently regular $\hat{u}^{inc}$,

$$\begin{aligned}\hat{g}^\varepsilon_0 &= \frac{1}{2\pi\varepsilon}\int_{\Gamma^\varepsilon} \hat{u}^{inc}(\omega,\boldsymbol{x})d\Gamma_{\boldsymbol{x}} = \hat{u}^{inc}(\omega,0) + O(\varepsilon),\\ \sum_{n\in\mathbb{Z}\setminus\{0\}} |\hat{g}^\varepsilon_n|^2 &= (2\pi\varepsilon)^{-1} \inf_{c\in\mathbb{C}} \|\hat{g}^\varepsilon - c\|^2_{L^2(\Gamma_\varepsilon)}\\ &\lesssim \varepsilon^{-1}\int_{\Gamma^\varepsilon} |\hat{u}^{inc}(\omega,\boldsymbol{y}) - \hat{u}^{inc}(\omega,0)|^2 d\Gamma_{\boldsymbol{y}} = O(\varepsilon^2).\end{aligned}$$

Therefore,

$$\hat{u}^\varepsilon(\omega,\rho\hat{s}_\theta) = -\frac{i\pi}{2}H_0^{(1)}(\omega\rho)\hat{u}^{inc}(\omega,0)\log^{-1}\varepsilon + o(\log^{-1}\varepsilon).$$

If, in the frequency domain, $\hat{u}^{inc}(\omega,0) \neq 0$, as $\varepsilon \to 0$, we cannot expect that $\hat{u}^\varepsilon(\omega,\rho\hat{s}_\theta)$ decays to 0 faster than $\log^{-1}\varepsilon$. The above argument can be translated into the time domain using the Plancherel identity and bounds on Hankel functions in $\mathbb{C}^+$. This is confirmed by the numerical experiment of the next section.

2.3.2. Time-domain numerical experiment. We compute the field scattered by a single obstacle ($N = 1$, $R = 1$, $\boldsymbol{c} = \boldsymbol{0}$) on the interval $(0,T)$, $T = 8$. The incident field is given by $u^{inc}(t,\boldsymbol{x}) = -\mathrm{e}^{-20(t-\boldsymbol{d}\cdot\boldsymbol{x}-1)^2}$, with $\boldsymbol{d} = (0,1)$. The solution is computed using the time-domain BEM, semi-discretized in time using the trapezoid rule Convolution Quadrature method [29, 27, 28], and in space using the Galerkin method with the basis functions $\{\mathrm{e}^{im\theta_\ell}\}_{m=-N_s}^{N_s}$ on the ℓth obstacle. Let us remark that the convolution quadrature requires the knowledge of the Fourier-Laplace transform of the Green function (or a method for its numerical evaluation), and does not need its time-domain analogue. The results are illustrated in Figure 1. We observe a good agreement of the results with the lower bound $\|u^\varepsilon(.,\boldsymbol{x}_0)\|_{L^\infty(0,T)} \ge c_T \log^{-1}\varepsilon$.

2.4. Motivation for designing a new asymptotic model. It is rather natural to ask whether it is necessary to construct a Foldy-Lax model in the time domain, if one could simply rewrite the

available frequency domain Foldy-Lax models in the time domain by applying the inverse Fourier-Laplace transform. In this section we demonstrate that such a procedure can possibly yield a potentially unstable model. Our starting point is the Foldy-Lax model analyzed in [9], which is $O(\varepsilon/\log\varepsilon)$-accurate in the frequency domain. We prove in this section that there exist geometric configurations for which this model is unstable.

2.4.1. Foldy-Lax model of [9]. In [9] it was suggested to approximate the field $\hat{u}^\varepsilon(\boldsymbol{x})$ by the following linear combination:

$$\hat{u}^\varepsilon(\boldsymbol{x}) \approx \hat{u}^\varepsilon_{FL}(\boldsymbol{x}) = \sum_{k\in\mathcal{N}} \frac{G_\omega(\|\boldsymbol{x}-\boldsymbol{c}_k\|)}{G_\omega(r_k^\varepsilon)}\hat{\lambda}^\varepsilon_{FL,k}, \quad \text{where } \hat{\boldsymbol{\lambda}}^\varepsilon_{FL} \in \mathbb{C}^N \text{ solves} \tag{2.8}$$

$$\hat{\lambda}^\varepsilon_{FL,n} + \sum_{k\in\mathcal{N}\setminus\{n\}} \frac{G_\omega(\|\boldsymbol{c}_n-\boldsymbol{c}_k\|)}{G_\omega(r_k^\varepsilon)}\hat{\lambda}^\varepsilon_{FL,k} = -\hat{u}^{inc}(\boldsymbol{c}_n), \quad n=1,\dots,N. \tag{2.9}$$

To rewrite the above in the time domain, first of all we remark that $\hat{\boldsymbol{\lambda}}^\varepsilon_{FL}$ is frequency-dependent, and thus is a Fourier-Laplace transform of a time-dependent distribution (which, moreover, one can show to be causal). With $\hat{\mu}^\varepsilon_{FL,n} = (G_\omega(r_n^\varepsilon))^{-1}\hat{\lambda}^\varepsilon_{FL,n}$, the time-domain Foldy-Lax approximation of the scattered field reads:

$$\begin{aligned} u^\varepsilon(t,\boldsymbol{x}) \approx u^\varepsilon_{FL}(t,\boldsymbol{x}) &= \sum_{k\in\mathcal{N}} \mathcal{G}(t,\|\boldsymbol{x}-\boldsymbol{c}_k\|) *_t \mu^\varepsilon_{FL,k} \\ &= \frac{1}{2\pi}\sum_{k\in\mathcal{N}} \int_0^t \frac{\mathbb{1}_{t-\tau>\|\boldsymbol{x}-\boldsymbol{c}_k\|}}{\sqrt{(t-\tau)^2-\|\boldsymbol{x}-\boldsymbol{c}_k\|^2}}\mu^\varepsilon_{FL,k}(\tau)d\tau, \end{aligned} \tag{FL1}$$

where the functions $\boldsymbol{\mu}^\varepsilon_{FL} : \mathbb{R}_+ \to \mathbb{R}^N$ satisfy, for all $n=1,\dots,N$,

$$\mathcal{G}(t,r_n^\varepsilon) *_t \mu^\varepsilon_{FL,n} + \sum_{k\in\mathcal{N}\setminus\{n\}} \mathcal{G}(t,\|\boldsymbol{c}_n-\boldsymbol{c}_k\|) *_t \mu^\varepsilon_{FL,k} = -u^{inc}(t,\boldsymbol{c}_n). \tag{FL2}$$

It is possible to show that, for $N\le 2$, the model (FL1-FL2) is uniformly stable, i.e. (2.4) holds for $\widetilde{u}^\varepsilon = u^\varepsilon_{FL}$. However, when $N>2$, this may no longer be the case; in particular, the model (FL1-FL2) exhibits instabilities when the distance between the particles is comparable to their size.

2.4.2. Instability of the model (FL1-FL2). For a particular geometry consisting of three particles that are located in the vertices of an equilateral triangle, s.t. the distance between them is smaller than their diameter, the Foldy-Lax model (FL1-FL2) is unstable, as formalized in the statement below.

PROPOSITION 2.1. *Let $N=3$ and $R_i=r$ for all i. Let $\|\boldsymbol{c}_i-\boldsymbol{c}_j\|=c>0$ for all $i\neq j$ (in other words, the centers of the particles are located in the vertices of an equilateral triangle of side length c). Assume that $c/r<4$.*

Then there exist u_0, $u_1\in C_0^\infty(\Omega^c)$, a compact $K\subset\Omega^c$ and $A,C>0$ s.t.

$$\limsup_{t\to+\infty}(\mathrm{e}^{-At}\|u^1_{FL}(t,.)\|_{L^2(K)}) \ge C.$$

Let us examine (FL1), (FL2). Evidently, the temporal behaviour of u^1_{FL} is closely related to the behaviour of $\boldsymbol{\lambda}^1_{FL}$. In order to show that $t\mapsto\|\boldsymbol{\lambda}^1_{FL}(t)\|$ admits an exponential growth, we will prove that its Fourier-Laplace transform has poles with a strictly positive imaginary part. The poles of $\hat{\boldsymbol{\lambda}}^1_{FL}$ are closely related to the points ω where the matrix in the left-hand side of (2.9) is not invertible. Let us denote this matrix for the geometry described in Proposition 2.1 by $\Lambda(\omega)$:

$$\Lambda_{nk}(\omega) = \delta_{nk} + (1-\delta_{nk})P(\omega), \qquad P(\omega) = \frac{H_0^{(1)}(\omega c)}{H_0^{(1)}(\omega r)}, \quad k,n=1,\dots,N.$$

We then have the following result.

LEMMA 2.2. *Under assumptions of Proposition 2.1, with* $\eta = cr^{-1} < 4$,
(i) The matrix $\Lambda = \Lambda(\omega)$ *is not invertible for a countable set of frequencies* $\omega_n \in \mathbb{C}^+$, $n \in \mathbb{Z}$.
(ii) These frequencies satisfy

$$\lim_{n\to\pm\infty} \operatorname{Im}\omega_n = \frac{1}{r(\eta-1)} \log\frac{2}{\sqrt{\eta}} > 0. \tag{2.10}$$

(iii) The respective eigenvalues are simple, moreover $\operatorname{Ker}\Lambda(\omega_n) = \operatorname{span}\{(1,1,1)\}$.

Proof. We present the complete proof in Appendix A, while here we will briefly outline how (i) and (ii) are proven. One can show that the points $\omega \in \mathbb{C}^+$ where the matrix Λ is not invertible are the roots $\omega \in \mathbb{C}^+$ of the equation $P(\omega) = -1/2$. From the known asymptotics of the Hankel functions it follows that

$$P(\omega) = \eta^{-\frac{1}{2}} \mathrm{e}^{i(\eta-1)\omega r} + o(1), \quad |\omega| \to +\infty.$$

The inverse function theorem can then be used to prove that the roots of $P(\omega) = -1/2$ are close to the roots of $\eta^{-\frac{1}{2}} \mathrm{e}^{i(\eta-1)\omega r} = -1/2$, which, in turn, are given by

$$\omega_{\infty,n} = \frac{1}{r(\eta-1)} \left((2n+1)\pi + i \log\frac{2}{\sqrt{\eta}} \right), \quad n \in \mathbb{Z}. \tag{2.11}$$

Evidently, $\operatorname{Im}\omega_{\infty,n} > 0$ for $\eta < 4$. ∎

Proof of Proposition 2.1. For brevity, we will omit the index 1 in $\boldsymbol{\lambda}^1_{FL}$ and u^1_{FL}. First of all, let us prove the result for $\boldsymbol{\lambda}_{FL}(t)$, and next discuss how to extend the reasoning to u_{FL}. More precisely, we will show that there exist u_0, $u_1 \in C_0^\infty(\Omega^c)$, $c, B > 0$ s.t., for some sequence $t_n \to +\infty$, one has that $\|\boldsymbol{\lambda}_{FL}(t_n)\| \geq c\mathrm{e}^{Bt_n}$.

Let us assume the opposite, i.e. that for all u_0, $u_1 \in C_0^\infty(\Omega^c)$, for all $B > 0$,

$$\limsup_{t\to+\infty} \left(\mathrm{e}^{-Bt} \|\boldsymbol{\lambda}_{FL}(t)\| \right) = 0. \tag{2.12}$$

The assumption implies that for all $\delta > 0$, there exists $C_\delta > 0$, s.t.

$$\|\boldsymbol{\lambda}_{FL}(t)\| \leq C_\delta \mathrm{e}^{\delta t}, \quad \text{for all } t > 0.$$

Then $\omega \mapsto \hat{\boldsymbol{\lambda}}_{FL}$ is $\mathbb{C}^3$-valued analytic function in $\mathbb{C}^+$. We will arrive at contradiction by choosing u^{inc} so that $\hat{\boldsymbol{\lambda}}_{FL}$ has a pole in $\mathbb{C}^+$. Let us introduce

$$\boldsymbol{a}(\omega) = -\left(\hat{u}^{inc}(\omega, \boldsymbol{c}_k)\right)_{k=1}^3 \in \mathbb{C}^3, \quad \text{so that } \hat{\boldsymbol{\lambda}}_{FL}(\omega) = \Lambda(\omega)^{-1}\boldsymbol{a}(\omega).$$

In the vicinity of ω_n defined as in Lemma 2.2, one has that $\Lambda(\omega)^{-1} = (\omega-\omega_n)^{-1} P_{\mathbf{1}} + O(1)$, where $P_{\mathbf{1}}$ is an orthogonal projector on $\operatorname{Span}\{\mathbf{1} = (1,1,1)^t\}$. To show that $\hat{\boldsymbol{\lambda}}_{FL}$ has a pole in $\omega = \omega_n$, it suffices to find u_0, u_1 so that for some $n \in \mathbb{Z}$, $P_{\mathbf{1}}\boldsymbol{a}(\omega_n) \neq 0$.

Let us fix $n = n_*$. The choice of u_0, u_1 is then as follows. We fix $u_0 = 0$. Let a priori $\operatorname{supp} u_1 = K_0$, where K_0 is a compact in Ω^c. Without loss of generality, let us assume that K_0 includes a small ball in the vicinity of the midpoint $\boldsymbol{x}^*$ of the equilateral triangle formed by the points $\boldsymbol{c}_k$, $k = 1, \ldots, 3$. Then

$$\hat{u}^{inc}(\omega, \boldsymbol{x}) = -\int_{K_0} G_\omega(\|\boldsymbol{x}-\boldsymbol{y}\|) u_1(\boldsymbol{y}) d\boldsymbol{y},$$

and we need to choose u_1 so that

$$\alpha = (\mathbf{1}, \boldsymbol{a}(\omega_{n_*})) = -\int_{K_0} \sum_{k=1}^3 G_{\omega_{n_*}}(\|\boldsymbol{c}_k - \boldsymbol{y}\|) u_1(\boldsymbol{y}) d\boldsymbol{y} \neq 0. \tag{2.13}$$

Evidently, such a function $u_1(\boldsymbol{y}) \in C_0^\infty(K_0)$ exists, since otherwise one would have had $\sum_{k=1}^3 G_{\omega_{n_*}}(\|\boldsymbol{c}_k - \boldsymbol{y}\|) = 0$ for all $\boldsymbol{y} \in K_0$, and, in particular, $G_{\omega_{n_*}}(\|\boldsymbol{c}_k - \boldsymbol{x}^*\|) = 0$; this is impossible since $H_0^{(1)}(z)$ does not vanish in $\mathbb{C}^+$.

This construction ensures that $\hat{\boldsymbol{\lambda}}(\omega)$ has a pole in $\omega_{n_*} \in \mathbb{C}^+$, thus a contradiction to (2.12).

Let us now argue that with the above choice of the initial data, $\omega \mapsto \hat{u}_{FL}(\omega)$ is not L^2-analytic in $\mathbb{C}^+$; this will prove the statement of the proposition. By (2.8),

$$\hat{u}_{FL}(\omega, \boldsymbol{x}) = \sum_{k=1}^3 \frac{G_\omega(\|\boldsymbol{x} - \boldsymbol{c}_k\|)}{G_\omega(r)} \hat{\lambda}_{FL,k}.$$

In the vicinity of ω_{n_*}, $\hat{\boldsymbol{\lambda}}_{FL}(\omega) = (\omega - \omega_{n_*})^{-1}\alpha\mathbf{1} + O(1)$, cf. (2.13), and thus $\hat{u}_{FL}$ has the following expansion:

$$\hat{u}_{FL}(\omega, \boldsymbol{x}) = (\omega - \omega_{n_*})^{-1} \left(\boldsymbol{f}(\omega_{n_*}, \boldsymbol{x}), \mathbf{1}\right) + O(1), \quad f_k(\omega, \boldsymbol{x}) = \alpha \frac{G_\omega(\|\boldsymbol{x} - \boldsymbol{c}_k\|)}{G_\omega(r)}.$$

It remains to prove that there exists a compact K, s.t. $\hat{u}_{FL} : \mathbb{C}^+ \to L^2(K)$ is not analytic. For this it is sufficient to show that $(\boldsymbol{f}(\omega_{n_*}, \boldsymbol{x}), \mathbf{1}) \neq 0$ for $\boldsymbol{x}$ lying in a subset of K of a non-zero Lebesgue measure. In particular, we will choose K as a small ball around $\boldsymbol{x}^*$, where $\boldsymbol{x}^*$ is as defined above. We remark that

$$\boldsymbol{f}(\omega_{n_*}, \boldsymbol{x}^*) = \alpha \frac{G_{\omega_{n_*}}(\|\boldsymbol{x}^* - \boldsymbol{c}_k\|)}{G_{\omega_{n_*}}(r)} \mathbf{1} \neq 0,$$

because $z \mapsto H_0^{(1)}(z)$ does not vanish in $\mathbb{C}^+$. Moreover, $\boldsymbol{x} \mapsto \boldsymbol{f}(\omega_{n_*}, \boldsymbol{x})$ is continuous in the vicinity of $\boldsymbol{x}^*$, which proves the desired result. ∎

2.4.3. A numerical illustration to Lemma 2.2 and Proposition 2.1. To illustrate the statement of Lemma 2.2, we plot $E(\omega) = |P(\omega) + 1/2|$ in Figure 2 (see the proof of the lemma). We compare the numerically computed roots of $E(\omega)$ (zeros of $\det \Lambda(\omega)$ in $\mathbb{C}^+$) to the values $\omega_{\infty,n}$ cf. (2.11). As seen in Figure 2, for the chosen parameters, the values $\omega_{\infty,n}$ provide a good approximation to the roots of $E(\omega)$.

Let us now illustrate the statement of Proposition 2.1. Performing a direct numerical simulation of the problem in Proposition 2.1 is delicate. The difficulty stems from the time semidiscretization. The convolution quadrature method, cf. Section 2.3.2, can be shown to converge for this problem, see the analysis in [29], but the issue lies in its implementation, namely computation of the convolution weights. This is usually done in the Laplace domain using contour integration techniques [28], with the contour that depends on the final simulation time and the time step Δt, and this procedure may fail because of the presence of the resonances in $\mathbb{C}^+$. Hence it is difficult to ensure the convergence of the algorithm in this case, though the exponential blow-up is of course seen numerically. Because of such convergence problems, we computed the Foldy-Lax solution only on a fairly short time interval, where we could ensure the validity of the method used for approximating the convolution weights. We computed the Foldy-Lax

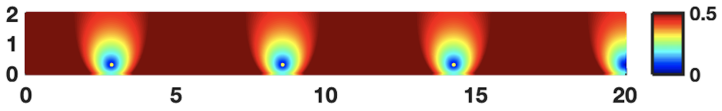

FIG. 2. $|P(\omega) + 1/2|$ *in the coordinates* $(\operatorname{Re}\omega, \operatorname{Im}\omega)$, $\eta = 2.1$ *and* $r = 1$. *The values* $\omega_{\infty,n}$ *are shown in white.*

solution u_{FL}^ε for the configuration of Proposition 2.1, with $r = 0.1$, $\boldsymbol{c}_i$ located in the vertices of the equilateral triangle with $\boldsymbol{c}_1 = (-0.105, 0)$, $\boldsymbol{c}_2 = (0.105, 0)$ and $\boldsymbol{c}_3 \approx (0, 0.1819)$ (so that $\eta = 2.1$), the incident field given by

$$u^{inc}(t, \boldsymbol{x}) = \mathrm{e}^{-20(t - x_2 - 2)^2} \sin(30(t - x_2 - 2)),$$

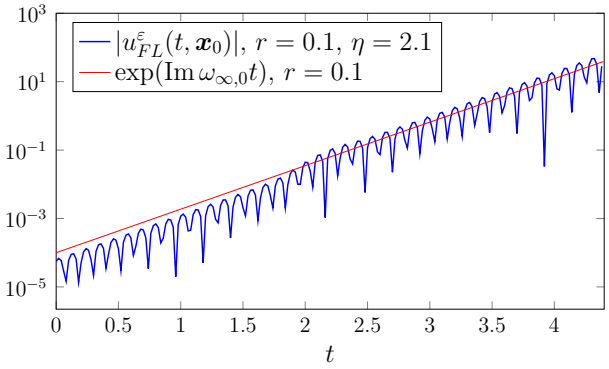

FIG. 3. *The dependence of the absolute value of the solution $u^\varepsilon_{FL}(t,\boldsymbol{x}_0)$, $\boldsymbol{x}_0=(0.2,0.2)$ on time, computed for the experiment of Section 2.4.3 (with $r=0.1$).*

and the final simulation time $T=4.4$. An illustration to this experiment is given in Figure 3. As seen from the proofs of Proposition 2.1 and Lemma 2.2, the exponential growth rate A of u^ε_{FL} is defined by the imaginary part of the roots of $P(\omega)=-1/2$. The numerically computed rate of the exponential growth of the field is close to $\operatorname{Im}\omega_{\infty,0}$, where $\omega_{\infty,0}=28.56+2.93i$. This is not surprising: the smallest root of $|P(\omega)+1/2|$ with positive real and imaginary parts is approximately $\omega\approx 28.38+2.99i$.

2.4.4. Discussion. Proposition 2.1 states that for some geometric configurations, the Foldy-Lax model (FL1-FL2) may exhibit instabilities (i.e. it is not uniformly stable). However, we have a proof only for the case when the particles are very close to each other. Moreover, as $\varepsilon\to 0$, one can prove that the three-particle configuration of Proposition 2.1 with $r_j^\varepsilon=\varepsilon r$ becomes again stable. For the moment, we do not know whether for any system of particles there exists $\varepsilon_0>0$ depending on N, d_*, s.t. (FL1-FL2) is stable for all $\varepsilon<\varepsilon_0$ (we conjecture that this is the case).

According to (2.10), as $r\to 0$, the exponential growth rate becomes more pronounced. On the other hand, upon examining the proof of Lemma 2.2, and in particular (2.11), we can expect that for a fixed n, $\operatorname{Re}\omega_n$ also grows with $r\to 0$, and therefore, in order to observe the exponential growth rate in practice, one may need to excite high frequencies, where the model (FL1-FL2) most likely looses its validity.

These features of the model (FL1-FL2) indicate its lack of robustness, although, in view of the above arguments, many more experiments are needed to conclude about its applicability.

In this paper we develop an alternative Foldy-Lax model, which is uniformly stable and $O(\varepsilon^2)$-convergent. One of the advantages of the new model is that its derivation is not limited to circular geometries (though we analyse the error only the circular geometry case) and it is stable for any geometric configuration where the particles do not touch each other. Let us remark that the new model can be seen as a perturbation of the Foldy-Lax model (FL1-FL2), with an error between the coefficients that define the two models being of $O(\varepsilon^2)$ for a fixed frequency (see Section 3.3.4). We will present more experiments comparing the two models in Section 6.2.

3. Galerkin Foldy-Lax model.

We start by defining the Galerkin Foldy-Lax model in the frequency domain, and next write it in the time domain.

3.1. Frequency domain.

We will look for a solution to (2.5) in terms of the single layer potential of an unknown density $\hat{\boldsymbol{\mu}}^\varepsilon$:

$$\hat{u}^\varepsilon(\boldsymbol{x})=\hat{\mathcal{S}}^\varepsilon\hat{\boldsymbol{\mu}}^\varepsilon(\boldsymbol{x})=\int_{\Gamma^\varepsilon}G_\omega(\|\boldsymbol{x}-\boldsymbol{y}\|)\hat{\boldsymbol{\mu}}^\varepsilon(\boldsymbol{y})d\Gamma_{\boldsymbol{y}},\quad \boldsymbol{x}\in\Omega^{\varepsilon,c}. \tag{3.1}$$

The operator $\hat{\mathcal{S}}^\varepsilon \in \mathcal{L}(H^{-1/2}(\Gamma^\varepsilon), H^1_{loc}(\mathbb{R}^d \setminus \Gamma^\varepsilon))$. Using boundary conditions, we obtain from the above the following boundary integral equation, with $\hat{\mathbb{S}}^\varepsilon := \gamma_0 \hat{\mathcal{S}}^\varepsilon \in \mathcal{L}(H^{-1/2}(\Gamma^\varepsilon), H^{1/2}(\Gamma^\varepsilon))$,

$$\hat{g}^\varepsilon(\boldsymbol{x}) = \hat{\mathbb{S}}^\varepsilon \hat{\boldsymbol{\mu}}^\varepsilon(\boldsymbol{x}) = \int_{\Gamma^\varepsilon} G_\omega(\|\boldsymbol{x}-\boldsymbol{y}\|)\hat{\boldsymbol{\mu}}^\varepsilon(\boldsymbol{y})d\Gamma_{\boldsymbol{y}}, \quad \boldsymbol{x} \in \Gamma^\varepsilon. \tag{3.2}$$

Introducing

$$\hat{\mathbb{S}}^\varepsilon_{nk} : H^{-1/2}(\Gamma^\varepsilon_k) \to H^{1/2}(\Gamma^\varepsilon_n), \quad n,k \in \mathcal{N},$$

defined for a sufficiently regular ϕ by

$$(\hat{\mathbb{S}}^\varepsilon_{nk}\phi)(\boldsymbol{x}) = \int_{\Gamma^\varepsilon_k} G_\omega(\|\boldsymbol{x}-\boldsymbol{y}\|)\phi(\boldsymbol{y})d\Gamma_{\boldsymbol{y}}, \quad \boldsymbol{x} \in \Gamma^\varepsilon_n, \tag{3.3}$$

we can further rewrite the equation (3.2) as follows:

$$\hat{g}^\varepsilon_n(\boldsymbol{x}) = \hat{\mathbb{S}}^\varepsilon_{nn}\hat{\boldsymbol{\mu}}^\varepsilon_n + \sum_{k\in\mathcal{N}\setminus\{n\}} \hat{\mathbb{S}}^\varepsilon_{nk}\hat{\boldsymbol{\mu}}^\varepsilon_k, \quad n \in \mathcal{N}. \tag{3.4}$$

The above can be rewritten as a variational formulation: find $\hat{\boldsymbol{\mu}}^\varepsilon \in H^{-1/2}(\Gamma^\varepsilon)$, s.t.

$$\langle \boldsymbol{\phi}, \hat{\boldsymbol{g}}^\varepsilon\rangle = \langle \boldsymbol{\phi}, \hat{\mathbb{S}}^\varepsilon \hat{\boldsymbol{\mu}}^\varepsilon_G\rangle, \quad \text{for all } \boldsymbol{\phi} \in H^{-1/2}(\Gamma^\varepsilon). \tag{3.5}$$

Let us now introduce the following coarse Galerkin space:

$$\mathcal{V}^\varepsilon_0 \subset H^{-1/2}(\Gamma^\varepsilon), \quad \mathcal{V}^\varepsilon_0 = \prod_{n=1}^N \mathcal{V}_0(\Gamma^\varepsilon_n), \qquad \mathcal{V}_0(\Gamma^\varepsilon_n) = \operatorname{span}\{1,\, \boldsymbol{x} \in \Gamma^\varepsilon_n\}. \tag{3.6}$$

Evidently, $\mathcal{V}^\varepsilon_0$ is an N-dimensional space, with the basis $\{\mathbf{e}^{\varepsilon,n}(\boldsymbol{x})\}_{n=1}^N$ defined as

$$\mathbf{e}^{\varepsilon,n}(\boldsymbol{x}) = \begin{cases} 1, & \boldsymbol{x} \in \Gamma^\varepsilon_n, \\ 0, & \text{otherwise.} \end{cases}$$

The main idea is to discretize (3.5) by using the Galerkin method with the trial and test space $\mathcal{V}^\varepsilon_0$. Such a discretization rewrites: find $\hat{\boldsymbol{\mu}}^\varepsilon_G := \sum_{n\in\mathcal{N}} \hat{\mu}^\varepsilon_{G,n}\mathbf{e}^{\varepsilon,n}$, $\hat{\mu}^\varepsilon_{G,n} \in \mathbb{C}$ (the index 'G' stands for 'Galerkin'), s.t.

$$\langle \mathbf{e}^{\varepsilon,n}, \hat{\boldsymbol{g}}^\varepsilon\rangle = \langle \mathbf{e}^{\varepsilon,n}, \hat{\mathbb{S}}^\varepsilon \hat{\boldsymbol{\mu}}^\varepsilon_G\rangle, \text{ for all } n \in \mathcal{N}, \tag{3.7}$$

and yields the following system of equations, cf. (3.4):

$$\begin{aligned} \int_{\Gamma^\varepsilon_n} \hat{g}^\varepsilon_n(\boldsymbol{x})d\Gamma_{\boldsymbol{x}} &= \hat{\mu}^\varepsilon_{G,n} \iint_{\Gamma^\varepsilon_n\times\Gamma^\varepsilon_n} G_\omega(\|\boldsymbol{x}-\boldsymbol{y}\|)d\Gamma_{\boldsymbol{y}}\, d\Gamma_{\boldsymbol{x}} \\ &\quad + \sum_{k\in\mathcal{N}\setminus\{n\}} \hat{\mu}^\varepsilon_{G,k} \iint_{\Gamma^\varepsilon_n\times\Gamma^\varepsilon_k} G_\omega(\|\boldsymbol{x}-\boldsymbol{y}\|)d\Gamma_{\boldsymbol{x}}\, d\Gamma_{\boldsymbol{y}}, \quad n \in \mathcal{N}. \end{aligned} \tag{3.8}$$

Let us remark that the Lebesgue integrals in the above are well-defined because the function $(\boldsymbol{x},\boldsymbol{y}) \mapsto G_\omega(\|\boldsymbol{x}-\boldsymbol{y}\|)$ belongs to $L^1(\Gamma^\varepsilon_n \times \Gamma^\varepsilon_k)$ for all n,k.

Knowing the coefficients $\hat{\boldsymbol{\mu}}^\varepsilon_G$, we can reconstruct an approximation $\hat{u}^\varepsilon_G$ to the exact solution u^ε according to (3.1):

$$\hat{u}^\varepsilon_G(\boldsymbol{x}) = \sum_{k=1}^N \hat{\mu}^\varepsilon_{G,k} \int_{\Gamma^\varepsilon_k} G_\omega(\|\boldsymbol{x}-\boldsymbol{y}\|)d\Gamma_{\boldsymbol{y}}, \quad \boldsymbol{x} \in \Omega^{\varepsilon,c}. \tag{3.9}$$

We will call the system of equations (3.8) and the reconstruction formula (3.9) the frequency-domain Galerkin Foldy-Lax model.

3.2. Time domain. Let us rewrite (3.8) in the time domain. Recall that the time-domain single layer potential is defined as the inverse Fourier-Laplace transform of the operator $\hat{\mathcal{S}}^\varepsilon$, more precisely, it acts as the following convolution:

$$\mathcal{S}^\varepsilon(\partial_t)\boldsymbol{\phi}(t,\boldsymbol{x}) = \int_0^t \int_{\Gamma^\varepsilon} \mathcal{G}(t-\tau, \boldsymbol{x}-\boldsymbol{y})\boldsymbol{\phi}(\tau,\boldsymbol{y}) d\Gamma_{\boldsymbol{y}}\, d\tau, \quad \boldsymbol{x} \in \Omega^{\varepsilon,c}. \tag{3.10}$$

Its trace is again continuous across Γ^ε, and is denoted by

$$\mathbb{S}^\varepsilon(\partial_t)\boldsymbol{\phi}(t,\boldsymbol{x}) = \int_0^t \int_{\Gamma^\varepsilon} \mathcal{G}(t-\tau, \boldsymbol{x}-\boldsymbol{y})\boldsymbol{\phi}(\tau,\boldsymbol{y}) d\Gamma_{\boldsymbol{y}}\, d\tau, \quad \boldsymbol{x} \in \Gamma^\varepsilon.$$

With the above definitions, similarly to Section 2.4.1, (3.7) rewrites

$$\langle \mathbf{e}^{\varepsilon,n}, \boldsymbol{g}^\varepsilon(t,.)\rangle = \langle \mathbf{e}^{\varepsilon,n}, \mathbb{S}^\varepsilon(\partial_t)\boldsymbol{\mu}_G^\varepsilon(t,.)\rangle, \text{ for all } n \in \mathcal{N}. \tag{3.11}$$

In other words, with

$$\mathcal{G}_{nk}^\varepsilon(t) = \mathcal{F}^{-1} \iint_{\Gamma_n^\varepsilon \times \Gamma_k^\varepsilon} G_\omega(\|\boldsymbol{x}-\boldsymbol{y}\|) d\Gamma_{\boldsymbol{x}} d\Gamma_{\boldsymbol{y}} = \iint_{\Gamma_n^\varepsilon \times \Gamma_k^\varepsilon} \mathcal{G}(t, \|\boldsymbol{x}-\boldsymbol{y}\|) d\boldsymbol{x}\, d\boldsymbol{y}, \tag{3.12}$$

the linear system of equations (3.8) in the time domain becomes a convolutional system of equations for $\boldsymbol{\mu}_G^\varepsilon : \mathbb{R}^+ \to \mathbb{R}^N$:

$$\begin{aligned} \int_{\Gamma_n^\varepsilon} g_n^\varepsilon(t,\boldsymbol{x}) d\Gamma_{\boldsymbol{x}} &= \int_0^t \mathcal{G}_{nn}^\varepsilon(t-\tau)\mu_n^\varepsilon(\tau) d\tau \\ &\quad + \sum_{k \in \mathcal{N}\setminus\{n\}} \int_0^t \mathcal{G}_{nk}^\varepsilon(t-\tau)\mu_k^\varepsilon(\tau) d\tau, \quad n \in \mathcal{N}. \end{aligned} \tag{GFL1}$$

Knowing the approximate density $\boldsymbol{\mu}_G^\varepsilon$, we restore the solution according to (3.10):

$$u_G^\varepsilon(t,\boldsymbol{x}) = \sum_{k\in\mathcal{N}} \int_0^t \left(\int_{\Gamma_k^\varepsilon} \mathcal{G}(t-\tau, \boldsymbol{x}-\boldsymbol{y}) d\Gamma_{\boldsymbol{y}} \right) \mu_{G,k}^\varepsilon(\tau) d\tau. \tag{GFL2}$$

Remark 1. *Let us remark that the above model is a priori stable for each $0 < \varepsilon \leq 1$. This is formalized in Theorem 4.1 and in Proposition 4.3. The reason for this is that the system of equations in (GFL1) stems from the Galerkin semidiscretization of the single-layer boundary integral operator $\mathbb{S}^\varepsilon(\partial_t)$. By applying the Fourier-Laplace transform to (GFL1) we obtain (3.7); for each $\omega \in \mathbb{C}^+$, the problem (3.7) is well-posed because of the coercivity of the single layer boundary integral operator $\mathrm{Im}\langle \hat{\mathbb{S}}^\varepsilon v, \overline{\omega v}\rangle \gtrsim c_1(\varepsilon,\omega)\|v\|^2_{H^{-1/2}(\Gamma^\varepsilon)}$. This allows also to obtain a bound $\|\hat{\boldsymbol{\mu}}_G^\varepsilon\|_{-1/2} \lesssim c_2(\varepsilon,\omega)\|\hat{\boldsymbol{g}}^\varepsilon\|_{1/2}$ in the frequency domain, which can be translated into a stability bound. This bound in turn can be used to obtain a stability bound for $\hat{u}_G^\varepsilon$. See the proof of Proposition 4.3 for a more detailed description of this approach.*

3.3. Galerkin Foldy-Lax model for circles. The Galerkin Foldy-Lax model can be defined for arbitrary geometries Ω_j^ε. Its practical implementation relies on the evaluation of the quantities (3.12) (computing the respective double integrals). In the case of the circular scatterers, this can be done analytically, exploiting the Graf addition theorem, on one hand, and the fact that constant functions are eigenfunctions of the single-layer boundary integral operator on a circle, on the other hand.

3.3.1. Galerkin Foldy-Lax model in the frequency domain.

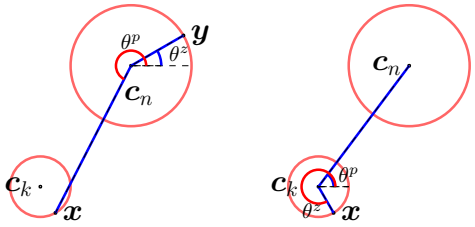

FIG. 4. *An illustration to the two applications of the Graf addition theorem.*

Derivation of the system of equations for unknown coefficients. We start with the variational formulation (3.7), which we rewrite in accordance with (3.4):

$$\langle \mathbf{e}^{\varepsilon,n}, \hat{\boldsymbol{g}}^{\varepsilon}\rangle = \langle \mathbf{e}^{\varepsilon,n}, \hat{\mathbb{S}}^{\varepsilon}_{nn}\mathbf{e}^{\varepsilon,n}\rangle \hat{\mu}^{\varepsilon}_{G,n} + \sum_{k\in\mathcal{N}\setminus\{n\}} \langle \mathbf{e}^{\varepsilon,n}, \hat{\mathbb{S}}^{\varepsilon}_{nk}\mathbf{e}^{\varepsilon,k}\rangle \hat{\mu}^{\varepsilon}_{G,k}. \tag{3.13}$$

Let us rewrite the right-hand side of the above identity. The operator $\hat{\mathbb{S}}^{\varepsilon}_{nn}$ is normal, as proven in [8]; moreover, its (non-normalized) eigenfunctions are $\{\mathrm{e}^{ik\theta_n(\boldsymbol{x})}\}_{k\in\mathbb{Z}}$, and eigenvalues are given by [22, 21],

$$\begin{aligned} &\hat{\mathbb{S}}^{\varepsilon}_{nn}\mathrm{e}^{ik\theta_n} = \frac{i\pi r_n^{\varepsilon}}{2} H^{(1)}_{|k|}(\omega r_n^{\varepsilon}) J_{|k|}(\omega r_n^{\varepsilon})\mathrm{e}^{ik\theta_n}, \text{ therefore} \\ &\langle \boldsymbol{e}^{\varepsilon,n}, \hat{\mathbb{S}}^{\varepsilon}_{nn}\boldsymbol{e}^{\varepsilon,n}\rangle = i\pi^2 (r_n^{\varepsilon})^2 H^{(1)}_0(\omega r_n^{\varepsilon}) J_0(\omega r_n^{\varepsilon}). \end{aligned} \tag{3.14}$$

The operator $\hat{\mathbb{S}}^{\varepsilon}_{nk}$ can also be rewritten in a more convenient form, by using the Graf addition theorem [1, 9.1.79]. According to it, for $z, p \in \mathbb{C}$, s.t. $p = |p|\mathrm{e}^{i\theta^p}$, $z = |z|\mathrm{e}^{i\theta^z}$, with $|p| > |z|$, and $w = p - z = |w|\mathrm{e}^{i\theta^w}$, $\chi = \theta^w - \theta^p$, it holds that

$$H^{(1)}_m(\omega||p|\mathrm{e}^{i\theta^p} - |z|\mathrm{e}^{i\theta^z}|) = \mathrm{e}^{-im\chi} \sum_{k\in\mathbb{Z}} H^{(1)}_{m+k}(\omega|p|) J_k(\omega|z|)\mathrm{e}^{ik(\theta^p-\theta^z)}. \tag{3.15}$$

Given $\boldsymbol{x} \in \Gamma^{\varepsilon}_k$, $\boldsymbol{y} \in \Gamma^{\varepsilon}_n$, first we apply the Graf theorem to $H^{(1)}_0(\omega\|\boldsymbol{x}-\boldsymbol{y}\|)$, with $p = \|\boldsymbol{x}-\boldsymbol{c}_n\|\mathrm{e}^{i\theta_n(\boldsymbol{x})}$ and $z = \|\boldsymbol{y}-\boldsymbol{c}_n\|\mathrm{e}^{i\theta_n(\boldsymbol{y})}$. We obtain its expansion into the series of $H_m(\omega\|\boldsymbol{x}-\boldsymbol{c}_m\|)$, and next we re-apply the Graf theorem to each of the terms of the series, with $p = \|\boldsymbol{c}_n - \boldsymbol{c}_k\|\mathrm{e}^{i\theta_k(\boldsymbol{c}_n)}$ and $z = \|\boldsymbol{x}-\boldsymbol{c}_k\|\mathrm{e}^{i\theta_k(\boldsymbol{x})}$ (in this latter case $w = p - z = \|\boldsymbol{x}-\boldsymbol{c}_n\|\mathrm{e}^{i\theta_n(\boldsymbol{x})}$, $\theta_n(\boldsymbol{c}_k) = \pi + \theta_k(\boldsymbol{c}_n)$ and $\chi = \theta_n(\boldsymbol{x}) - \theta_n(\boldsymbol{c}_k)$). These two applications are illustrated in Figure 4. We finally obtain the following expansion:

$$\begin{aligned} H^{(1)}_0(\omega\|\boldsymbol{x}-\boldsymbol{y}\|) = &\sum_{m=-\infty}^{\infty} J_m(\omega r_n^{\varepsilon})\mathrm{e}^{-im\theta_n(\boldsymbol{y})} \\ &\times \sum_{j=-\infty}^{\infty} H_{m+j}(\omega\|\boldsymbol{c}_n-\boldsymbol{c}_k\|)\mathrm{e}^{i(m\theta_n(\boldsymbol{c}_k)+j\theta_k(\boldsymbol{c}_n))} J_j(\omega r_k^{\varepsilon})\mathrm{e}^{ik\theta_k(\boldsymbol{x})}. \end{aligned}$$

Replacing $H^{(1)}_0$ in the definition of $\hat{\mathbb{S}}^{\varepsilon}_{nk}$ by the above expression yields

$$\langle \boldsymbol{e}^{n,\varepsilon}, \hat{\mathbb{S}}^{\varepsilon}_{nk}\boldsymbol{e}^{k,\varepsilon}\rangle = i\pi^2 r_k^{\varepsilon} r_n^{\varepsilon} J_0(\omega r_k^{\varepsilon}) J_0(\omega r_n^{\varepsilon}) H^{(1)}_0(\omega\|\boldsymbol{c}_k - \boldsymbol{c}_n\|). \tag{3.16}$$

Therefore, the Foldy-Lax model (3.13) then can be rewritten in the following form:

$$\begin{aligned} \int_{\Gamma^{\varepsilon}_n} \hat{g}^{\varepsilon}(\boldsymbol{x}) d\Gamma_{\boldsymbol{x}} = &\, i\pi^2 (r_n^{\varepsilon})^2 H^{(1)}_0(\omega r_n^{\varepsilon}) J_0(\omega r_n^{\varepsilon}) \hat{\mu}^{\varepsilon}_{G,n} \\ &+ i\pi^2 \sum_{k\in\mathcal{N}\setminus\{n\}} r_k^{\varepsilon} r_n^{\varepsilon} J_0(\omega r_k^{\varepsilon}) J_0(\omega r_n^{\varepsilon}) H^{(1)}_0(\omega\|\boldsymbol{c}_k - \boldsymbol{c}_n\|)\hat{\mu}^{\varepsilon}_{G,k}. \end{aligned} \tag{3.17}$$

Approximation of the field. Once the coefficients $\hat{\boldsymbol{\mu}}_G^\varepsilon$ are found by solving the system of equations (3.17), it remains to approximate the field $\hat{u}^\varepsilon$. We start with (3.9), which we further rewrite by using the Graf addition theorem (3.15):

$$\begin{aligned}\hat{u}_G^\varepsilon &= \frac{i}{4}\sum_{k\in\mathcal{N}}\hat{\mu}_{G,k}^\varepsilon\int_{\Gamma_k^\varepsilon}H_0^{(1)}(\omega\|\boldsymbol{x}-\boldsymbol{y}\|)d\Gamma_{\boldsymbol{y}}\\ &= \frac{i}{4}\sum_{k\in\mathcal{N}}\hat{\mu}_{G,k}^\varepsilon H_0^{(1)}(\omega\|\boldsymbol{x}-\boldsymbol{c}_k\|)\int_{\Gamma_k^\varepsilon}J_0(\omega\|\boldsymbol{y}-\boldsymbol{c}_k\|)d\Gamma_{\boldsymbol{y}}\\ &= \frac{i\pi}{2}\sum_{k\in\mathcal{N}}\hat{\mu}_{G,k}^\varepsilon r_k^\varepsilon H_0^{(1)}(\omega\|\boldsymbol{x}-\boldsymbol{c}_k\|)J_0(\omega r_k^\varepsilon).\end{aligned}\tag{3.18}$$

3.3.2. Galerkin Foldy-Lax model in the time domain. To rewrite the Galerkin Foldy-Lax model for circular obstacles in the time domain, let us introduce the following causal distributions (with 'sc' standing for 'scaled', compared to the analogous definitions in Section 3.2):

$$\begin{aligned}\mathcal{G}_{nn}^{sc,\varepsilon} &= \mathcal{F}^{-1}\frac{i\pi r_n^\varepsilon}{2}J_0(\omega r_n^\varepsilon)H_0^{(1)}(\omega r_n^\varepsilon),\\ \mathcal{G}_{nk}^{sc,\varepsilon} &= \mathcal{F}^{-1}\frac{i\pi r_k^\varepsilon}{2}J_0(\omega r_k^\varepsilon)J_0(\omega r_n^\varepsilon)H_0^{(1)}(\omega\|\boldsymbol{c}_k-\boldsymbol{c}_n\|),\quad k\neq n,\\ \mathcal{G}_k^{sc,\varepsilon}(\boldsymbol{x}) &= \mathcal{F}^{-1}\frac{i\pi r_k^\varepsilon}{2}H_0(\omega\|\boldsymbol{x}-\boldsymbol{c}_k\|)J_0(\omega r_k^\varepsilon).\end{aligned}$$

Then the Galerkin Foldy-Lax model (3.17), (3.18) in the time domain rewrites as

$$\begin{aligned}-\frac{1}{2\pi}\int_0^{2\pi}u^{inc}(t,\boldsymbol{c}_n+r_n^\varepsilon\hat{s}_\theta)d\theta &= \mathcal{G}_{nn}^{sc,\varepsilon}*_t\mu_{G,n}^\varepsilon+\sum_{k\in\mathcal{N}\setminus\{n\}}\mathcal{G}_{nk}^{sc,\varepsilon}*_t\mu_{G,k}^\varepsilon,\quad n\in\mathcal{N},\\ u_G^\varepsilon(t,\boldsymbol{x}) &= \sum_{k\in\mathcal{N}}\mathcal{G}_k^{sc,\varepsilon}(\boldsymbol{x})*_t\mu_{G,k}^\varepsilon.\end{aligned}\tag{3.19}$$

3.3.3. Numerical illustration of the stability of the Galerkin Foldy-Lax model for the configuration of Proposition 2.1. Let us illustrate the stability of the Galerkin Foldy-Lax model for the configuration described in Proposition 2.1. For this we use the same data as in Section 2.4.3. The field $u_G^\varepsilon(t,\boldsymbol{x}_0)$ is shown in Figure 5. It remains bounded, unlike u_{FL}^ε, cf. Figure 2, although we see that the solution obtained with the help of the asymptotic model is quite far from the reference solution, computed with the help of high-order BEM.

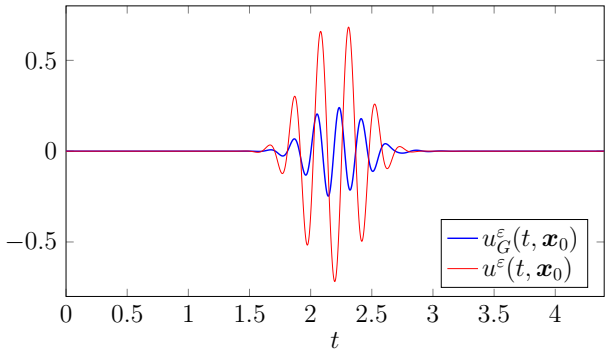

FIG. 5. *An illustration to the numerical experiment of Section 3.3.3. The dependence of the approximate solution* $u_G^\varepsilon(t,\boldsymbol{x}_0)$ *and the reference solution* $u^\varepsilon(t,\boldsymbol{x}_0)$ *at* $\boldsymbol{x}_0=(0.2,0.2)$ *on time.*

3.3.4. Connection to the Foldy-Lax model (2.9). The goal of this section is to show the relation between the original Foldy-Lax model and the new Galerkin one; we will show it in the frequency domain, i.e. for (2.9) and (3.17). We start by rewriting (3.17) in a form similar to (2.9). Let us consider the left-hand side of (2.9). First, $\hat{u}^{inc}(\boldsymbol{x})$ satisfies the homogeneous Helmholtz equation inside $B(\boldsymbol{c}_n, r_n^\varepsilon)$, therefore

$$\hat{u}^{inc}(\boldsymbol{c}_n + \rho\hat{s}_\theta) = -\sum_{m\in\mathbb{Z}} \hat{g}^\varepsilon_{n,m} \frac{J_m(\omega\rho)}{J_m(\omega r_n^\varepsilon)} \mathrm{e}^{-im\theta}, \qquad \rho < r_n^\varepsilon.$$

Because $J_m(0) = \delta_{0m}$,

$$-J_0(\omega r_n^\varepsilon)\hat{u}^{inc}(\boldsymbol{c}_n) = \hat{g}^\varepsilon_{n,0} = (2\pi r_n^\varepsilon)^{-1} \int_{\Gamma_n^\varepsilon} \hat{g}^\varepsilon(\boldsymbol{x}) d\Gamma_{\boldsymbol{x}}. \tag{3.20}$$

Next, let us rewrite the right-hand side of (2.9). Let

$$\hat{\lambda}^\varepsilon_{G,n} = \frac{i\pi}{2} r_n^\varepsilon H_0^{(1)}(\omega r_n^\varepsilon)\hat{\mu}^\varepsilon_{G,n}.$$

Replacing the left-hand side of (3.17) by (3.20) and $\hat{\boldsymbol{\mu}}^\varepsilon_G$ by its expression of $\hat{\boldsymbol{\lambda}}^\varepsilon_G$ yields

$$-\hat{u}^{inc}(\boldsymbol{c}_n) = \hat{\lambda}^\varepsilon_{G,n} + \sum_{k\in\mathcal{N}\setminus\{n\}} J_0(\omega r_k^\varepsilon) \frac{H_0^{(1)}(\omega\|\boldsymbol{c}_k - \boldsymbol{c}_n\|)}{H_0^{(1)}(\omega r_k^\varepsilon)} \hat{\lambda}^\varepsilon_{G,k}, \quad n \in \mathcal{N}. \tag{3.21}$$

And the field approximation then reads

$$-\hat{u}^\varepsilon_G(\boldsymbol{x}) = \sum_{k\in\mathcal{N}} J_0(\omega r_k^\varepsilon) \frac{H_0^{(1)}(\omega\|\boldsymbol{x} - \boldsymbol{c}_k\|)}{H_0^{(1)}(\omega r_k^\varepsilon)} \hat{\lambda}^\varepsilon_{G,k}. \tag{3.22}$$

We recognize in (3.21) the system of equations (2.9), and in (3.22) the approximation (2.8), modulo the term $J_0(\omega r_k^\varepsilon)$. For a fixed frequency ω, as $r_n^\varepsilon \to 0$, $J_0(\omega r_n^\varepsilon) = 1 + O(\varepsilon^2)$, and thus approximating $J_0(\omega r_n^\varepsilon)$ by 1 does not seem to affect the convergence rates of the model, at least in the frequency domain [9]. However, in the time domain, the absence of this term is accountable for a potential lack of stability.

4. Convergence Analysis. We aim at obtaining an estimate of the type

$$\|u^\varepsilon(t) - u^\varepsilon_G(t)\|_{L^2(K)} < C \times \mathrm{error}(\varepsilon).$$

We will specify the type of dependence (e.g. polynomial) of the constant C on the number of particles N, the minimal distance between particles d_*, simulation time t, the largest and smallest radii R^* and R_*, and make explicit the dependence of the error on a certain norm of the data u^{inc}.

In the analysis, we never use an assumption about N being a fixed number with respect to $\varepsilon > 0$, or $d_*^\varepsilon > d_* = \mathrm{const}$. This enables us to extend our results to the case when N and d_*^ε depend on the asymptotic parameter ε (Section 5).

4.1. Main results. Let us first introduce a technical assumption.

Assumption 1. *We assume that the incident field satisfies*

$$u^{inc} \in H^9(0,T;H^3(\mathbb{R}^2)).$$

Such a regularity assumption holds true notably when u_0, $u_1 \in C_0^\infty(\mathbb{R}^2)$.

Let us also introduce the weighted norm

$$\|v\|^2_{H^m_\varepsilon(0,T;X)} := \sum_{k=0}^m \varepsilon^k \|\partial_t^k v\|^2_{L^2(0,T;X)}.$$

Evidently, it can be bounded by ε-independent norm. Nonetheless, we would like to use such a norm in the convergence estimates, where suitable, since it takes into account the ratio of the wavelength and the asymptotic parameter ε: for $v(t) = \mathrm{e}^{iwt}$, with $w > 0$, the norm $\|v\|_{H^m_\varepsilon(0,T)} \lesssim T\big(\sum_{k=0}^{m} (\varepsilon w)^2\big)^{1/2}$.

The principal result of this section is summarized below. It shows that the Galerkin Foldy-Lax method yields $O(\varepsilon^2)$ error in the far-field, and $O(\varepsilon)$ error in the near-field (at the distance $O(\varepsilon)$ to the scatterers).

THEOREM 4.1 (Convergence of u^ε_G). *Let Assumption 1 hold true. Let $\delta = \delta_\varepsilon > 0$, and $\boldsymbol{x}_\varepsilon \in \Omega^{\varepsilon+\delta_\varepsilon,c}$. Then, for all $0 < \varepsilon \leq 1$, $0 < t < T$, the field u^ε_G satisfies the following error bound, with a constant C_G depending polynomially on $R^*, R_*^{-1}, T, N, \underline{d_*}^{-1}$:*

$$\|u^\varepsilon_G(t, \boldsymbol{x}_\varepsilon) - u^\varepsilon(t, \boldsymbol{x}_\varepsilon)\| \leq \varepsilon^2 \times \max(1, \delta_\varepsilon^{-1}) C_G \|\partial_t^6 u^{inc}\|_{H^3_\varepsilon(0,T;H^3(\mathbb{R}^2))}.$$

In particular,

- *when $\delta_\varepsilon = \text{const}$ (far-field), then*
$$\|u^\varepsilon_G(t, \boldsymbol{x}_\varepsilon) - u^\varepsilon(t, \boldsymbol{x}_\varepsilon)\| = O(\varepsilon^2).$$
- *when $\delta_\varepsilon = \varepsilon^\alpha$, with $\alpha \in (0, 2)$ (near-field), then*
$$\|u^\varepsilon_G(t, \boldsymbol{x}_\varepsilon) - u^\varepsilon(t, \boldsymbol{x}_\varepsilon)\| = O(\varepsilon^{2-\alpha}).$$

The proof of this theorem can be found in Section 4.6. It yields immediately the following result.

COROLLARY 4.2. *Under Assumption 1, the Galerkin Foldy-Lax model is convergent and uniformly stable, as defined in the end of Section 2.1.*

Proof. See Appendix B. ∎

Theorem 4.1 relies on the following result about the convergence of the density $\boldsymbol{\mu}^\varepsilon$.

PROPOSITION 4.3 (Convergence of the density). *Let Assumption 1 hold true. Let $T > 0$. For all $0 < \varepsilon \leq 1$, the density $\boldsymbol{\mu}^\varepsilon_G \in L^\infty(0, T; \mathcal{V}_0^\varepsilon)$ satisfies the following bound, with the constant $C_{\mu 0}$ depending polynomially on R^*, R_*^{-1}, T, N and $\underline{d_*}^{-1}$:*

$$\|\boldsymbol{\mu}^\varepsilon_G\|_{L^\infty(0,T;H^{-1/2}(\Gamma_\varepsilon))} \leq \varepsilon^{-1/2} \times C_{\mu 0} \|\partial_t^2 u^{inc}\|^2_{H^1_\varepsilon(0,T;H^2(\mathbb{R}^2))}.$$

The error between the exact density and its approximation satisfies, with the constant $C_{\mu,G}$ depending polynomially on R^*, R_*^{-1}, T, N and $\underline{d_*}^{-1}$:

$$\|\boldsymbol{e}^\varepsilon\|_{L^\infty(0,T;H^{-1/2}(\Gamma^\varepsilon))} \leq \varepsilon \times C_{\mu,G} \|\partial_t^6 u^{inc}\|_{H^3_\varepsilon(0,T;H^3(\mathbb{R}^2)))}.$$

The proof of this proposition is presented in Section 4.5. The above proposition states two results:

- the $H^{-1/2}(\Gamma^\varepsilon)$-norm of the density $\boldsymbol{\mu}^\varepsilon_G(t)$ grows at most as $O(\varepsilon^{-1/2})$; this implies in particular that $\|\boldsymbol{\mu}^\varepsilon_G(t)\|_{L^\infty(\Gamma^\varepsilon)} \lesssim \varepsilon^{-1}$.
- the Galerkin Foldy-Lax method approximates the density $\boldsymbol{\mu}^\varepsilon_G$ with the error $O(\varepsilon)$, i.e. we can expect the relative error in the density approximation to be of order $O(\varepsilon^{3/2})$.

The growth of the density $\boldsymbol{\mu}^\varepsilon_G$ with ε^{-1} is due to the choice of the Foldy-Lax unknown $\boldsymbol{\mu}^\varepsilon$ as the jump of the normal trace of the field that satisfies the Dirichelt problem for the wave equation inside and outside of the obstacles (with the data $\boldsymbol{g}^\varepsilon$). It is possible to rescale the Galerkin Foldy-Lax formulation in order to avoid this problem, by taking as the new unknown

$$\lambda^\varepsilon_k = \mathbb{S}^\varepsilon_{kk}(\partial_t)\mu^\varepsilon_k, \quad k = 1, \ldots, N.$$

The Galerkin method applied to the integral formulation with this new unknown will yield a problem equivalent to (3.11), because constant functions are eigenfunctions of $\hat{\mathbb{S}}^\varepsilon_{kk}$. The analysis of the Foldy-Lax formulation obtained with this definition of the density is out of scope of the present article, since, conceptually, it will not differ much from the analysis presented here, however, requires some extra technical results.

REMARK 2. *Comparing Proposition 4.3 and Theorem 4.1, one may find it surprising that the error in the density of $O(\varepsilon)$ can produce an error of $O(\varepsilon^2)$ in the field. See Section 4.6 for a detailed explanation to such a 'super-convergence' phenomenon.*

4.2. Main identity for the error in the frequency domain. We start by performing the analysis in the frequency domain, as it is classical in the time-domain boundary integral equation community [2, 38], by considering the case of the frequencies with absorption ($\omega \in \mathbb{C}^+$), and next argue how the respective estimates can be translated into the time domain.

4.2.1. Decomposition of spaces. Let us decompose the space $H^{1/2}(\Gamma^\varepsilon)$ into a direct sum of the spaces (orthogonal with respect to $L^2(\Gamma^\varepsilon)$-scalar product)

$$H^{1/2}(\Gamma^\varepsilon) = \mathcal{V}_0^\varepsilon \dot{+} H_*^{1/2}(\Gamma^\varepsilon),$$

where $\mathcal{V}_0^\varepsilon$ was defined in (3.6) as follows:

$$\mathcal{V}_0^\varepsilon = \prod_{n\in\mathcal{N}} \mathcal{V}_0(\Gamma_n^\varepsilon), \qquad \mathcal{V}_0(\Gamma_n^\varepsilon) = \operatorname{span}\{1,\, \boldsymbol{x} \in \Gamma_n^\varepsilon\}, \quad \text{and}$$
$$H_*^{1/2}(\Gamma^\varepsilon) = \{\boldsymbol{v} \in H^{1/2}(\Gamma^\varepsilon) : (\mathbf{e}^{\varepsilon,n}, \boldsymbol{v})_{L^2(\Gamma^\varepsilon)} = 0, \ \text{ for all } n \in \mathcal{N}\}.$$

The respective $L^2(\Gamma^\varepsilon)$-orthogonal projector on the space $\mathcal{V}_0^\varepsilon$ is denoted by $\mathbb{P}_0^\varepsilon$, and on the space $H_*^{1/2}(\Gamma^\varepsilon)$ by $\mathbb{P}_\perp^\varepsilon$. For any $\boldsymbol{v} \in H^{1/2}(\Gamma^\varepsilon)$, we introduce the decomposition $\boldsymbol{v} = \boldsymbol{v}_0 \dot{+} \boldsymbol{v}_\perp$, with $\boldsymbol{v}_0 \in \mathcal{V}_0^\varepsilon$, $\boldsymbol{v}_\perp \in H_*^{1/2}(\Gamma^\varepsilon)$. In a similar manner we decompose

$$H^{-1/2}(\Gamma^\varepsilon) = \mathcal{V}_0^\varepsilon \dot{+} H_*^{-1/2}(\Gamma^\varepsilon), \quad \text{where}$$
$$H_*^{-1/2}(\Gamma^\varepsilon) = \{\boldsymbol{v} \in H^{-1/2}(\Gamma^\varepsilon) : \langle \boldsymbol{v}, \mathbf{e}^{\varepsilon,n}\rangle = 0, \ \text{ for all } n \in \mathcal{N}\}.$$

The respective adjoint projectors will be denoted by $\mathbb{P}_0^{\varepsilon,*}$ and $\mathbb{P}_\perp^{\varepsilon,*}$. Again, any $\boldsymbol{v} \in H^{-1/2}(\Gamma^\varepsilon)$ can be decomposed as $\boldsymbol{v} = \boldsymbol{v}_0 \dot{+} \boldsymbol{v}_\perp$, with $\boldsymbol{v}_0 \in \mathcal{V}_0^\varepsilon$, $\boldsymbol{v}_\perp \in H_*^{-1/2}(\Gamma^\varepsilon)$.

It remains to introduce the following operators:

$$\hat{\mathbb{S}}_{00}^\varepsilon := \mathbb{P}_0^\varepsilon \hat{\mathbb{S}}^\varepsilon \mathbb{P}_0^{\varepsilon,*}, \quad \hat{\mathbb{S}}_{0\perp}^\varepsilon = \mathbb{P}_0^\varepsilon \hat{\mathbb{S}}^\varepsilon \mathbb{P}_\perp^{\varepsilon,*}, \quad \hat{\mathbb{S}}_{\perp 0}^\varepsilon = \mathbb{P}_\perp^\varepsilon \hat{\mathbb{S}}^\varepsilon \mathbb{P}_0^{\varepsilon,*}, \quad \hat{\mathbb{S}}_{\perp\perp}^\varepsilon = \mathbb{P}_\perp^\varepsilon \hat{\mathbb{S}}^\varepsilon \mathbb{P}_\perp^{\varepsilon,*}.$$

The main idea of the error analysis is to exploit different scaling of the norms of these operators with respect to $\varepsilon \to 0$.

Remark 3. *Remark that there should be no confusion between $\hat{\mathbb{S}}_{00}^\varepsilon$ defined above and the operators $\hat{\mathbb{S}}_{kk}^\varepsilon$, $k = 1, \dots, N$, corresponding to the single layer boundary integral operators for a single obstacle, cf. (3.3).*

4.2.2. Error expression in the frequency domain. With the decomposition of the spaces introduced in the previous section, we rewrite the Galerkin Foldy-Lax model as: find $\hat{\boldsymbol{\mu}}_G^\varepsilon \in \mathcal{V}_0^\varepsilon$, s.t.

$$\hat{\boldsymbol{g}}_0^\varepsilon = \hat{\mathbb{S}}_{00}^\varepsilon \hat{\boldsymbol{\mu}}_G^\varepsilon. \tag{4.1}$$

The exact solution $\hat{\boldsymbol{\mu}}^\varepsilon$ satisfies the system

$$\begin{pmatrix} \hat{\mathbb{S}}_{00}^\varepsilon & \hat{\mathbb{S}}_{0\perp}^\varepsilon \\ \hat{\mathbb{S}}_{\perp 0}^\varepsilon & \hat{\mathbb{S}}_{\perp\perp}^\varepsilon \end{pmatrix} \begin{pmatrix} \hat{\boldsymbol{\mu}}_0^\varepsilon \\ \hat{\boldsymbol{\mu}}_\perp^\varepsilon \end{pmatrix} = \begin{pmatrix} \hat{\boldsymbol{g}}_0^\varepsilon \\ \hat{\boldsymbol{g}}_\perp^\varepsilon \end{pmatrix}.$$

From the above it is straightforward to obtain an equation for the error $\hat{\boldsymbol{e}}^\varepsilon = \hat{\boldsymbol{\mu}}^\varepsilon - \hat{\boldsymbol{\mu}}_G^\varepsilon$:

$$\begin{pmatrix} \hat{\mathbb{S}}_{00}^\varepsilon & \hat{\mathbb{S}}_{0\perp}^\varepsilon \\ \hat{\mathbb{S}}_{\perp 0}^\varepsilon & \hat{\mathbb{S}}_{\perp\perp}^\varepsilon \end{pmatrix} \begin{pmatrix} \hat{\boldsymbol{e}}_0^\varepsilon \\ \hat{\boldsymbol{e}}_\perp^\varepsilon \end{pmatrix} = \begin{pmatrix} 0 \\ \hat{\boldsymbol{g}}_\perp^\varepsilon - \hat{\mathbb{S}}_{\perp 0}^\varepsilon \hat{\boldsymbol{\mu}}_G^\varepsilon \end{pmatrix}.$$

The constant component of the error can be obtained by the usual Schur complement:

$$\hat{\boldsymbol{e}}_0^\varepsilon = \left(\hat{\mathbb{S}}_{00}^\varepsilon\right)^{-1} \hat{\mathbb{S}}_{0\perp}^\varepsilon \, \hat{\boldsymbol{e}}_\perp^\varepsilon, \tag{4.2}$$

and the non-constant component is nothing else than

$$\hat{\boldsymbol{e}}^\varepsilon_\perp = \mathbb{P}^{\varepsilon,*}_\perp(\hat{\mathbb{S}}^\varepsilon)^{-1}\mathbb{P}^\varepsilon_\perp(\hat{\boldsymbol{g}}^\varepsilon_\perp - \hat{\mathbb{S}}^\varepsilon_{\perp 0}\hat{\boldsymbol{\mu}}^\varepsilon_G) = \mathbb{P}^{\varepsilon,*}_\perp(\hat{\mathbb{S}}^\varepsilon)^{-1}\mathbb{P}^\varepsilon_\perp(\hat{\boldsymbol{g}}^\varepsilon_\perp - \hat{\mathbb{S}}^\varepsilon_{\perp 0}\big(\hat{\mathbb{S}}^\varepsilon_{00}\big)^{-1}\hat{\boldsymbol{g}}^\varepsilon_0).$$

Next, we estimate

$$\begin{aligned}
&\|\hat{\boldsymbol{e}}^\varepsilon_0\|_{-1/2} \le \|\big(\hat{\mathbb{S}}^\varepsilon_{00}\big)^{-1}\|\|\hat{\mathbb{S}}^\varepsilon_{0\perp}\|\,\|\hat{\boldsymbol{e}}^\varepsilon_\perp\|_{-1/2},\\
&\|\hat{\boldsymbol{e}}^\varepsilon_\perp\|_{-1/2} \le \|\mathbb{P}^{\varepsilon,*}_\perp(\hat{\mathbb{S}}^\varepsilon)^{-1}\mathbb{P}^\varepsilon_\perp\|\left(\|\hat{\boldsymbol{g}}^\varepsilon_\perp\|_{1/2} + \|\hat{\mathbb{S}}^\varepsilon_{\perp 0}\|\|\big(\hat{\mathbb{S}}^\varepsilon_{00}\big)^{-1}\|\|\hat{\boldsymbol{g}}^\varepsilon_0\|_{1/2}\right).
\end{aligned} \tag{4.3}$$

Thus, the convergence of the Galerkin Foldy-Lax model relies on the estimates of the data $\hat{\boldsymbol{g}}^\varepsilon$ and on the estimates on the operator norms of the (inverses of) restrictions of $\hat{\mathbb{S}}^\varepsilon$ to different subspaces, as $\varepsilon \to 0$.

Let us anticipate the results that we will prove in the sections that follow. For the data, we will see that as $\varepsilon \to 0$, it is a constant component of $\hat{\boldsymbol{g}}^\varepsilon$ that provides the most significant contribution in the norm of $\|\hat{\boldsymbol{g}}^\varepsilon\|_{H^{1/2}(\Gamma^\varepsilon)}$:

$$\|\hat{\boldsymbol{g}}^\varepsilon_0\|_{1/2} = O(\varepsilon^{1/2}), \quad \|\hat{\boldsymbol{g}}^\varepsilon_\perp\|_{1/2} = O(\varepsilon).$$

For the operators, this is as well the case: the most significant contribution to $\big(\hat{\mathbb{S}}^\varepsilon\big)^{-1}$ is provided by the inverse of $\hat{\mathbb{S}}^\varepsilon_{00}$, which scales as $O(\varepsilon^{-1})$. Moreover, as $\varepsilon \to 0$, the operator $\hat{\mathbb{S}}^\varepsilon$ approaches a block-diagonal operator. This is reflected below:

$$\|\big(\hat{\mathbb{S}}^\varepsilon_{00}\big)^{-1}\| = O(\varepsilon^{-1}), \quad \|\mathbb{P}^{\varepsilon,*}_\perp(\hat{\mathbb{S}}^\varepsilon)^{-1}\mathbb{P}^\varepsilon_\perp\| = O(1), \quad \|\hat{\mathbb{S}}^\varepsilon_{0\perp}\| = \|\hat{\mathbb{S}}^\varepsilon_{\perp 0}\| = O(\varepsilon^{3/2}).$$

These estimates, combined with (4.3), will imply the following error behaviour:

$$\|\hat{\boldsymbol{e}}^\varepsilon_\perp\|_{-1/2} = O(\varepsilon), \quad \|\hat{\boldsymbol{e}}^\varepsilon_0\|_{-1/2} = O(\varepsilon^{3/2}).$$

We proceed as follows. Because our final goal is to obtain time-domain estimates, we

- first obtain estimates on the data, directly in the time domain;
- next obtain frequency-domain estimates on the operators, explicit in the frequency and in the asymptotic parameter;
- translate all the estimates into the time domain.

4.3. Estimates on the data in the time domain. The two main results of this section are Propositions 4.6 and 4.7, which relate the norms of $\boldsymbol{g}^\varepsilon_\perp$ and $\boldsymbol{g}^\varepsilon_0$ on the boundary Γ^ε to the ε-independent norm of the incident field u^{inc}. The proof of these propositions relies on two auxiliary lemmas, formulated for the case of a single circle of a fixed radius $r > 0$. We will make use of the same decomposition of the spaces, as the one introduced in Section 4.2.1, however, for the case of the single boundary $\mathcal{C}_r$. The projection operators corresponding to $\mathbb{P}^\varepsilon_0$ and $\mathbb{P}^\varepsilon_\perp$ will be denoted by P_0 and $P_\perp$. We start with estimating $P_0\gamma_0 v$.

LEMMA 4.4. *Let $0 < R \le +\infty$. Then there exists $C > 0$ s.t., for all $0 < r < R$, $v \in H^2(B(0,R))$,*

$$\|P_0\gamma_0 v\|_{L^2(\mathcal{C}_r)} \le Cr^{1/2}\|v\|_{H^2(B(0,R))}.$$

Proof. Evidently, $\|P_0\gamma_0 v\|_{L^2(\mathcal{C}_r)} \le (2\pi r)^{1/2}\|v\|_{L^\infty(\mathcal{C}_r)}$. The remaining part of the result follows by the Sobolev embedding theorem [16, Theorem 1.4.4.1]. ∎

REMARK 4. *We state the above result with $H^2(B(0,R))$ instead of a more optimal $L^\infty(B(0,R))$ space, because it is better adapted to the energy wave equation which is used later.*

Next, let us estimate $P_\perp\gamma_0 v$.

LEMMA 4.5. *Let $0 < R \le +\infty$, $\delta > 0$. Then there exists $C > 0$ s.t., for all $0 < r < R$, s.t. for all $0 < r < R$, $v \in H^3(B(0,R))$,*

$$\|P_\perp\gamma_0 v\|_{H^{1/2}(\mathcal{C}_r)} \le Cr\max(1,r)\|v\|_{H^3(B(0,R))}.$$

Proof. Decomposing $\gamma_0 v$ into its Fourier series (2.6) yields

$$\|P_\perp \gamma_0 v\|_{H^{1/2}(\mathcal{C}_r)} = r \sum_{m\in\mathbb{Z}\setminus\{0\}} \left(1+\frac{m^2}{r^2}\right)^{1/2} |v_m|^2 \le 2\max(1,r) \sum_{m\in\mathbb{Z}\setminus\{0\}} m|v_m|^2.$$

To estimate the above, we use the seminorm (2.7). Defining $\hat{\boldsymbol{s}}_\theta = (\cos\theta, \sin\theta)$, we rewrite it in the following way:

$$\|P_\perp v\|^2_{\mathcal{H}^{1/2}(\mathcal{C}_r)} = \int_0^{2\pi}\int_0^{2\pi} \frac{|v(r\hat{\boldsymbol{s}}_\theta) - v(r\hat{\boldsymbol{s}}_\psi)|^2}{|\hat{\boldsymbol{s}}_\theta - \hat{\boldsymbol{s}}_\psi|^2} d\theta d\psi \lesssim r^2 \sup_{\boldsymbol{x}\in B(0,r)} |\nabla v(\boldsymbol{x})|^2.$$

The latter quantity is bounded by the Sobolev embedding theorem. ∎

The above two lemmas then allow us to estimate $\boldsymbol{g}_0^\varepsilon$ and $\boldsymbol{g}_\perp^\varepsilon$.

PROPOSITION 4.6. *Let $\ell \in \mathbb{N}$, and let for all $t \ge 0$, $\partial_t^\ell u^{inc}(t) \in H^2(\mathbb{R}^2)$. There exists $c_0 > 0$, depending polynomially on R^*, s.t.*

$$\|\partial_t^\ell \boldsymbol{g}_0^\varepsilon(t)\|_{L^2(\Gamma^\varepsilon)} \le c_0 \varepsilon^{1/2} N^{1/2} \|\partial_t^\ell u^{inc}(t)\|_{H^2(\mathbb{R}^2)}, \quad t \ge 0.$$

Proof. We prove the result for $\ell = 0$; for $\ell > 0$ the proof is a straightforward extension. By Lemma 4.4, we have the bound

$$\sum_{n\in\mathcal{N}} \|\boldsymbol{g}_0^\varepsilon(t)\|^2_{L^2(\Gamma_n^\varepsilon)} \lesssim \sum_{n\in\mathcal{N}} r_n^\varepsilon \|u^{inc}(t)\|^2_{H^{1+\delta}(\mathbb{R}^2)} \le R^* N\varepsilon \|u^{inc}(t)\|^2_{H^{1+\delta}(\mathbb{R}^2)}.$$ ∎

The counterpart of Lemma 4.5, which relates $\boldsymbol{g}_\perp^\varepsilon$ to u^{inc}, is given below.

PROPOSITION 4.7. *Let $\ell \in \mathbb{N}$, and let, for all $t \ge 0$, $\partial_t^\ell u^{inc}(t) \in H^3(\mathbb{R}^2)$. There exists $c_\perp > 0$, depending polynomially on R^*, s.t. for all $t \ge 0$,*

$$\|\partial_t^\ell \boldsymbol{g}_\perp^\varepsilon(t)\|_{H^{1/2}(\Gamma^\varepsilon)} \le c_\perp \varepsilon N^{1/2} \|\partial_t^\ell u^{inc}(t)\|_{H^3(\mathbb{R}^2)}.$$

Proof. The proof mimics almost verbatim the proof Proposition 4.6. ∎

REMARK 5. *The above bounds translate obviously into the frequency domain.*

4.4. Estimates on the operators in the frequency domain. The goal of this section is to prove the following bounds, with constants depending on the frequency:

$$\|\big(\hat{\mathbb{S}}_{00}^\varepsilon\big)^{-1}\| = O(\varepsilon^{-1}), \quad \|\hat{\mathbb{S}}_{0\perp}^\varepsilon\| = \|\hat{\mathbb{S}}_{\perp 0}^\varepsilon\| = O(\varepsilon^{3/2}), \quad \|\mathbb{P}_\perp^{\varepsilon,*}(\hat{\mathbb{S}}^\varepsilon)^{-1}\mathbb{P}_\perp^\varepsilon\| = O(1).$$

4.4.1. Lifting lemmas. The proof on the estimates on the norms $\|(\mathbb{S}_{00}^\varepsilon)^{-1}\|$ and $\|\mathbb{P}_\perp^{\varepsilon,*}(\hat{\mathbb{S}}^\varepsilon)^{-1}\mathbb{P}_\perp^\varepsilon\|$ is typically done by showing the coercivity of the underlying operators, and a certain lifting lemma, see [2]. The difficulty in our case lies in deriving the lifting lemma with estimates explicit in the small parameter $\varepsilon > 0$. To do so, we will base our considerations on the idea from the recent work by Hassan and Stamm [17], where the three-dimensional electrostatic problem in the exterior of multiple spheres is considered. They adapt the lifting lemma to their geometry, and we will make use of their construction, with some modifications due to the nature of our model (the Helmholtz equation rather than electrostatics).

We proceed as follows:

1. in Lemmas 4.9, 4.10, we formulate the lifting bounds explicit in $\operatorname{diam}\mathcal{O}$ for the case when $\mathcal{O} = B(0,r)$, and the data is either constant or orthogonal to a constant. Moreover, we will need an estimate on the L^2-norm of the solution inside

$$B_{r,r+d} = B(0, r+d) \setminus \overline{B(0,r)}.$$

2. we extend these results to the case of multiple scatterers in Proposition 4.11.

Lifting lemmas for a single obstacle. We start by recalling the lifting lemma of [2], in the form presented in the monograph by Sayas [38].

PROPOSITION 4.8 (Proposition 2.5.1 in [38]). *Let $\mathcal{O}$ be a Lipschitz domain. Then there exists $C_{\mathcal{O}} > 0$, s.t. for all $\xi \in H^{1/2}(\partial\mathcal{O})$ and all $a > 0$, the solution $v \in H^1(\mathcal{O})$ to the Dirichlet problem*

$$-\Delta v + a^2 v = 0 \text{ in } \mathcal{O}, \quad \gamma_0 v = \xi,$$

is bounded as follows: $\|v\|_{a,\mathcal{O}} \leq C_{\mathcal{O}} \max(1, a^{1/2}) \|\xi\|_{H^{1/2}(\mathcal{O})}$.

Let us single out an explicit dependence of $C_{\mathcal{O}}$ on $\operatorname{diam}\mathcal{O}$ for the case when $\mathcal{O}$ is a circle $B(0,r)$. We start by considering the case when the data is constant on C_r.

LEMMA 4.9 (Lifting lemma for constants). *Let $a, r > 0$, and $V^r \in H^1(\mathbb{R}^2)$ satisfy the interior boundary value problem*

$$-\Delta V^r + a^2 V^r = 0 \text{ in } B(0,r), \quad \gamma_0^- V^r = 1,$$

and the exterior boundary value problem

$$-\Delta V^r + a^2 V^r = 0 \text{ in } B^c(0,r), \quad \gamma_0^+ V^r = 1.$$

Then, for all $d > 0$,

$$\|V^r\|^2_{a,B(0,r+d)} \lesssim \max(1, ar), \tag{4.4}$$

$$\|V^r\|^2_{L^2(B_{r,r+d})} \lesssim rd + d^2. \tag{4.5}$$

Proof. The solution V^r is defined via the modified Bessel functions:

$$V^r(\rho) = \begin{cases} \frac{I_0(a\rho)}{I_0(ar)} & \rho < r, \\ \\ \frac{K_0(a\rho)}{K_0(ar)} & \rho > r. \end{cases} \tag{4.6}$$

Proof of the bound (4.5). Using Lemma C.2 to bound $K_0(a\rho)/K_0(ar)$,

$$\|V^r\|^2_{L^2(B_{r,r+d})} = 2\pi \int_r^{r+d} \left| \frac{K_0(a\rho)}{K_0(ar)} \right|^2 \rho d\rho \lesssim d(r+d).$$

Proof of the bound (4.4). To prove this result, one could have used an explicit expression for V^r (4.6) and next proved some bounds on the modified Bessel functions. We have tried this approach, however, the final bound that we managed to obtain did not improve significantly over the bound obtained from a simple scaling argument (see Remark 6 below), which we will present below.

We start by bounding $\|V^r\|^2_{a,B(0,r+d)} \leq \|V^r\|^2_{a,\mathbb{R}^2}$. In what follows, we use the fact that V^r is rotation invariant, and we make its dependence on a explicit by writing $V^r(\rho, a)$ instead of $V^r(\rho)$. By a scaling argument, one can verify that $V^r(\rho, a) = V^1(\frac{\rho}{r}, ar)$. Moreover (where we use $V^r \in H^1(\mathbb{R}^2)$):

$$\|V^r(., a)\|^2_{a,\mathbb{R}^2} = \int_0^{+\infty} \left(|\partial_\rho V^r(\rho, a)|^2 + a^2 |V^r(\rho, a)|^2 \right) \rho d\rho = \|V^1(., ar)\|^2_{ar,\mathbb{R}^2}. \tag{4.7}$$

To obtain (4.4), it suffices to bound

$$\|V^1(., ar)\|^2_{ar,\mathbb{R}^2} = \|V^1(., ar)\|^2_{ar,B(0,1)} + \|V^1(., ar)\|^2_{ar,B^c(0,1)},$$

which is done by applying Proposition 4.8 twice, first with $\mathcal{O} = B(0,1)$ and next with $\mathcal{O} = B^c(0,1)$. ∎

REMARK 6. *A bound for $\|V^r\|^2_{a,B(0,r+d)}$ that we obtained by bounding modified Bessel functions reads:*

$$\|V^r\|^2_{a,B(0,r+d)} \lesssim \begin{cases} -\frac{1}{\log(a(r+d)}, & a(r+d)<1/2, \\ \max(1,ar), & a(r+d)>1/2. \end{cases}$$

I.e., by using the scaling approach, we lose logarithmic terms at low frequencies.

A similar scaling approach can be used in order to prove a lifting lemma for the case when the boundary data is orthogonal to the space $\mathcal{V}_0^\varepsilon$.

LEMMA 4.10 (Lifting lemma for elements of $H^{1/2}_*(\mathcal{C}_r)$). *Given $a, r > 0$, $g^r \in H^{1/2}_*(\mathcal{C}_r)$, let $V^r \in H^1(\mathbb{R}^2)$ satisfy the interior boundary value problem*

$$-\Delta V^r + a^2 V^r = 0 \text{ in } B(0,r), \quad \gamma_0^- V^r = g^r,$$

and the exterior boundary value problem

$$-\Delta V^r + a^2 V^r = 0 \text{ in } B^c(0,r), \quad \gamma_0^+ V^r = g^r.$$

Then, for all $d > 0$, V^r satisfies the following bounds:

$$\|V^r\|^2_{a,B(0,r+d)} \lesssim \max(1,ar)\|g^r\|^2_{H^{1/2}(\mathcal{C}_r)}, \tag{4.8}$$

$$\|V^r\|^2_{L^2(B_{r,r+d})} \lesssim rd\|g^r\|^2_{H^{1/2}(\mathcal{C}_r)}. \tag{4.9}$$

Proof. Provided that $g^r = \sum_{m\in\mathbb{Z}\setminus\{0\}} g^r_m \mathrm{e}^{im\theta}$, the solution to the above BVPs can be written explicitly:

$$V^r(\rho,\theta) = \sum_{m\in\mathbb{Z}\setminus\{0\}} v^r_m(\rho)\mathrm{e}^{im\theta}, \quad v^r_m(\rho) = \begin{cases} \frac{I_{|m|}(a\rho)}{I_{|m|}(ar)} g^r_m \mathrm{e}^{im\theta}, & \rho < r, \\ \frac{K_{|m|}(a\rho)}{K_{|m|}(ar)} g^r_m \mathrm{e}^{im\theta}, & \rho > r. \end{cases} \tag{4.10}$$

Proof of the bound (4.9). We start by bounding $\|v^r_m\|^2_{L^2(B_{r,r+d})}$. With Lemma C.3, for $m \geq 1$, we have

$$\int_r^{r+d} \left|\frac{K_m(a\rho)}{K_m(ar)}\right|^2 \rho d\rho \lesssim r^{2m} \int_r^{r+d} \rho^{-2m+1} d\rho \lesssim rd.$$

From the definition of $V^r(\rho,\theta)$, it is straightforward to see that

$$\|V^r\|^2_{L^2(B_{r,r+d})} \lesssim rd \sum_{m\in\mathbb{Z}\setminus\{0\}} |g^r_m|^2 \lesssim rd \sum_{m\in\mathbb{Z}\setminus\{0\}} |m||g^r_m|^2 \lesssim rd\|g^r\|^2_{H^{1/2}(\mathcal{C}^r)}.$$

Proof of the bound (4.8). For the same reason as in the proof of Lemma 4.9, we will use the scaling argument to prove (4.8), see also Remark 7 below. Again, we will bound $\|V^r\|^2_{a,B(0,r+d)} \lesssim \|V^r\|^2_{a,\mathbb{R}^2}$.

First of all, let us introduce $g^1(\boldsymbol{x}) := g^r(r\boldsymbol{x})$, for $\boldsymbol{x} \in \mathcal{C}_1$. Let $V^1(\rho, b) \in H^1(\mathbb{R}^2)$ be a solution to the following exterior and interior problems:

$$\begin{aligned} &-\Delta V^1 + b^2 V^1 = 0 \text{ in } B(0,1), \quad \gamma_0^- V^1 = g^1, \\ &-\Delta V^1 + b^2 V^1 = 0 \text{ in } B^c(0,1), \quad \gamma_0^+ V^1 = g^1. \end{aligned}$$

Again, by a scaling argument, one can verify that $V^r(\rho, a) = V^1(\frac{\rho}{r}, ar)$, and one has the norm identity (4.7). It remains to use Proposition 4.8 which yields

$$\|V^r(.,a)\|^2_{a,\mathcal{O}_r} \leq C\max(1,ar)\|g^1\|^2_{H^{1/2}(\mathcal{C}_1)}. \tag{4.11}$$

Here the constant C is independent of r, but encodes some information about the circular shape of the scatterer. The functions g^1, g^r are defined by their Fourier series, for $\boldsymbol{x} = (\cos\theta, \sin\theta)$,

$$g^1(\boldsymbol{x}) = g^r(r\boldsymbol{x}) = \sum_{m\in\mathbb{Z}\setminus\{0\}} g^1_m \mathrm{e}^{im\theta} = \sum_{m\in\mathbb{Z}\setminus\{0\}} g^r_m \mathrm{e}^{im\theta}.$$

We remark that

$$\begin{aligned}\|g^1\|^2_{H^{1/2}(\mathcal{C}_1)} &= \sum_{m\in\mathbb{Z}\setminus\{0\}} (1+m^2)^{1/2}|g^1_m|^2 \le 2\sum_{m\in\mathbb{Z}\setminus\{0\}} |m||g^1_m|^2 \\ &\le 2r\sum_{m\in\mathbb{Z}} (1+\frac{m^2}{r^2})^{1/2}|g^r_m|^2 = \|g^r\|^2_{H^{1/2}(\mathcal{C}_r)},\end{aligned}$$

which, with (4.11), yields the desired inequality. ∎

Remark 7. *Unlike for Lemma 4.9, the direct estimates by bounding modified Hankel and Bessel functions did not improve over the straightforward scaling bound.*

Before proving the lifting lemma for multiple circles, let us introduce an auxiliary truncation function.

Preliminaries: an auxiliary truncation function. In what follows, we will extensively use the following truncation function. Let

$$\chi_{r,d}(\rho) = \begin{cases} 1, & \rho \in [r, r+d/4), \\ 0, & \rho > r + d/2, \\ p_{r,d}(\rho), & \text{otherwise}, \end{cases} \tag{4.12}$$

with $p_{r,d} = \sum_{k=0}^{7} a_k(\rho - r - d/2)^k$, with the coefficients a_k chosen so that $\chi_{r,d} \in C^3(\mathbb{R}_{\ge 0})$. One can verify that $a_k = c_k/d^k$ (with some c_k independent of d and r), for $k \ge 4$, and $a_3 = a_2 = a_1 = a_0 = 0$. We then introduce

$$\chi^\varepsilon_n(\boldsymbol{x}) := \chi_{r^\varepsilon_n, \underline{d^\varepsilon_*}}(\|\boldsymbol{x} - \boldsymbol{c}_n\|), \quad \chi^\varepsilon(\boldsymbol{x}) := \sum_{n\in\mathcal{N}} \chi^\varepsilon_n(\boldsymbol{x}). \tag{4.13}$$

With this definition,

$$\operatorname{supp}\chi^\varepsilon_n \cap \operatorname{supp}\chi^\varepsilon_k = \emptyset, \quad \text{if } n \ne k, \tag{4.14}$$

$$\operatorname{supp}\chi^\varepsilon_n \subseteq \overline{B}(\boldsymbol{c}_n, r^\varepsilon_n + \underline{d^\varepsilon_*}/2). \tag{4.15}$$

It is then straightforward to see that

$$\|\chi^\varepsilon\|_{L^\infty(\mathbb{R}^2)} \lesssim 1, \quad \|\chi^\varepsilon\|_{W^{s,\infty}(\mathbb{R}^2)} \lesssim \left(\underline{d^\varepsilon_*}\right)^{-s}, \quad s \ge 0. \tag{4.16}$$

Lifting lemma for multiple scatterers. The two lifting lemmas and the definition of the truncation function enable us to prove the following proposition.

Proposition 4.11 (Lifting lemma for multiple scatterers). *Let $a > 0$, $\boldsymbol{\lambda} \in H^{1/2}(\Gamma^\varepsilon)$, and $\Lambda^\varepsilon \in H^1(\mathbb{R}^2)$ satisfy the following two boundary-value problems:*

$$\begin{aligned} &-\Delta\Lambda^\varepsilon + a^2\Lambda^\varepsilon = 0 \text{ in } \Omega^\varepsilon, \quad \gamma_0^-\Lambda^\varepsilon = \boldsymbol{\lambda}, \\ &-\Delta\Lambda^\varepsilon + a^2\Lambda^\varepsilon = 0 \text{ in } \Omega^{\varepsilon,c}, \quad \gamma_0^+\Lambda^\varepsilon = \boldsymbol{\lambda}. \end{aligned}$$

Let us define

$$C_0(\varepsilon, d^\varepsilon_*) := 1 + \frac{\varepsilon}{\underline{d^\varepsilon_*}}. \tag{4.17}$$

If $\boldsymbol{\lambda} \in \mathcal{V}_0^\varepsilon$, then, with a constant $c_{m,0}$ depending polynomially on R_*^{-1} and R^*,

$$\|\Lambda^\varepsilon\|^2_{a,\mathbb{R}^2} \le c_{m,0}\varepsilon^{-1}\max(1,\varepsilon a)C_0(\varepsilon, d_*^\varepsilon)\|\boldsymbol{\lambda}\|^2_{H^{1/2}(\Gamma^\varepsilon)}.$$

If $\boldsymbol{\lambda} \in H_*^{1/2}(\Gamma^\varepsilon)$, then, with a constant $c_{m,\perp}$ depending polynomially on R_*^{-1} and R^*,

$$\|\Lambda^\varepsilon\|^2_{a,\mathbb{R}^2} \le c_{m,\perp}\max(1,\varepsilon a)C_0(\varepsilon, d_*^\varepsilon)\|\boldsymbol{\lambda}\|^2_{H^{1/2}(\Gamma^\varepsilon)}.$$

REMARK 8. *The index 'm' in $c_{m,0}$, $c_{m,\perp}$ stands for 'multiple'.*

Proof. First of all, we remark that $\Lambda^\varepsilon = \arg\min_{v\in H^1(\mathbb{R}^2):\,\gamma_0^\pm v=\boldsymbol{\lambda}} \|v\|_{a,\mathbb{R}^2}$. Therefore, in order to bound $\|\Lambda^\varepsilon\|_{a,\mathbb{R}^2}$, we can construct a lifting $v \in H^1(\mathbb{R}^2)$ of $\boldsymbol{\lambda}$, obtain an explicit stability bound $\|v\|_{a,\mathbb{R}^2} \le C_\varepsilon\|\boldsymbol{\lambda}\|_{H^{1/2}(\Gamma^\varepsilon)}$, and conclude that $\|\Lambda^\varepsilon\|_{a,\mathbb{R}^2} \le C_\varepsilon\|\boldsymbol{\lambda}\|_{H^{1/2}(\Gamma^\varepsilon)}$. Let us define the following lifting of $\boldsymbol{\lambda}$ (where χ_n^ε are as in (4.13)):

$$\Lambda_\chi^\varepsilon := \sum_{n\in\mathcal{N}} \Lambda_n^\varepsilon \chi_n^\varepsilon,$$

where each $\Lambda_n^\varepsilon \in H^1(\mathbb{R}^2)$ solves the following exterior and interior boundary value problems, with $\lambda_n \in H^{1/2}(\Gamma_n^\varepsilon)$,

$$\begin{aligned} -\Delta\Lambda_n^\varepsilon + a\,\Lambda_n^\varepsilon = 0 \text{ in } \Omega_n^\varepsilon, \quad \gamma_0^-\Lambda_n^\varepsilon = \lambda_n,\\ -\Delta\Lambda_n^\varepsilon + a\,\Lambda_n^\varepsilon = 0 \text{ in } \Omega_n^{\varepsilon,c}, \quad \gamma_0^+\Lambda_n^\varepsilon = \lambda_n. \end{aligned} \tag{4.18}$$

We next relate $\|\Lambda_\chi^\varepsilon\|^2_{a,\mathbb{R}^2}$ to the norms $\|\Lambda_n^\varepsilon\|^2_{a,\mathbb{R}^2}$, which we will bound based on Lemmas 4.9, 4.10. By definition,

$$\|\Lambda_\chi^\varepsilon\|^2_{a,\mathbb{R}^2} = a^2\|\sum_{n\in\mathcal{N}}\chi_n^\varepsilon\Lambda_n^\varepsilon\|^2 + \|\sum_{n\in\mathcal{N}}\chi_n^\varepsilon\nabla\Lambda_n^\varepsilon\|^2 + \|\sum_{n\in\mathcal{N}}\nabla\chi_n^\varepsilon\Lambda_n^\varepsilon\|^2.$$

By the property (4.14), we have that

$$\begin{aligned} \|\Lambda_\chi^\varepsilon\|^2_{a,\mathbb{R}^2} &= a^2\sum_{n\in\mathcal{N}}\|\chi_n^\varepsilon\Lambda_n^\varepsilon\|^2 + \sum_{n\in\mathcal{N}}\|\chi_n^\varepsilon\nabla\Lambda_n^\varepsilon\|^2 + \sum_{n\in\mathcal{N}}\|\nabla\chi_n^\varepsilon\Lambda_n^\varepsilon\|^2\\ &\le \sum_{n\in\mathcal{N}}\|\chi_n^\varepsilon\|^2_{L^\infty}\|\Lambda_n^\varepsilon\|^2_{a,\operatorname{supp}\chi_n^\varepsilon} + \sum_{n\in\mathcal{N}}\|\nabla\chi_n^\varepsilon\|^2_{L^\infty}\|\Lambda_n^\varepsilon\|^2_{\operatorname{supp}\nabla\chi_n^\varepsilon}\\ &\overset{(4.14)}{=} \|\chi^\varepsilon\|^2_{L^\infty}\sum_{n\in\mathcal{N}}\|\Lambda_n^\varepsilon\|^2_{a,\operatorname{supp}\chi_n^\varepsilon} + \|\nabla\chi^\varepsilon\|^2_{L^\infty}\sum_{n\in\mathcal{N}}\|\Lambda_n^\varepsilon\|^2_{\operatorname{supp}\nabla\chi_n^\varepsilon}\\ &\overset{(4.16)}{\lesssim} \sum_{n\in\mathcal{N}}\|\Lambda_n^\varepsilon\|^2_{a,\operatorname{supp}\chi_n^\varepsilon} + (\underline{d_*^\varepsilon})^{-2}\sum_{n\in\mathcal{N}}\|\Lambda_n^\varepsilon\|^2_{\operatorname{supp}\nabla\chi_n^\varepsilon}. \end{aligned} \tag{4.19}$$

It remains to bound all the above quantities, by recalling that, see (4.15), $\operatorname{supp}\nabla\chi_n^\varepsilon \subset \overline{B(\boldsymbol{c}_n, r_n^\varepsilon + \underline{d_*^\varepsilon}/2)}\setminus B(\boldsymbol{c}_n, r_n^\varepsilon)$. We consider two cases: $\boldsymbol{\lambda} \in \mathcal{V}_0^\varepsilon$ and $\boldsymbol{\lambda} \in H_*^{1/2}(\Gamma^\varepsilon)$.

Case 1. Bounds for $\boldsymbol{\lambda} \in \mathcal{V}_0^\varepsilon$. A straightforward application of Lemma 4.9 yields

$$\|\Lambda_\chi^\varepsilon\|^2_{a,\mathbb{R}^2} \lesssim \sum_{n=1}^N \max(1, ar_n^\varepsilon)|\lambda_{n,0}|^2 + (\underline{d_*^\varepsilon})^{-2}\sum_{n=1}^N \underline{d_*^\varepsilon}(r_n^\varepsilon + \underline{d_*^\varepsilon})|\lambda_{n,0}|^2.$$

Because $\|\boldsymbol{\lambda}\|^2_{H^{1/2}(\Gamma^\varepsilon)} = 2\pi\sum_{n\in\mathcal{N}} r_n^\varepsilon|\lambda_{n,0}|^2$, we have the following bound, with a constant $C_1 > 0$ depending on R_*^{-1} and R^* polynomially:

$$\|\Lambda_\chi^\varepsilon\|^2_{a,\mathbb{R}^2} \le C_1\varepsilon^{-1}\left(\max(1,\varepsilon a) + \frac{\varepsilon}{\underline{d_*^\varepsilon}} + 1\right)\|\boldsymbol{\lambda}\|^2_{H^{1/2}(\Gamma^\varepsilon)}.$$

By bounding $1 \leq \max(1, a\varepsilon)$, the bound of the proposition follows straightforwardly from the above.

Case 2. Bounds for $\boldsymbol{\lambda} \in H_*^{1/2}(\Gamma^\varepsilon)$. An application of bounds of Lemma 4.10 to bound the right-hand side of the inequality (4.19) yields the following bound, with a constant C_2 depending on on R_*^{-1} and R^* polynomially:

$$\|\Lambda_\chi^\varepsilon\|^2_{a,\mathbb{R}^2} \leq C_2 \left(\max(1, \varepsilon a) + \frac{\varepsilon}{d_*^\varepsilon} \right) \|\boldsymbol{\lambda}\|^2_{H^{1/2}(\Gamma^\varepsilon)}. \qquad \square$$

The bound in the statement of the proposition is then obtained like in Case 1.

4.4.2. An estimate on $\|\big(\hat{\mathbb{S}}_{00}^\varepsilon\big)^{-1}\|$. To obtain the operator norm estimates, we will need some auxiliary notation.

Auxiliary notation. We define a normal to Ω^ε so that points into the exterior of Ω^ε. Given a function $\phi \in H^1(\mathbb{R}^2 \setminus \Gamma^\varepsilon)$, we define by $\gamma_0^+\phi$ and $\gamma_1^+\phi$ its exterior trace and its exterior normal trace, by $\gamma_0^-\phi$ and $\gamma_1^-\phi$ its interior traces, and by $[\gamma_0\phi]$, $[\gamma_1\phi]$ the respective jumps:

$$[\gamma_0\phi] = \gamma_0^-\phi - \gamma_0^+\phi, \quad [\gamma_1\phi] = \gamma_1^-\phi - \gamma_1^+\phi.$$

Estimate on the operator norm. Given $\boldsymbol{\eta} \in H^{1/2}(\Gamma^\varepsilon)$, we denote $v_\eta^\varepsilon := \hat{\mathcal{S}}^\varepsilon\boldsymbol{\eta} \in H^1(\mathbb{R}^2)$. We remark that v_η^ε solves the following transmission problem:

$$\begin{aligned} &-\Delta v_\eta^\varepsilon - \omega^2 v_\eta^\varepsilon = 0 \text{ in } \mathbb{R}^2 \setminus \Gamma^\varepsilon, \\ &[\gamma_0 v_\eta^\varepsilon] = 0, \quad [\gamma_1 v_\eta^\varepsilon] = \boldsymbol{\eta}, \end{aligned} \tag{4.20}$$

and, moreover, $\gamma_0 v_\eta^\varepsilon = \hat{\mathbb{S}}^\varepsilon\boldsymbol{\eta}$.

THEOREM 4.12. *Let $\omega \in \mathbb{C}^+$. The operator $\hat{\mathbb{S}}_{00}^\varepsilon : \mathcal{V}_0^\varepsilon \to \mathcal{V}_0^\varepsilon$ satisfies, with a constant $c_{m,0}$ as in Proposition 4.11,*

$$\|\big(\hat{\mathbb{S}}_{00}^\varepsilon\big)^{-1}\| \leq c_{m,0} \frac{|\omega|}{\operatorname{Im}\omega} C_0(\varepsilon, d_*^\varepsilon) \varepsilon^{-1} \max(1, \varepsilon|\omega|).$$

Proof. As usual in the theory of time-domain boundary integal equations, we will prove a coercivity bound on $\hat{\mathbb{S}}_{00}^\varepsilon$, cf. [2]. Let $\boldsymbol{\eta} \in \mathcal{V}_0^\varepsilon$. Then

$$\mathbb{P}_0^\varepsilon \gamma_0 v_\eta^\varepsilon = \mathbb{P}_0^\varepsilon \hat{\mathbb{S}}^\varepsilon \mathbb{P}_0^{\varepsilon,*} \boldsymbol{\eta} = \hat{\mathbb{S}}_{00}^\varepsilon \boldsymbol{\eta}.$$

Therefore, since $\boldsymbol{\eta} \in \mathcal{V}_0^\varepsilon$,

$$\langle \boldsymbol{\eta}, \overline{\hat{\mathbb{S}}^\varepsilon\boldsymbol{\eta}} \rangle = \langle \boldsymbol{\eta}, \overline{\hat{\mathbb{S}}_{00}^\varepsilon\boldsymbol{\eta}} \rangle.$$

Hence,

$$-\operatorname{Im}\langle \boldsymbol{\eta}, \overline{\omega\hat{\mathbb{S}}_{00}^\varepsilon\boldsymbol{\eta}} \rangle = -\langle \boldsymbol{\eta}, \overline{\omega\hat{\mathbb{S}}^\varepsilon\boldsymbol{\eta}} \rangle = \operatorname{Im}\omega \|v_\eta^\varepsilon\|^2_{|\omega|,\mathbb{R}^2}, \tag{4.21}$$

where the last identity holds because of the Green formula. Next, we need to obtain an upper bound on $\boldsymbol{\eta}$ in terms of v_η^ε, which is done in a classical way:

$$\|\boldsymbol{\eta}\|_{H^{-1/2}(\Gamma^\varepsilon)} = \sup_{\boldsymbol{\lambda} \in \mathcal{V}_0^\varepsilon \setminus \{0\}} \frac{\langle \boldsymbol{\eta}, \overline{\boldsymbol{\lambda}} \rangle}{\|\boldsymbol{\lambda}\|_{H^{-1/2}(\Gamma^\varepsilon)}} = \sup_{\boldsymbol{\lambda} \in \mathcal{V}_0^\varepsilon \setminus \{0\}} \inf_{\substack{\Lambda \in H^1(\mathbb{R}^2): \\ \gamma_0\Lambda = \boldsymbol{\lambda}}} \frac{\langle \boldsymbol{\eta}, \overline{\gamma_0\Lambda} \rangle}{\|\boldsymbol{\lambda}\|_{H^{-1/2}(\Gamma^\varepsilon)}}.$$

By the Green identity,

$$\langle \boldsymbol{\eta}, \overline{\gamma_0\Lambda} \rangle = -\int_{\mathbb{R}^2} \nabla v_\eta^\varepsilon \overline{\nabla\Lambda}\, d\boldsymbol{x} - \omega^2 \int_{\mathbb{R}^2} v_\eta^\varepsilon \overline{\Lambda}\, d\boldsymbol{x}.$$

Then

$$\|\boldsymbol{\eta}\|_{H^{-1/2}(\Gamma^\varepsilon)} \le \|v_\eta^\varepsilon\|_{|\omega|,\mathbb{R}^2} \sup_{\boldsymbol{\lambda}\in\mathcal{V}_0^\varepsilon\setminus\{0\}} \inf_{\substack{\Lambda\in H^1(\mathbb{R}^2):\\ \gamma_0\Lambda=\boldsymbol{\lambda}}} \frac{\|\Lambda\|_{|\omega|,\mathbb{R}^2}}{\|\boldsymbol{\lambda}\|_{H^{-1/2}(\Gamma^\varepsilon)}}. \tag{4.22}$$

The $\inf_{\Lambda\in H^1(\mathbb{R}^2):\,\gamma_0\Lambda=\boldsymbol{\lambda}} \frac{\|\Lambda\|_{|\omega|,\mathbb{R}^2}}{\|\boldsymbol{\lambda}\|_{H^{-1/2}(\Gamma^\varepsilon)}}$ is realized for $\Lambda=\Lambda^\varepsilon$, where Λ^ε is from Proposition 4.11, with $a=|\omega|$. With the notation of Proposition 4.11, we obtain

$$\|\boldsymbol{\eta}\|^2_{H^{-1/2}(\Gamma^\varepsilon)} \le c_{m,0}\varepsilon^{-1}\max(1,\varepsilon|\omega|)C_0(\varepsilon,d_*^\varepsilon)\|v_\eta^\varepsilon\|^2_{|\omega|,\mathbb{R}^2}.$$

Therefore, from (4.21) and the above, we obtain the coercivity bound

$$-\operatorname{Im}\langle\boldsymbol{\eta},\overline{\omega\hat{\mathbb{S}}^\varepsilon_{00}\boldsymbol{\eta}}\rangle \ge \varepsilon\, c_{m,0}^{-1}\,\min(1,(\varepsilon|\omega|)^{-1})\,\operatorname{Im}\omega\, C_0^{-1}(\varepsilon,d_*^\varepsilon)\|\boldsymbol{\eta}\|^2_{H^{-1/2}(\Gamma^\varepsilon)},$$

and the bound for the inverse $\left(\hat{\mathbb{S}}^\varepsilon_{00}\right)^{-1}$ stated in the theorem follows from the above. ∎

4.4.3. An estimate on $\|\mathbb{P}_\perp^{\varepsilon,*}(\hat{\mathbb{S}}^\varepsilon)^{-1}\mathbb{P}_\perp^\varepsilon\|$. In the theorem below we show that $\|\mathbb{P}_\perp^{\varepsilon,*}(\hat{\mathbb{S}}^\varepsilon)^{-1}\mathbb{P}_\perp^\varepsilon\| = O(1)$, and thus this term does not have an effect on the asymptotic error estimate.

Theorem 4.13. *Let $\omega\in\mathbb{C}^+$. The operator $\hat{\mathbb{S}}^\varepsilon : H^{-1/2}(\Gamma^\varepsilon)\to H^{1/2}(\Gamma^\varepsilon)$ satisfies, with $c_{m,\perp}$ like in Proposition 4.11,*

$$\|\mathbb{P}_\perp^{\varepsilon,*}(\hat{\mathbb{S}}^\varepsilon)^{-1}\mathbb{P}_\perp^\varepsilon\| \le c_{m,\perp}\frac{|\omega|}{\operatorname{Im}\omega}C_0(\varepsilon,d_*^\varepsilon)\max(1,\varepsilon|\omega|).$$

Proof. Let $\boldsymbol{\lambda}\in H_*^{1/2}(\Gamma^\varepsilon)$, and $\boldsymbol{\eta}=(\hat{\mathbb{S}}^\varepsilon)^{-1}\boldsymbol{\lambda}\equiv(\hat{\mathbb{S}}^\varepsilon)^{-1}\mathbb{P}_\perp^\varepsilon\boldsymbol{\lambda}$. Our goal is to find an estimate on $\boldsymbol{\eta}_\perp=\mathbb{P}_\perp^{\varepsilon,*}(\hat{\mathbb{S}}^\varepsilon)^{-1}\mathbb{P}_\perp^\varepsilon\boldsymbol{\lambda}$ by $\boldsymbol{\lambda}$. For this we remark that

$$\langle\boldsymbol{\eta},\overline{\hat{\mathbb{S}}^\varepsilon\boldsymbol{\eta}}\rangle=\langle\boldsymbol{\eta},\overline{\boldsymbol{\lambda}}\rangle=\langle\boldsymbol{\eta}_\perp,\overline{\boldsymbol{\lambda}}\rangle,$$

because $\boldsymbol{\lambda}\in H_*^{1/2}(\Gamma^\varepsilon)$. We proceed now like in the proof of Theorem 4.12. We define $v_\eta^\varepsilon:=\hat{\mathcal{S}}^\varepsilon\boldsymbol{\eta}\in H^1(\mathbb{R}^2)$ the solution to the transmission problem (4.20). The Green identity yields

$$-\operatorname{Im}\langle\boldsymbol{\eta}_\perp,\overline{\omega\boldsymbol{\lambda}}\rangle=\operatorname{Im}\omega\|v_\eta^\varepsilon\|^2_{|\omega|,\mathbb{R}^2}.$$

It remains to estimate $\boldsymbol{\eta}_\perp$ by $\|v_\eta^\varepsilon\|_{|\omega|,\mathbb{R}^2}$, like in (4.22):

$$\|\boldsymbol{\eta}_\perp\| \le \|v_\eta^\varepsilon\|_{|\omega|,H^1(\mathbb{R}^2)} \sup_{\boldsymbol{\lambda}\in H_*^{1/2}(\Gamma^\varepsilon)\setminus\{0\}} \inf_{\substack{\Lambda\in H^1(\mathbb{R}^2):\\ \gamma_0\Lambda=\boldsymbol{\lambda}}} \frac{\|\Lambda\|_{|\omega|,\mathbb{R}^2}}{\|\boldsymbol{\lambda}\|}.$$

The desired estimate again follows from Proposition 4.11. We have

$$-\operatorname{Im}\langle\boldsymbol{\eta}_\perp,\overline{\omega\boldsymbol{\lambda}}\rangle \ge c_{m,\perp}^{-1}\operatorname{Im}\omega\min(1,(\varepsilon|\omega|)^{-1})C_0^{-1}(\varepsilon,d_*^\varepsilon)\|\boldsymbol{\eta}_\perp\|^2_{H^{-1/2}(\Gamma^\varepsilon)},$$

which yields the estimate in the statement of the theorem. ∎

4.4.4. An estimate on $\|\hat{\mathbb{S}}^\varepsilon_{0\perp}\|$ and $\|\hat{\mathbb{S}}^\varepsilon_{\perp 0}\|$. The upper bounds on the norms of these operators will be obtained in a different manner compared to the proofs of Theorems 4.12 and 4.13. The first result shows that it is sufficient to obtain a bound on either of the norms $\|\hat{\mathbb{S}}^\varepsilon_{0\perp}\|$ or $\|\hat{\mathbb{S}}^\varepsilon_{\perp 0}\|$.

Proposition 4.14. $\|\hat{\mathbb{S}}^\varepsilon_{\perp 0}\|=\|\hat{\mathbb{S}}^\varepsilon_{0\perp}\|$.

Proof. We start with

$$\|\hat{\mathbb{S}}^\varepsilon_{0\perp}\| = \sup_{\boldsymbol{\mu}\in\mathcal{V}^\varepsilon_0}\sup_{\boldsymbol{\lambda}\in H^{-1/2}_*(\Gamma^\varepsilon)} \frac{\langle \boldsymbol{\mu}, \hat{\mathbb{S}}^\varepsilon\boldsymbol{\lambda}\rangle}{\|\boldsymbol{\lambda}\|_{H^{-1/2}(\Gamma^\varepsilon)}\|\boldsymbol{\mu}\|_{H^{-1/2}(\Gamma^\varepsilon)}},$$
$$\|\hat{\mathbb{S}}^\varepsilon_{\perp 0}\| = \sup_{\boldsymbol{\mu}\in\mathcal{V}^\varepsilon_0}\sup_{\boldsymbol{\lambda}\in H^{-1/2}_*(\Gamma^\varepsilon)} \frac{\langle \boldsymbol{\lambda}, \hat{\mathbb{S}}^\varepsilon\boldsymbol{\mu}\rangle}{\|\boldsymbol{\lambda}\|_{H^{-1/2}(\Gamma^\varepsilon)}\|\boldsymbol{\mu}\|_{H^{-1/2}(\Gamma^\varepsilon)}}.$$

With the notation like in (4.20), third Green's identity yields

$$\langle \boldsymbol{\mu}, \hat{\mathbb{S}}^\varepsilon\boldsymbol{\lambda}\rangle - \langle \boldsymbol{\lambda}, \hat{\mathbb{S}}^\varepsilon\boldsymbol{\mu}\rangle = -\int_{\mathbb{R}^2\setminus\Gamma^\varepsilon}(\Delta v^\varepsilon_\mu - \omega^2 v^\varepsilon_\mu)v^\varepsilon_\lambda + \int_{\mathbb{R}^2\setminus\Gamma^\varepsilon}(\Delta v^\varepsilon_\lambda - \omega^2 v^\varepsilon_\lambda)v^\varepsilon_\mu = 0,$$

and hence the desired result. ∎

Before proving the main theorem of this section, let us state an auxiliary lemma, which we will use also later.

LEMMA 4.15. *Let $\omega\in\mathbb{C}^+$, $r>0$, and the point $\boldsymbol{x}\in B^c(0,r)$ be such that $\operatorname{dist}(\boldsymbol{x}, B(0,r)) = d$. Let $h:\mathcal{C}_r\to\mathbb{C}$ be defined by $h(\boldsymbol{y}) = \mathcal{G}_\omega(\boldsymbol{y}-\boldsymbol{x})$. Then the following bounds hold true:*

$$\|h\|_{L^2(\mathcal{C}_r)} \lesssim r^{1/2}\min\left(\max\left(1, \log\frac{1}{d\operatorname{Im}\omega}\right), |\omega d|^{-1/2}\right),$$
$$\|h_\perp\|_{H^{1/2}(\mathcal{C}_r)} \lesssim r\max(1, r^{1/2})d^{-1}\max(1, |\omega d|^{1/2}).$$

Proof. Evidently, $\|h\|^2_{L^2(\mathcal{C}_r)} \lesssim \|h\|^2_{L^\infty(\mathcal{C}_r)} r$. For all $\boldsymbol{y}\in C_r$, the function $\omega\mapsto\mathcal{G}_\omega(\boldsymbol{y})$ is analytic in $\omega\in\mathbb{C}^+$ and its restriction to $\mathbb{C}^+$ is continuous to $\mathbb{R}\setminus\{0\}$. Therefore, we make use of the following bound that stems from the asymptotic behaviour of the Hankel functions for $\omega\in\mathbb{C}^+$, when $\omega\to 0$ and when $|\omega|\to+\infty$, cf. [14, Section 10.8, Section 10.17]:

$$|h(\boldsymbol{y})| \lesssim \min\left(\max\left(1, \log\frac{1}{|\omega|\|\boldsymbol{x}-\boldsymbol{y}\|}\right), \frac{1}{|\omega|^{1/2}\|\boldsymbol{x}-\boldsymbol{y}\|^{1/2}}\right).$$

To obtain the desired bound we use $\operatorname{Im}\omega < |\omega|$.

To compute $\|h_\perp\|_{H^{1/2}(\mathcal{C}_r)}$, we proceed as follows: first of all,

$$\|h_\perp\|^2_{L^2(\mathcal{C}_r)} = \inf_{c\in\mathbb{C}}\|h-c\| \le \|\mathcal{G}_\omega(.-\boldsymbol{x}) - \mathcal{G}_\omega(-\boldsymbol{x})\|^2_{L^2(\mathcal{C}_r)}$$
$$\lesssim \|\nabla\mathcal{G}_\omega(.-\boldsymbol{x})\|^2_{L^\infty(B(0,r))}r^3.$$

Because $\frac{d}{dz}H^{(0)}_0(z) = -H^{(0)}_1(z)$,

$$|\nabla_{\boldsymbol{y}}\mathcal{G}_\omega(\boldsymbol{y}-\boldsymbol{x})| \lesssim |\omega||H^{(1)}_1(\omega\|\boldsymbol{y}-\boldsymbol{x}\|)| \lesssim |\omega|\max\left(\frac{1}{|\omega|\|\boldsymbol{y}-\boldsymbol{x}\|}, \frac{1}{\sqrt{|\omega\|\boldsymbol{y}-\boldsymbol{x}\|}}\right),$$

and we again used the fact that the restriction $z\mapsto H^{(1)}_1(z)$ to $\mathbb{C}^+$ is analytic, and continuous to $\mathbb{R}\setminus\{0\}$, in order to obtain the above bound from its asymptotics, cf. [14, Section 10.8, Section 10.17]. This finally yields

$$\|h_\perp\|^2_{L^2(\mathcal{C}_r)} \lesssim r^3d^{-2}\max(1, |\omega|d).$$

Next, to obtain a complete bound for $\|h_\perp\|_{H^{1/2}(\mathcal{C}_r)}$, it remains to compute its Sobolev-Slobodeckii seminorm, where we again use the Lipschitz regularity of h:

$$\|h_\perp\|^2_{\mathcal{H}^{1/2}(\mathcal{C}_r)} = \int_{\mathcal{C}_r}\int_{\mathcal{C}_r}\frac{|h(\boldsymbol{y})-h(\boldsymbol{y}')|^2}{\|\boldsymbol{y}-\boldsymbol{y}'\|^2}d\Gamma_{\boldsymbol{y}}d\Gamma_{\boldsymbol{y}'} \lesssim r^2d^{-2}\max(1, |\omega|d).$$

∎

Finally we have all the necessary results to formulate and prove the principal result of this section.

THEOREM 4.16. *Let $\omega \in \mathbb{C}^+$. Then the following bound holds for all $\varepsilon > 0$, with a constant $C_{0\perp}$ depending on R_*^{-1} and R^* polynomially:*

$$\|\hat{\mathbb{S}}^\varepsilon_{\perp 0}\| = \|\hat{\mathbb{S}}^\varepsilon_{0\perp}\| \le C_{0\perp}\varepsilon^{3/2} N(\underline{d}^\varepsilon_*)^{-1}|\omega| \max(1, (\operatorname{Im}\omega)^{-1}).$$

Proof. We use an explicit representation of $\hat{\mathbb{S}}^\varepsilon_{0\perp}$.

Let $\boldsymbol{\eta} = \hat{\mathbb{S}}^\varepsilon \boldsymbol{\lambda}$, with $\boldsymbol{\lambda} \in H_*^{-1/2}(\Gamma^\varepsilon)$. Our goal is to bound $\boldsymbol{\eta}_0$ by $\boldsymbol{\lambda}$; by the density argument it suffices to obtain the bound for $\boldsymbol{\lambda}$ sufficiently regular (e.g. $\boldsymbol{\lambda} \in C^0(\Gamma^\varepsilon)$). On Γ^ε_ℓ, it holds that

$$\eta_\ell = \hat{S}^\varepsilon_{\ell\ell}\lambda_\ell + \sum_{n\in\mathcal{N}\setminus\{\ell\}} \hat{\mathbb{S}}^\varepsilon_{\ell n}\lambda_n.$$

Since $\boldsymbol{\lambda} \in H_*^{-1/2}(\Gamma^\varepsilon)$, by (3.14) it follows that $\hat{\mathbb{S}}^\varepsilon_{\ell\ell}\lambda_\ell \in H_*^{1/2}(\Gamma^\varepsilon_\ell)$. Therefore, we have, after integrating both sides of the above over Γ^ε_ℓ,

$$r^\varepsilon_\ell \eta_{\ell,0} = \frac{1}{2\pi} \sum_{n\in\mathcal{N}\setminus\{\ell\}} \int_{\Gamma^\varepsilon_\ell}\int_{\Gamma^\varepsilon_n} \mathcal{G}_\omega(\boldsymbol{x}-\boldsymbol{y})\lambda_n(\boldsymbol{y}) d\Gamma_{\boldsymbol{y}}\, d\Gamma_{\boldsymbol{x}}.$$

It remains to use the definition of $\|\boldsymbol{\eta}_0\|^2_{L^2(\Gamma^\varepsilon)}$ and the Cauchy-Schwarz inequality:

$$\begin{aligned}\|\boldsymbol{\eta}_0\|^2_{L^2(\Gamma^\varepsilon)} &\lesssim \sum_{\ell\in\mathcal{N}} (r^\varepsilon_\ell)^{-1} \left| \sum_{n\in\mathcal{N}\setminus\{\ell\}} \iint\limits_{\Gamma^\varepsilon_\ell\times\Gamma^\varepsilon_n} \mathcal{G}_\omega(\boldsymbol{x}-\boldsymbol{y})\lambda_n(\boldsymbol{y}) d\Gamma_{\boldsymbol{y}} d\Gamma_{\boldsymbol{x}} \right|^2 \\ &\lesssim R_*^{-1}\varepsilon \sum_{\ell\in\mathcal{N}} \left| \sum_{n\in\mathcal{N}\setminus\{\ell\}} r^\varepsilon_\ell \sup_{\boldsymbol{x}\in\Gamma^\varepsilon_\ell} \left| \int_{\Gamma^\varepsilon_n} H_0(\omega\|\boldsymbol{x}-\boldsymbol{y}\|)\lambda_n(\boldsymbol{y}) d\Gamma_{\boldsymbol{y}} \right| \right|^2. \end{aligned} \tag{4.23}$$

We then use the bound of Lemma 4.15 to obtain, with C_1 depending polynomially on R^* and R_*^{-1}, for $\boldsymbol{x} \in \Gamma^\varepsilon_\ell$:

$$\left| \int_{\Gamma^\varepsilon_n} H_0(\omega\|\boldsymbol{x}-\boldsymbol{y}\|)\lambda_n(\boldsymbol{y}) d\Gamma_{\boldsymbol{y}} \right| \le C_1\varepsilon/d^\varepsilon_* \max(1, |\omega d^\varepsilon_*|^{1/2}) \|\lambda_n\|_{H_*^{-1/2}(\Gamma^\varepsilon_m)}.$$

The rest follows by the Cauchy-Schwarz inequality and by remarking that

$$\begin{aligned}(d^\varepsilon_*)^{-1}\max(1, |\omega d^\varepsilon_*|^{1/2}) &\le \max(1, (d^\varepsilon_*)^{-1})\max(1, |\omega|) \\ &\le \max(1, (d^\varepsilon_*)^{-1})|\omega|\max(1, (\operatorname{Im}\omega)^{-1}).\end{aligned}$$

∎

We have now finished with the proofs of auxiliary results, namely, the bounds on the data and the bounds on the operators. In the section that follows we will use these ingredients to prove Proposition 4.3 about convergence of the Galerkin approximation of the density, and next make use of its results in order to prove the principal statement of Section 4, namely Theorem 4.1.

4.5. Proof of Proposition 4.3. *Step 1. Stability bound for the density.* To obtain a time-domain bound on $\boldsymbol{\mu}^\varepsilon_G$, we proceed as follows.

First, we use the stability bounds provided in Theorem 4.12 in order to obtain a bound on $\|\hat{\boldsymbol{\mu}}^0_G\|_{-1/2}$ (recall that, cf. (4.1), $\hat{\boldsymbol{\mu}}^\varepsilon_G = (\hat{\mathbb{S}}^\varepsilon_{00})^{-1}\hat{\boldsymbol{g}}^\varepsilon_0$). Next we rewrite the obtained bound in the time domain, using the Plancherel identity. Next, we bound $\|\partial^k_t \boldsymbol{g}^\varepsilon_0\|_{1/2}$ by a certain ε-independent norm of u^{inc}, as stated in Section 4.3.

Step 1.1. Stability bound on the density in the frequency domain. With Theorem 4.12, we have the

following stability bound on the density in the frequency domain, with $C_G > 0$ depending polynomially on R_*^{-1}, R^*:

$$\|\hat{\boldsymbol{\mu}}_G^\varepsilon\|_{-1/2} \leq C_G \varepsilon^{-1} C_0(\varepsilon, d_*^\varepsilon) \max(1, \varepsilon|\omega|) \frac{|\omega|}{\operatorname{Im}\omega} \|\hat{\boldsymbol{g}}_0^\varepsilon\|_{1/2}, \quad \text{for all } \omega \in \mathbb{C}^+. \tag{4.24}$$

Step 1.2. Passing to the time-domain. Rewriting the bound (4.24) in the time domain is quite classical, and, e.g. can be found in the monograph [38], or [3], [5], see the references therein. For the convenience of the reader, we will outline the corresponding procedure below.

First of all, we remark that the function $\omega \mapsto \hat{\boldsymbol{\mu}}_G^\varepsilon(\omega)$ is $H^{-1/2}(\Gamma^\varepsilon)$-analytic in $\mathbb{C}^+$. This follows from the analyticity of $\omega \mapsto \hat{\mathbb{S}}_{00}^\varepsilon \in \mathcal{L}\left(H^{-1/2}(\Gamma^\varepsilon), H^{1/2}(\Gamma^\varepsilon)\right)$ and $\omega \mapsto \hat{\boldsymbol{g}}_0^\varepsilon \in H^{1/2}(\Gamma^\varepsilon)$. Moreover, the bound (4.24) indicates that, indeed, $\hat{\boldsymbol{\mu}}_G^\varepsilon$ is the Fourier-Laplace transform of a causal $\mathcal{V}_0^\varepsilon$-valued distribution (cf. [13]). Moreover, $\boldsymbol{\mu}_G^\varepsilon(t)$ vanishes with all its derivatives in the vicinity of 0 as a convolution of a causal operator-valued distribution $\mathbb{S}_{00}(\partial_t)$ with $\boldsymbol{g}_0^\varepsilon(t)$, which itself vanishes with all its derivatives in the vicinity of 0.

To translate the obtained frequency-domain bounds to the time-domain, we proceed as follows. Let $T > 0$. First, we use the Plancherel identity and the causality of $\boldsymbol{\mu}_G^\varepsilon$ to obtain the following inequality, valid for any $\eta > 0$,

$$\begin{aligned}\int_{\mathbb{R}^+} \mathrm{e}^{-2\eta t} \|\boldsymbol{\mu}_G^\varepsilon(t)\|_{-1/2}^2 dt = \frac{1}{2\pi} \int_{\mathbb{R}} \|\hat{\boldsymbol{\mu}}_G^\varepsilon(\omega + i\eta)\|_{-1/2}^2 d\omega \lesssim C_G^2 \varepsilon^{-2} C_0^2(\varepsilon, d_*^\varepsilon) \eta^{-2} \\ \times \int_{\mathbb{R}} (1 + \varepsilon^2 |\omega + i\eta|^2) |\omega + i\eta|^2 \|\hat{\boldsymbol{g}}_0^\varepsilon(\omega + i\eta)\|_{1/2}^2 d\omega,\end{aligned}$$

where C_G is like in Theorem 4.12, and the latter inequality was obtained from the bound of Theorem 4.12 by using $\max(a, b) \leq a + b$. Next, we bound in the above

$$(1 + \varepsilon^2 |\omega + i\eta|^2) \|\hat{\boldsymbol{g}}_0^\varepsilon(\omega + i\eta)\|_{1/2}^2 \leq \|(1 - i(\omega + i\eta)\varepsilon) \hat{\boldsymbol{g}}_0^\varepsilon(\omega + i\eta)\|_{1/2}^2,$$

which allows to apply the Plancherel identity again to the right-hand-side of the above inequality, in order to obtain a bound on $\boldsymbol{\mu}_G^\varepsilon$ by $\boldsymbol{g}_0^\varepsilon$, rather than its Fourier-Laplace transform. In particular, recalling that $\boldsymbol{g}_0^\varepsilon$ vanishes with all its derivatives in the vicinity of 0, and choosing $\eta = \frac{1}{T}$ yields the following bound

$$\begin{aligned}\int_{\mathbb{R}^+} \mathrm{e}^{-2t/T} \|\boldsymbol{\mu}_G^\varepsilon(t)\|_{-1/2}^2 dt \lesssim C_G^2 C_0^2(\varepsilon, d_*^\varepsilon) \varepsilon^{-2} T^2 \\ \times \int_{\mathbb{R}^+} \mathrm{e}^{-2t/T} \|(1 + \varepsilon\partial_t) \partial_t \boldsymbol{g}_0^\varepsilon(t)\|_{1/2}^2 dt.\end{aligned} \tag{4.25}$$

Our goal is now to replace in the above the integrals over $\mathbb{R}_+$ by the integrals over $(0, T)$. For this we will use of the causality argument. More precisely, because $\boldsymbol{\mu}_G^\varepsilon = \left(\mathbb{S}_{00}^\varepsilon(\partial_t)\right)^{-1} \boldsymbol{g}_0^\varepsilon$, the density $\boldsymbol{\mu}_G^\varepsilon(t)$ depends only on $\boldsymbol{g}_0^\varepsilon(\tau)$ for $\tau \leq t$. Hence, if $\boldsymbol{g}_{T,0}^\varepsilon$ is s.t.

$$\boldsymbol{g}_{T,0}^\varepsilon = \boldsymbol{g}_0^\varepsilon \text{ on } (-\infty, T),$$

and

$$\boldsymbol{\mu}_{G,T}^\varepsilon = \left(\mathbb{S}_{00}^\varepsilon(\partial_t)\right)^{-1} \boldsymbol{g}_{0,T}^\varepsilon,$$

then we have that $\boldsymbol{\mu}_G^\varepsilon = \boldsymbol{\mu}_{G,T}^\varepsilon$ on $(-\infty, T)$. Moreover, if $\boldsymbol{g}_{0,T}^\varepsilon$ is sufficiently regular, the bound (4.25) holds with $\boldsymbol{\mu}_G^\varepsilon$, $\boldsymbol{g}_0^\varepsilon$ replaced respectively by $\boldsymbol{\mu}_{G,T}^\varepsilon$, $\boldsymbol{g}_{0,T}^\varepsilon$. We choose $\boldsymbol{g}_{0,T}^\varepsilon$ so that (cf. the proof of Proposition 3.2.2 in [38])

$$(1 + \varepsilon\partial_t) \partial_t \boldsymbol{g}_0^\varepsilon(t) = 0 \text{ on } (T, \infty), \quad \partial_t^\ell \boldsymbol{g}_{0,T}^\varepsilon(T) = \partial_t^\ell \boldsymbol{g}_0^\varepsilon(T), \text{ for } \ell = 0, 1.$$

With this choice, (4.25) becomes

$$\begin{aligned}\int_{\mathbb{R}^+} \mathrm{e}^{-2t/T} \|\boldsymbol{\mu}_{G,T}^\varepsilon(t)\|_{-1/2}^2 dt \lesssim C_G^2 C_0^2(\varepsilon, d_*^\varepsilon) \varepsilon^{-2} T^2 \\ \times \int_0^T \mathrm{e}^{-2t/T} \|(1 + \varepsilon\partial_t) \partial_t \boldsymbol{g}_0^\varepsilon(t)\|_{1/2}^2 dt.\end{aligned} \tag{4.26}$$

We use $\boldsymbol{\mu}^\varepsilon_{G,T}(t) = \boldsymbol{\mu}^\varepsilon_G(t)$ on $(0,T)$ and $1 > \mathrm{e}^{-t/T} > \mathrm{e}^{-1}$ on $(0,T)$ to obtain further

$$\int_0^T \|\boldsymbol{\mu}^\varepsilon_G(t)\|^2_{-1/2}dt \lesssim C_G^2 C_0^2(\varepsilon, d^\varepsilon_*)\varepsilon^{-2}T^2 \int_0^T \|(1+\varepsilon\partial_t)\partial_t \boldsymbol{g}^\varepsilon_0(t)\|^2_{1/2}dt. \tag{4.27}$$

We thus have obtained a time-domain bound on $\boldsymbol{\mu}^\varepsilon_G$ in terms of $\boldsymbol{g}^\varepsilon_0$. To get a stronger $L^\infty(0,T;H^{-1/2}(\Gamma^\varepsilon))$-bound on $\boldsymbol{\mu}^\varepsilon_G$, we use

$$\|\boldsymbol{\mu}^\varepsilon_G\|_{L^\infty(0,T;\mathcal{V}^\varepsilon_0)} \le T^{1/2}\|\partial_t\boldsymbol{\mu}^\varepsilon_G\|_{L^2(0,T;\mathcal{V}^\varepsilon_0)},$$

and the bound on $\|\partial_t\boldsymbol{\mu}^\varepsilon_G\|_{L^2(0,T;H^{-1/2}(\Gamma^\varepsilon))}$ can be obtained like (4.27).

Step 1.3. Bounding the right-hand side with respect to u^{inc}. Finally, to obtain the bound in the statement of the proposition, we use in (4.27) the estimate of Proposition 4.6. It yields the following bound, where the constant C'_G depends on R^* and R_*^{-1} polynomially:

$$\|\boldsymbol{\mu}^\varepsilon_G\|^2_{L^\infty(0,T;\mathcal{V}^\varepsilon_0)} \le C'_G C_0^2(\varepsilon, d^\varepsilon_*)\varepsilon^{-1}T^3 N\|\partial_t^2 u^{inc}\|^2_{H^1_\varepsilon(0,T;H^2(\mathbb{R}^2))}.$$

Bounding $C_0(\varepsilon, d^\varepsilon_*) < 1 + 1/\underline{d_*}$, see its definition (4.17), yields the desired stability bound in the statement of the proposition.

Step 2. Error bounds. The bounds on the density errors can be computed like in the previous case, by making use of the results of Theorems 4.12, 4.13, 4.16 and Propositions 4.6, 4.7. In order to avoid technicalities, we will not specify explicit dependence of the constants in the error estimates on $T, N, \underline{d_*}^{-1}$, since it is clear that the resulting bounds will depend on them polynomially. In what follows, the constants $C_{i,G,\perp}$, $C_{i,G,0}$, $i \in \mathbb{N}$, depend on polynomially on $T, N, \underline{d_*}^{-1}, R^*, R_*^{-1}$.

Step 2.1. One error bound for the orthogonal component of the density. Our next goal is to estimate the error $\boldsymbol{e}^\varepsilon_\perp$. With Theorems 4.12, 4.13, 4.16, and using the same arguments as in the previous step, the frequency-domain bound (4.3) can be rewritten:

$$\begin{aligned}\|\hat{\boldsymbol{e}}^\varepsilon_\perp\|_{-1/2} \le C_{1,G,\perp}\frac{|\omega|}{\operatorname{Im}\omega}\max(1,\varepsilon|\omega|)\big(&\|\hat{\boldsymbol{g}}^\varepsilon_\perp\|_{1/2}\\ &+\varepsilon^{1/2}\frac{|\omega|^2}{\operatorname{Im}\omega}\max(1,(\operatorname{Im}\omega)^{-1})\max(1,\varepsilon|\omega|)\|\hat{\boldsymbol{g}}^\varepsilon_0\|_{1/2}\big).\end{aligned} \tag{4.28}$$

Using the same arguments as in Step 1 yields the following bound:

$$\begin{aligned}\|\boldsymbol{e}^\varepsilon_\perp\|_{L^\infty(0,T;H^{-1/2}(\Gamma^\varepsilon))} &\le C_{2,G,\perp}\big(\|\partial_t^2\boldsymbol{g}^\varepsilon_\perp\|_{H^1_\varepsilon(0,T;H^{1/2}(\Gamma^\varepsilon))} + \varepsilon^{1/2}\|\partial_t^4\boldsymbol{g}^\varepsilon_0\|_{H^2_\varepsilon(0,T;\mathcal{V}^\varepsilon_0)}\big)\\ &\le C_{3,G,\perp}\big(\|\partial_t^4\boldsymbol{g}^\varepsilon_\perp\|_{H^1_\varepsilon(0,T;H^{1/2}(\Gamma^\varepsilon))} + \varepsilon^{1/2}\|\partial_t^4\boldsymbol{g}^\varepsilon_0\|_{H^2_\varepsilon(0,T;\mathcal{V}^\varepsilon_0)}\big),\end{aligned} \tag{4.29}$$

where in the last bound we used the property $\|v\|_{L^2(0,T)} \le T\|\partial_t v\|_{L^2(0,T)}$ for $v(0) = 0$.

Step 2.2. One error bound for the constant component of the density. With Theorems 4.12, 4.16, the frequency-domain bound (4.3) for $\hat{\boldsymbol{e}}^\varepsilon_0$ can be rewritten as follows:

$$\|\hat{\boldsymbol{e}}^\varepsilon_0\|_{-1/2} \le C_{1,G,0}\varepsilon^{1/2}\frac{|\omega|^2}{\operatorname{Im}\omega}\max(1,\varepsilon|\omega|)\max(1,(\operatorname{Im}\omega)^{-1})\|\hat{\boldsymbol{e}}^\varepsilon_\perp\|_{1/2}. \tag{4.30}$$

Repeating the same procedure as before yields the bound

$$\begin{aligned}\|\boldsymbol{e}^\varepsilon_0\|_{L^\infty(0,T;H^{-1/2}(\Gamma^\varepsilon))} &\le \varepsilon^{1/2}\\ &\times C_{2,G,0}\big(\|\partial_t^6\boldsymbol{g}^\varepsilon_\perp\|_{H^2_\varepsilon(0,T;H^{1/2}(\Gamma^\varepsilon))} + \varepsilon^{1/2}\|\partial_t^6\boldsymbol{g}^\varepsilon_0\|_{H^3_\varepsilon(0,T;H^{1/2}(\Gamma^\varepsilon))}\big).\end{aligned} \tag{4.31}$$

Step 2.3. Obtaining the final error bounds. It remains to sum up (4.31), (4.29) and apply the bounds of Propositions 4.6 and 4.7, so that the error is bounded by some Sobolev norms of the field u^{inc}. This yields the desired bound. Let us remark that with the bounds of Propositions 4.6 and 4.7,

$$\|\hat{\boldsymbol{e}}^\varepsilon_\perp\|_{-1/2} = O(\varepsilon) \quad \text{and} \quad \|\hat{\boldsymbol{e}}^\varepsilon_0\|_{-1/2} = O(\varepsilon^{3/2}). \tag{4.32}$$

This fact is not reflected in the statement of the proposition, but will be of use later.

4.6. Proof of Theorem 4.1. Let $\delta_\varepsilon > 0$, and let $\boldsymbol{x}_\varepsilon \in \Omega^{\varepsilon+\delta_\varepsilon,c}$. This in particular implies that $\operatorname{dist}(\boldsymbol{x}_\varepsilon, \Omega^{\varepsilon,c}) \geq \delta_\varepsilon$. First, we will obtain an explicit in frequency bound for the error

$$\hat{\nu}^\varepsilon := \hat{u}^\varepsilon(\omega, \boldsymbol{x}_\varepsilon) - \hat{u}^\varepsilon_G(\omega, \boldsymbol{x}_\varepsilon),$$

and next translate it into the time domain like in the proof of Proposition 4.3.

We use an explicit representation of $\hat{\nu}^\varepsilon$, valid for sufficiently regular $\hat{\boldsymbol{e}}^\varepsilon$:

$$\begin{aligned}
&\hat{\nu}^\varepsilon = \hat{\nu}^\varepsilon_0 + \hat{\nu}^\varepsilon_\perp,\\
&\hat{\nu}^\varepsilon_0 := \int_{\Gamma^\varepsilon} \mathcal{G}_\omega(\boldsymbol{x}_\varepsilon - \boldsymbol{y})\hat{\boldsymbol{e}}^\varepsilon_0(\boldsymbol{y})d\Gamma_{\boldsymbol{y}}, \quad \hat{\nu}^\varepsilon_\perp := \int_{\Gamma^\varepsilon} \mathcal{G}_\omega(\boldsymbol{x}_\varepsilon - \boldsymbol{y})\hat{\boldsymbol{e}}^\varepsilon_\perp(\boldsymbol{y})d\Gamma_{\boldsymbol{y}}.
\end{aligned}$$

We would like to show that the far-field error behaves as $\|\hat{\nu}^\varepsilon\| = O(\varepsilon^2)$, while the density error looses an order of ε: $\|\hat{\boldsymbol{e}}^\varepsilon\|_{H^{-1/2}(\Gamma^\varepsilon)} = O(\varepsilon)$, cf. Proposition 4.3. In order to obtain such a super-convergence result, we will treat the terms $\hat{\nu}^\varepsilon_0$ and $\hat{\nu}^\varepsilon_\perp$ separately, in order to make use of the different scalings of the error components (4.32). We will explain the interest in this approach afterwards.

In what follows, by $C_{i,G}$, $i \in \mathbb{N}$, we will denote a constant depending polynomially on R^*, R_*^{-1}, N, $\underline{d_*}^{-1}$, and, where appropriate, on T.

We start with the error generated by the constant component of the density error:

$$\begin{aligned}
|\hat{\nu}^\varepsilon_0|^2 &\leq \left| \sum_{n\in\mathcal{N}} \int_{\Gamma^\varepsilon_n} \mathcal{G}_\omega(\boldsymbol{x}_\varepsilon - \boldsymbol{y})\hat{e}^\varepsilon_{n,0}(\boldsymbol{y})d\Gamma_{\boldsymbol{y}} \right|^2\\
&\leq N \sup_n \|\mathcal{G}_\omega(\boldsymbol{x}_\varepsilon - .)\|^2_{L^2(\Gamma^\varepsilon_n)} \|\hat{\boldsymbol{e}}^\varepsilon_0\|^2_{L^2(\Gamma^\varepsilon)},
\end{aligned} \tag{4.33}$$

and the desired bound for $\hat{\nu}^\varepsilon_0$ follows from (4.30) and Lemma 4.15 (the latter used in a simplified form):

$$\begin{aligned}
|\hat{\nu}^\varepsilon_0| &\leq C_{1,G}\varepsilon \frac{|\omega|^2}{\operatorname{Im}\omega} \max(1, (\operatorname{Im}\omega)^{-1}) \max(1, \varepsilon|\omega|)\\
&\quad \times \max(1, \log\frac{1}{\delta_\varepsilon \operatorname{Im}\omega}) \|\hat{\boldsymbol{e}}^\varepsilon_\perp\|_{-1/2}\\
&\lesssim C_{1,G}\varepsilon \frac{|\omega|^2}{\operatorname{Im}\omega} \max(1, (\operatorname{Im}\omega)^{-1}) \max(1, \varepsilon|\omega|)\\
&\quad \times \max(1, \log\frac{1}{\delta_\varepsilon}) \max(1, \log\frac{1}{\operatorname{Im}\omega}) \|\hat{\boldsymbol{e}}^\varepsilon_\perp\|_{-1/2},
\end{aligned} \tag{4.34}$$

where in the latter inequality we used $\max(1, a+b) \leq \max(1,a) + \max(1,b) \leq \max(1,a)(1+\max(1,b)) \leq 2\max(1,a)\max(1,b)$. In a similar manner, using the result of Lemma 4.15, we can bound the field error generated by the error in the orthogonal component of the density:

$$\begin{aligned}
|\hat{\nu}^\varepsilon_\perp| &\leq C_{2,G}\varepsilon\delta_\varepsilon^{-1} \max(1, |\omega\delta_\varepsilon|^{1/2}) \|\hat{\boldsymbol{e}}^\varepsilon_\perp\|_{-1/2}\\
&\leq C_{2,G}\varepsilon\delta_\varepsilon^{-1} \max(1, \delta_\varepsilon^{1/2}) |\omega| \max(1, (\operatorname{Im}\omega)^{-1}) \|\hat{\boldsymbol{e}}^\varepsilon_\perp\|_{-1/2},
\end{aligned} \tag{4.35}$$

where to obtain the last bound we used in particular $\max(1, |\omega|^{1/2}) < \max(1, |\omega|) < |\omega| \max(1, (\operatorname{Im}\omega)^{-1})$.

At this point we can see the interest in splitting $\hat{\nu}^\varepsilon$ into two components. When $\delta_\varepsilon = \text{const}$, both $|\hat{\nu}^\varepsilon_0|$ and $|\hat{\nu}^\varepsilon_\perp|$ have the same scaling with respect to ε: they behave as $O(\varepsilon\|\hat{\boldsymbol{e}}^\varepsilon_\perp\|_{-1/2}) = O(\varepsilon^2)$, cf. (4.32). Had we used from the beginning the same argument as we used to obtain (4.35), we would have the bound

$$|\hat{\nu}^\varepsilon| \lesssim \sup_n \|\mathcal{G}_\omega(\boldsymbol{x}_\varepsilon - .)\|_{H^{1/2}(\Gamma^\varepsilon_n)} \|\hat{\boldsymbol{e}}^\varepsilon\|_{H^{-1/2}(\Gamma^\varepsilon)},$$

which, with Lemma 4.15 and Proposition 4.3 would yield, for $\delta_\varepsilon = \text{const}$, $|\hat{\nu}^\varepsilon| = O(\varepsilon^{3/2})$. With bounds (4.34) and (4.35), and remarking that both $\max(1, \log\frac{1}{\delta_\varepsilon})$ and $\delta_\varepsilon^{-1}\max(1, \delta_\varepsilon^{1/2})$ are bounded

by $\max(1, \delta_\varepsilon^{-1})$, we arrive at the following expression:

$$|\hat{\nu}^\varepsilon| \le C_{3,G} \max(1, \delta_\varepsilon^{-1}) |\omega| \max(1, (\operatorname{Im}\omega)^{-1}) \\ \times \Big(\frac{|\omega|}{\operatorname{Im}\omega} \max(1, \log \frac{1}{\operatorname{Im}\omega}) \max(1, \varepsilon|\omega|) + 1 \Big) \|\hat{\boldsymbol{e}}_\perp^\varepsilon\|_{-1/2}.$$

It remains to replace in the above bound $\|\hat{\boldsymbol{e}}_\perp^\varepsilon\|_{-1/2}$ by its bound (4.28), and next proceed like in the proof of Proposition 4.3, by passing to the time-domain and next exploiting the results of Propositions 4.6 and 4.7, in order to bound $\|\partial_t^\ell \boldsymbol{g}^\varepsilon\|_{1/2}$ by some volume norms of the incident field $\|\partial_t^\ell u^{inc}\|$. This yields the desired result.

5. Extension of the results: a cluster of particles. The goal of this section is to show how the obtained convergence bounds can be adapted to the case when one studies a sound-soft scattering problem for the case when the centres of the particles and distances between them are no longer fixed with ε. We will assume that $N = O(\varepsilon^{-\gamma})$, and $d_*^\varepsilon = O(\varepsilon^\alpha)$, with $\gamma, \alpha \ge 0$. We will limit our discussion to the case when the particles fill a fixed volume, which implies that $N \lesssim \min(\varepsilon^{-2}, \varepsilon^{-2\alpha})$, thus

$$\gamma \le 2 \min(1, \alpha). \tag{5.1}$$

Our goal is to extend the (far-field) result of Theorem 4.1 to this case. In other words, we would like to bound the following quantity:

$$|\nu^\varepsilon(t)| = |u_G^\varepsilon(t, \boldsymbol{x}) - u^\varepsilon(t, \boldsymbol{x})|, \quad \boldsymbol{x} \in \Omega^c, \quad \operatorname{dist}(\boldsymbol{x}, \Omega^{\varepsilon, c}) = \delta > 0.$$

It is straightforward to verify that the only assumption used in our proofs was an assumption on the circles not touching each other. Therefore, as seen from the proof of Proposition 4.3 and Theorem 4.1, it suffices to (carefully) keep track of the dependence of the error bounds in the frequency domain on N, d_*^ε and ε. Like before, we will rely on the inequalities (4.3). For convenience, let us rewrite the bounds of Theorems 4.12, 4.16, 4.13, as well as of Propositions 4.6, 4.7. First, according to (4.17),

$$C_0(\varepsilon, d_*^\varepsilon) = 1 + \frac{\varepsilon}{d_*^\varepsilon} = O(\varepsilon^{1-\max(1,\alpha)}), \quad \varepsilon \to 0.$$

We then have the following bounds for the operator norms:

$$\|(\hat{\mathbb{S}}_{00}^\varepsilon)^{-1}\| = O(\varepsilon^{-\max(1,\alpha)}), \quad \|\mathbb{P}_\perp^{\varepsilon,*} (\hat{\mathbb{S}}^\varepsilon)^{-1} \mathbb{P}_\perp^\varepsilon\| = O(\varepsilon^{1-\max(1,\alpha)}), \\ \|\hat{\mathbb{S}}_{0\perp}^\varepsilon\| = \|\hat{\mathbb{S}}_{\perp 0}^\varepsilon\| = O(\varepsilon^{3/2-\gamma-\alpha}).$$

Moreover,

$$\|\hat{\boldsymbol{g}}_0^\varepsilon\|_{1/2} = O(\varepsilon^{1/2-\gamma/2}), \quad \|\hat{\boldsymbol{g}}_\perp^\varepsilon\|_{1/2} = O(\varepsilon^{1-\gamma/2}).$$

It remains to rewrite the inequalities (4.3):

$$\|\hat{\boldsymbol{e}}_\perp^\varepsilon\|_{-1/2} = O(\varepsilon^{2-\max(1,\alpha)-\frac{\gamma}{2}}) + O(\varepsilon^{3-3\gamma/2-\alpha-2\max(1,\alpha)}) = O(\varepsilon^{3-3\gamma/2-\alpha-2\max(1,\alpha)}), \\ \|\hat{\boldsymbol{e}}_0^\varepsilon\| = O(\varepsilon^{9/2-5\gamma/2-2\alpha-3\max(1,\alpha)}).$$

Finally, to obtain the bound for the field, we proceed like in the proof of Theorem 4.1. In particular, by (4.33) and Lemma 4.15, it follows that

$$|\hat{\nu}_0^\varepsilon| = O(\varepsilon^{-\gamma/2+1/2} \|\hat{\boldsymbol{e}}_0^\varepsilon\|_{-1/2}) \quad \text{and} \quad |\hat{\nu}_\perp^\varepsilon| = O(\varepsilon^{-\gamma/2+1} \|\hat{\boldsymbol{e}}_\perp^\varepsilon\|_{-1/2}).$$

Therefore,

$$|\hat{\nu}^\varepsilon| = O(\varepsilon^{5-3\gamma-2\alpha-3\max(1,\alpha)}).$$

Let us now consider the following cases.

Case 1. $\alpha \ge 1$. $|\hat{\nu}^\varepsilon| \ge$ const as $\varepsilon \to 0$, and, according to our estimates, the Galerkin Foldy-Lax model does not converge in this case.

Case 2. $\alpha < 1$. The error behaves as $|\hat{\nu}^\varepsilon| = O(\varepsilon^{2-3\gamma-2\alpha})$. For a particular case when $\gamma = 2\alpha$, we can expect the convergence rate of $O(\varepsilon^{2(1-4\alpha)})$ for $\alpha < \frac{1}{4}$.

6. Numerical experiments. In all the experiments we use the trapezoid convolution quadrature method for the time semi-discretization. The reference solutions are computed with the use of the spatial Galerkin BEM with $2N_s+1$ spectral Galerkin basis functions $\{e^{im\theta}\}_{m=-N_s}^{N_s}$ on each of the obstacles.

6.1. Numerical validation of Theorem 4.1 and Proposition 4.3. We study a configuration of $N=20$ particles with centres located on the boundary of a unit circle, see Figure 6, left. We start with the $R_i = R = 0.1$ (in this case $d_* \approx 0.11$). The incident field $u^{inc}(t,\boldsymbol{x}) = \mathrm{e}^{-100(t-\boldsymbol{d}\cdot\boldsymbol{x}-2)^2}$, $\boldsymbol{d}=(0,1)$, is approximately band-limited, with the smallest wavelength $\lambda_{min} \approx 0.12$. The simulations are performed on the time interval $(0,T)$, $T=8$. We change ε and compare $\boldsymbol{\mu}_G^\varepsilon(t)$ and $u_G^\varepsilon(t,\boldsymbol{x}_0)$ in the centre of the

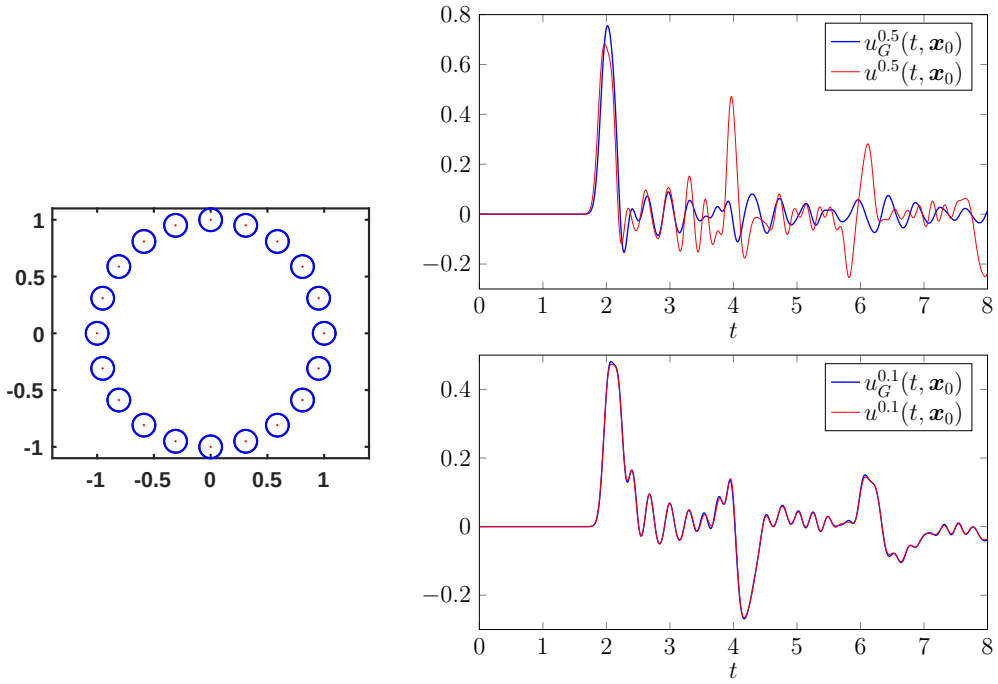

FIG. 6. *Left: the geometric configuration for the numerical experiment of Section 6 for $\varepsilon = 1$. Right: the dependence of the solutions $u^\varepsilon(t,\boldsymbol{x}_0)$ in $\boldsymbol{x}_0 = 0$ on time t obtained with the help of the Galerkin Foldy-Lax method and the high-order BEM for $\varepsilon R = 0.05$ (top) and $\varepsilon R = 0.01$ (bottom).*

circle $\boldsymbol{x}_0 = 0$ to the reference density $\boldsymbol{\mu}(t,\boldsymbol{x})$ and solution $u^\varepsilon(t,\boldsymbol{x}_0)$ by computing

$$e_\mu^\varepsilon = \|\boldsymbol{e}^\varepsilon\|_{L^\infty(0,T;H^{-1/2}(\Gamma^\varepsilon))}, \quad e_u^\varepsilon = \|u_G^\varepsilon(.,\boldsymbol{x}_0) - u^\varepsilon(.,\boldsymbol{x}_0)\|_{L^\infty(0,T)}. \tag{6.1}$$

The dependence of the solutions $u^\varepsilon(t,\boldsymbol{x}_0)$ and $u_G^\varepsilon(t,\boldsymbol{x}_0)$ on t is depicted in Figure 6, right. The dependence of e_μ^ε and e_u^ε on ε is shown in Figure 7, left. The numerical experiments support the claims of Proposition 4.3 and Theorem 4.1: as expected, $e_\mu^\varepsilon = O(\varepsilon)$ and $e_u^\varepsilon = O(\varepsilon^2)$.

6.2. Comparison with the Foldy-Lax model (FL1-FL2). The goal of this section is to compare the Foldy-Lax model (FL1-FL2) to the new Galerkin Foldy-Lax model. In the case when the Foldy-Lax model converges, we expect it to have the same convergence order as the Galerkin Foldy-Lax model, see Section 3.3.4, as well as Proposition 4.3. The reason for this is that the difference between the coefficients of the model is $O(\varepsilon^2)$, which is of convergence order of the solution.

We present two experiments: the first one in which the Foldy-Lax model (FL1-FL2) has a performance comparable to the Galerkin Foldy-Lax model, and the second one where the Galerkin Foldy-Lax model outperforms the Foldy-Lax model.

The first experiment is performed with the same data as in the previous section. In Figure 7, right, we depict e_u^ε defined for the Galerkin Foldy-Lax model in (6.1) and the analogous quantity $e_{FL,u}^\varepsilon$ for

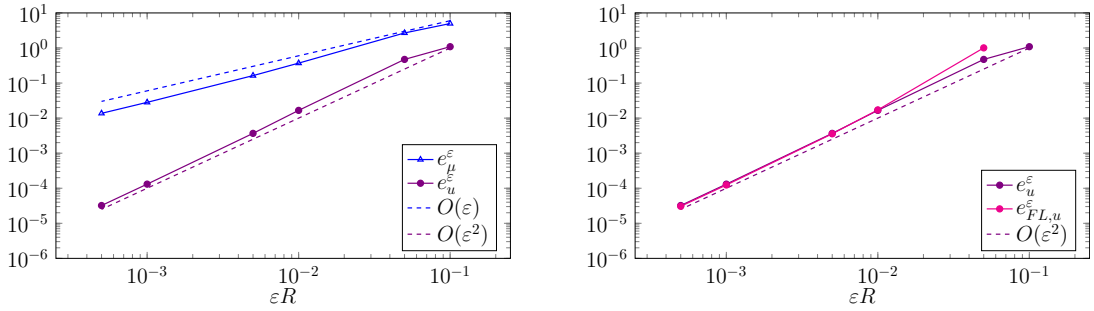

FIG. 7. *Left: an illustration to the experiment of Section 6.1. Convergence of the errors e_u^ε and e_μ^ε. Right: an illustration to the experiment of Section 6.2. Convergence of the error $e_{FL,u}^\varepsilon$.*

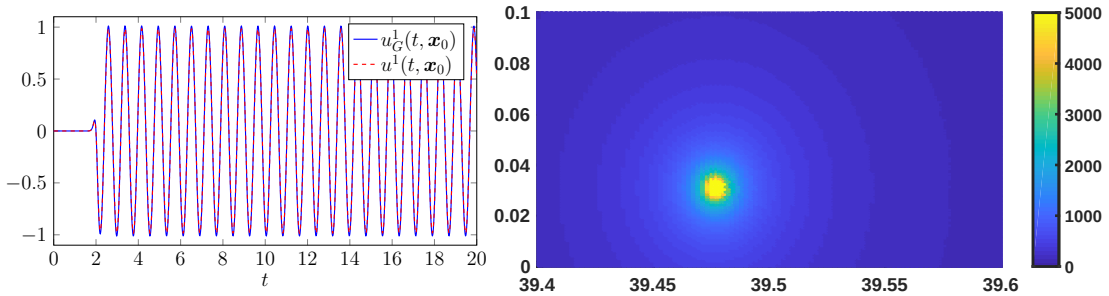

FIG. 8. *An illustration to the numerical experiment of Section 6.2. Left: The dependence of the solutions $u^1(t,\boldsymbol{x}_0)$ and $u_G^1(t,\boldsymbol{x}_0)$ on t. Right: the dependence of the condition number of the Foldy-Lax matrix (FL1) on ω plotted in the axis $(\operatorname{Re}\omega, \operatorname{Im}\omega)$.*

the Foldy-Lax model (FL1-FL2). We were not able to make the first experiment with $\varepsilon R = 0.1$ for the original Foldy-Lax model, since we observed an exponential blow-up of the solution on the given time interval. Nonetheless, for small ε, we see that the errors of the Galerkin Foldy-Lax model and the model (FL1-FL2) almost coincide (in some experiments it was even slightly lower in the latter case).

The second experiment is performed on longer times. We take $N = 16$ particles; the centers of the 15 particles of radius $R_i = 0.01$, $1 \le i \le 16$, are equidistant, and are located on the boundary of a circle of radius 0.1 centered in the origin, and the remaining particle of radius $R_{16} = 0.02$ is again centered in the origin. We set

$$u^{inc}(t,\boldsymbol{x}) = -\sin 8(t - s(\boldsymbol{x}))\mathcal{H}(t - s(\boldsymbol{x})), \quad s(\boldsymbol{x}) = x_2 + 2, \quad \mathcal{H}(t) = \frac{1}{1 + \mathrm{e}^{-20t}}.$$

We perform the simulations on the time interval $(0, T)$ with $T = 20$, and measure the field in the point $\boldsymbol{x}_0 = (0.07, 0)$. We show the reference solution versus the Galerkin Foldy-Lax approximation in Figure 8, left. The relative error between the two solutions does not exceed 4%. At the same time, the solution obtained with the Foldy-Lax model (FL1-FL2) explodes, at least for the chosen time step and the simulation time.[1] Numerically, we observe that the matrix in the right-hand side of (2.9) is not invertible for $\omega \approx 39.47 + 0.03i$, see Figure 8, right, and this probably accounts for the exponential growth of the computed solution.

7. Conclusions and open questions. In this work we have constructed an asymptotic model for scattering by small particles as a Galerkin discretization of the single-layer boundary integral formulation. This procedure yields a model a priori stable in the time-domain. For a particular case of scattering by circles, we have shown the second order convergence of the method, confirmed by the numerical experiments. Nonetheless, many questions still remain open, and we list them below:

[1] Remarkably, one still may have stability for larger time steps, see Section 3.3.3 for a related discussion.

1. optimality of the obtained estimates in regularity requirements;
2. construction of a (higher order) Galerkin Foldy-Lax model for particles of arbitrary shapes;
3. efficient numerical methods for such models, and comparison of their performance to the finite element method based simulations;
4. advantages/disadvantages in using other integral formulations (e.g. time-domain CFIE or direct integral formulation);
5. performance of Galerkin Foldy-Lax models purely in the frequency domain (in particular for the problems without absorption).

We plan to address some of these questions in future works, as well as extend the analysis to the 3D electromagnetic case.

Acknowledgements. I am grateful to Maxence Cassier (CNRS, Institut Fresnel), Patrick Joly (INRIA, IP Paris) for fruitful discussions. In particular, I thank Maxence for explaining the approach of [9], and Patrick for suggesting the name 'Galerkin Foldy-Lax'.

Appendix A. Proof of Lemma 2.2. We will rely on the following result.

LEMMA A.1. *[12, Chapter XII, Lemma 1.2] Let f be analytic on $B(0,R)$, $f(0)=0$, $|f'(0)|=\mu>0$, and $|f(z)|\leq M$ for all $z\in B(0,R)$. Then*

$$f(B(0;R))\supset B\left(0;\frac{R^2\mu^2}{6M}\right).$$

We will also need an asymptotic behaviour of Hankel functions [36, pp. 266-267]. For all $z\in\overline{\mathbb{C}^+}$ (where for $x<0$ we write $H_m^{(1)}(x)=\lim_{\nu\to 0+}H_m^{(1)}(x+i\nu)$):

$$H_0^{(1)}(z)=\left(\frac{2}{\pi z}\right)^{\frac{1}{2}}\mathrm{e}^{i(z-\frac{\pi}{4})}\left(1+O(|z|^{-1})\right),\quad |z|\to+\infty, \tag{A.1}$$

$$H_1^{(1)}(z)=\left(\frac{2}{\pi z}\right)^{\frac{1}{2}}\mathrm{e}^{i(z-\frac{3\pi}{4})}\left(1+O\left(|z|^{-1}\right)\right),\quad |z|\to+\infty. \tag{A.2}$$

Proof of Lemma 2.2. The matrix Λ with $\det\Lambda=1+2P^3-3P^2$ is not invertible for ω s.t. $P(\omega)\in\{-1/2,1\}$. It is possible to show that for $\omega\in\mathbb{C}^+$, $|P(\omega)|<1$, and therefore, $\Lambda(\omega)$ is not invertible in $\omega\in\mathbb{C}^+$, if and only if

$$P(\omega)=-1/2. \tag{A.3}$$

Proof of (i) and (ii). The set of the roots of (A.3) is at most countable, since $\omega\mapsto P(\omega)$ is analytic in $\mathbb{C}^+$. To show that there are infinitely many roots, we will rely on

- an explicit asymptotic behaviour of $P(\omega)$, which will allow us to obtain an ansatz for the location of the solutions of (A.3) in $\mathbb{C}^+$;
- Lemma A.1 which will that some solutions of (A.3) are close to this ansatz.

Step 1. Ansatz for the roots. By (A.1), for all $|\omega r|$ sufficiently large, we have that

$$P(\omega)=\frac{H_0^{(1)}(\omega\eta r)}{H_0^{(1)}(\omega r)}=\eta^{-\frac{1}{2}}\mathrm{e}^{i(\eta-1)\omega r}+O(|\omega|^{-1}). \tag{A.4}$$

The solutions of

$$\eta^{-1/2}\mathrm{e}^{i(\eta-1)\omega r}=-1/2 \tag{A.5}$$

are given by

$$\omega_{\infty,n}=\frac{1}{r(\eta-1)}\left((2n+1)\pi+i\log\frac{2}{\sqrt{\eta}}\right),\quad n\in\mathbb{Z}. \tag{A.6}$$

Because $1 < \sqrt{\eta} < 2$ by the assumption of the proposition, all these roots satisfy $\omega_{\infty,n} \in \mathbb{C}^+$, with $\operatorname{Im}\omega_{\infty,n}$ independent of n. As $n \to \infty$, we also have that $|\omega_{\infty,n}| = O(n)$. Moreover, $|\omega_{\infty,n+1} - \omega_{\infty,n}| = \frac{2\pi}{r(\eta-1)}$. Without loss of generality, in the proof we will consider the case $n > 0$.

Step 2. Roots of (A.3). Based on the above, let us show that countably many solutions of (A.3) lie in $\mathbb{C}^+$. Let us consider the following function:

$$p_n(\omega) := P(\omega) - P(\omega_{\infty,n}).$$

Remark that, by (A.4),

$$|P(\omega_{\infty,n}) + 1/2| \leq C_P n^{-1}, \quad C_P > 0. \tag{A.7}$$

We will show that for all n sufficiently large, there exists $\delta_n > 0$, s.t. $B(\omega_{\infty,n}, \delta_n) \subset \mathbb{C}^+$ and, with some $c_p > 0$,

$$p_n(B(\omega_{\infty,n}, \delta_n)) \supset B\left(0, c_p n^{-1}\right). \tag{A.8}$$

This will imply that the function

$$P(\omega) - 1/2 = p_n(\omega) + (P(\omega_{\infty,n}) - 1/2)$$

satisfies

$$P(B(\omega_{\infty,n}, \delta_n)) - 1/2 \supset B\left(0, (c_p + C_P)n^{-1}\right),$$

i.e. that there exists $\omega \in B(\omega_{\infty,n}, \delta_n)$ s.t. $P(\omega) = -1/2$. Let us remark that we will show a stronger result, namely, we will prove that in the above one can choose δ_n s.t. $\lim\limits_{n\to+\infty} \delta_n = 0$, which will yield the statement (ii).

It remains to prove (A.8). For this we will use Lemma A.1, applied to $f(.) = \widetilde{p}_n(.) = p_n(. + \omega_{\infty,n})$. A priori, we will choose δ_n so that

$$\delta_n < \frac{1}{2}\min(\operatorname{Im}\omega_{\infty,n}, \sup_k |\omega_{\infty,k+1} - \omega_{\infty,k}|) \leq \frac{1}{2r(\eta-1)}\log\frac{2}{\sqrt{\eta}}, \tag{A.9}$$

so that $B(\omega_{\infty,n}, \delta_n) \subset \mathbb{C}^+$, and $B(\omega_{\infty,n}, \delta_n) \cap B(\omega_{\infty,n+1}, \delta_{n+1}) = \emptyset$.

Let us now prove (A.8), based on Lemma A.1. We need a lower bound on $p_n'(\omega_{\infty,n})$ and an upper bound on p_n inside $B(\omega_{\infty,n}, \delta)$.

Step 2.1. A lower bound on $p_n'(\omega_{\infty,n})$. Because $(H_0^{(1)}(z))' = -H_1^{(1)}(z)$ ([1, 9.1.3, 9.1.28]), we have that

$$p_n'(\omega_{\infty,n}) = -c\frac{H_1^{(1)}(\omega_{\infty,n}c)}{H_0^{(1)}(\omega_{\infty,n}r)} + r\frac{H_1^{(1)}(\omega_{\infty,n}r)P(\omega_{\infty,n})}{H_0^{(1)}(\omega_{\infty,n}r)}. \tag{A.10}$$

We consider (A.10) for $n \to +\infty$, i.e. $|\omega_{\infty,n}| \to +\infty$. Using the asymptotic expansions (A.2), (A.4) and (A.7) in (A.10) results in the following expansion for p_n':

$$p_n'(\omega_{\infty,n}) = i\frac{c}{\sqrt{\eta}}\mathrm{e}^{i(\eta-1)\omega_{\infty,n}r} + \frac{ir}{2} + O(n^{-1}), \quad n \to +\infty.$$

Because $\omega_{\infty,n}$ solves (A.5), we have

$$p_n'(\omega_{\infty,n}) = -\frac{i(c-r)}{2} + O(n^{-1}),$$

hence for n sufficiently large we have

$$|p_n'(\omega_{\infty,n})| \geq \frac{r}{4}(\eta - 1). \tag{A.11}$$

Step 2.2. An upper bound on p_n. Again, we are interested in the case when $n \to +\infty$, and $\omega \in B(\omega_{\infty,n}, \delta)$.

From the definition of $p_n(\omega)$, the bound (A.7) and (A.4) it follows that, for all n sufficiently large, with some $C > 0$ independent of n,

$$|p_n(\omega)| \leq \eta^{-1/2} \mathrm{e}^{-(\eta-1)\,\mathrm{Im}\,\omega r} + \frac{1}{2} + Cn^{-1}.$$

For $\omega \in B(\omega_{\infty,n}, \delta) \subset \mathbb{C}^+$, and using $\eta > 1$, one sees that there exists $C_\eta > 0$ s.t.

$$|p_n(\omega)| \leq C_\eta, \text{ for all } n \text{ sufficiently large.} \tag{A.12}$$

Step 2.3. Proof of (A.8). Using (A.11) and (A.12), and applying Lemma A.1 to $\widetilde{p}_n(.) := p_n(. + \omega_{\infty,n})$, we conclude that, for all n sufficiently large

$$p_n(B(\omega_{\infty,n}, \delta_n)) \supset B\left(0; \frac{\delta_n^2 r^2 (\eta-1)^2}{96 C_\eta}\right).$$

To obtain the desired result, it remains to choose δ_n e.g. so that $|\delta_n| < n^{-1/2}$ (for all n sufficiently large (A.9) will be automatically satisfied).

To summarize, it follows that for all n sufficiently large, there exists $\omega_{k(n)} \in B(\omega_{\infty,n}; \delta_n) \subset \mathbb{C}^+$ s.t. (A.3) is satisfied with $\omega = \omega_{k(n)}$. *This proves (i).*

Because $\omega_{k(n)} \in B(\omega_{\infty,n}; \delta_n)$, $\delta_n \to 0$ as $n \to +\infty$, and using explicit expressions of $\omega_{\infty,n}$ in (A.6), *we see the validity of (ii).*

Finally, *(iii)* follows by considering an explicit expression of Λ, when $P(\omega) = -\frac{1}{2}$.

Appendix B. Proof of Corollary 4.2. The convergence property is immediate from Theorem 4.1 and (2.3). The uniform stability property relies on the triangle inequality

$$|u_G^\varepsilon(t, \boldsymbol{x}_\varepsilon)| \leq \text{error} + |u^\varepsilon(t, \boldsymbol{x}_\varepsilon)|.$$

It remains to bound $|u^\varepsilon(t, \boldsymbol{x}_\varepsilon)|$ and $\|\partial_t^6 u^{inc}\|_{H^3_\varepsilon(0,T;H^3(\mathbb{R}^2))}$ by some Sobolev norms of u_0, u_1. Let us sketch how this can be done.

To obtain a bound on u^ε we start by remarking that, by the Sobolev embedding theorem [16, Theorem 1.4.4.1], $|u^\varepsilon(t, \boldsymbol{x}_0)| \lesssim \|u^\varepsilon(t)\|_{H^2(B(\boldsymbol{x}_0,r))}$, where $r > 0$ is s.t. $B(\boldsymbol{x}_0, r) \subset \Omega^c$. To obtain a bound on $\|u^\varepsilon(t)\|_{H^2(B(\boldsymbol{x}_0,r))}$, we use the definition $u^\varepsilon = u^\varepsilon_{tot} - u^{inc}$ and the energy argument applied to u^ε_{tot} and u^{inc}. We proceed as follows.

By the triangle inequality, we have that

$$\|\partial_t u^\varepsilon(t)\|_{\Omega^c} + |u^\varepsilon(t)|_{H^1(\Omega^c)} \leq 2(\|u_0\| + \|u_1\|).$$

This immediately yields a bound on $|u^\varepsilon(t)|_{H^1(B(\boldsymbol{x}_0,r))}$.

To control $\|u^\varepsilon(t)\|_{B(\boldsymbol{x}_0,r)}$, we use that for $v(0) = 0$, $|v(t)| \leq t\|v'\|_{L^2(0,t)}$, thus

$$\|u^\varepsilon(t)\|_{\Omega^c} \leq 2t(\|u_0\| + \|u_1\|).$$

Finally, by using elliptic regularity results, cf. [34, Theorem 4.16], to bound $\|D^2 u^\varepsilon(t)\|_{B(\boldsymbol{x}_0,r)}$, it suffices to bound $\|\Delta u^\varepsilon(t)\|_{B(\boldsymbol{x}_0,r+\delta)}$, where $\delta > 0$ is s.t. $B(\boldsymbol{x}_0, r+\delta) \subset \Omega^c$. We have that $\|\Delta u^\varepsilon(t)\|_{B(\boldsymbol{x}_0,r+\delta)} = \|\partial_t^2 u^\varepsilon(t)\|_{B(\boldsymbol{x}_0,r+\delta)}$. The bound on $\|\partial_t^2 u^\varepsilon(t)\|_{B(\boldsymbol{x}_0,r+\delta)}$ can then be obtained by the triangle inequality and the energy argument applied to $\partial_t u^\varepsilon_{tot}$, $\partial_t u^{inc}$, which in their turn, solve the respective BVP and free space problem with the initial data $(u_1, \Delta u_0)$. This yields

$$\|D^2 u^\varepsilon(t)\|_{B(\boldsymbol{x}_0,r)} \lesssim \|\partial_t^2 u^\varepsilon(t)\|_{B(\boldsymbol{x}_0,r+\delta)} \leq 2(\|\Delta u_0\| + \|u_1\|).$$

To bound $\|\partial_t^6 u^{inc}\|_{H^3_\varepsilon(0,T;H^3(\mathbb{R}^2))}$ we remark that $\partial_t^k u^{inc}$ solves the wave equation, and, like before, make use of the initial data regularity and energy arguments. We leave the remaining details to the reader.

Appendix C. Estimates on Hankel functions.

LEMMA C.1. *Let $\omega, \rho > 0$. Then*

$$\sum_{n\in\mathbb{Z}\setminus\{0\}} \left|\frac{H_n^{(1)}(\omega\rho)}{H_n^{(1)}(\omega\varepsilon)}\right|^2 = O(\varepsilon^2), \quad \text{as } \varepsilon \to 0.$$

Proof. Since it holds that $H_n^{(1)}(z) = (-1)^n H_{-n}^{(1)}(z)$, see [14, §10.4], it suffices to derive a bound on $\sum_{n\in\mathbb{N}_+^*} \left|\frac{H_n^{(1)}(\omega\rho)}{H_n^{(1)}(\omega\varepsilon)}\right|^2$. First of all, by Lemma 7 in [9]

$$\frac{1}{|H_n^{(1)}(\omega\varepsilon)|} \le \frac{2(\omega\varepsilon)^{n-2}}{n!|H_2^{(1)}(\omega\varepsilon)|}, \quad \text{for } 0 < \omega\varepsilon < 1.$$

From the series expansion of $H_2^{(1)}$, cf. [14, §10.8 and 10.2.2], we conclude that there exists $\varepsilon_1 > 0$, $c_1 > 0$, s.t. for all $\varepsilon < \varepsilon_1$

$$\frac{1}{|H_n^{(1)}(\omega\varepsilon)|} \le c_1 \frac{(\omega\varepsilon)^n}{n!}. \tag{C.1}$$

Next, by the asymptotic expansions of Hankel functions as $n \to +\infty$ [14, §10.19], it follows that there exist $N_{\omega\rho}$, $c_2 > 0$, s.t. for all $n > N_{\omega\rho}$,

$$|H_n^{(1)}(\omega\rho)| \le c_2\sqrt{\frac{2}{\pi n}}\left(\frac{2n}{\mathrm{e}\omega\rho}\right)^n \le c_2(n-1)!\left(\frac{2}{\rho\omega}\right)^n. \tag{C.2}$$

Finally, we split the sum in the statement of the lemma into two terms and bound them using (C.1), (C.2), assuming in particular that $\varepsilon < \rho/2$:

$$\begin{aligned}\sum_{n\in\mathbb{N}_+^*} \left|\frac{H_n^{(1)}(\omega\rho)}{H_n^{(1)}(\omega\varepsilon)}\right|^2 &\le \sup_{0<n\le N_{\omega\rho}} |H_n^{(1)}(\omega\rho)|^2 \sum_{n=1}^{N_{\omega\rho}-1} |H_n^{(1)}(\omega\varepsilon)|^{-2} + \sum_{n=N_{\omega\rho}}^{+\infty} \left|\frac{H_n^{(1)}(\omega\rho)}{H_n^{(1)}(\omega\varepsilon)}\right|^2 \\ &\le C_{\omega\rho}\varepsilon^2.\end{aligned}$$

∎

LEMMA C.2. *For $\mu > 1$, all $x > 0$, $K_0(\mu x) < K_0(x)$.*

Proof. By [14, 10.32.9], the function

$$x \mapsto K_0(x) = \int_0^{+\infty} \mathrm{e}^{-x\cosh t} dt, \tag{C.3}$$

is strictly monotonically decreasing. ∎

LEMMA C.3. *For $\mu \ge 1$, $m \ge 1$, $x \in \mathbb{R}^+$, it holds that $K_m(\mu x) < \mu^{-m} K_m(x)$.*

Proof. By [14, 10.32.11], for all $\mu > 0$,

$$K_m(\mu x) = \frac{\Gamma(m+1/2)(2x)^m}{\sqrt{\pi}\mu^m} \int_0^{+\infty} \frac{\cos\mu t}{(t^2+x^2)^{m+1/2}} dt. \tag{C.4}$$

A straightforward computation yields

$$\operatorname{sign}\left(\mu^m K_m(\mu x) - K_m(x)\right) = \operatorname{sign} G(\mu, x),\ G(\mu, x) = \int_0^{+\infty} \frac{\cos\mu t - \cos t}{(t^2+x^2)^{m+1/2}} dt. \tag{C.5}$$

It remains to prove that for $\mu > 1$ the quantity in the right hand side is negative. Let $x > 0$ be fixed. We have $G(1, x) = 0$ and, integrating by parts (with $m \geq 1$),

$$\partial_\mu G(\mu, x) = -\int_0^{+\infty} \frac{t \sin \mu t}{(t^2 + x^2)^{m+1/2}} dt = -\frac{\mu}{(2m-1)} \int_0^{+\infty} \frac{\cos \mu t}{(t^2 + x^2)^{m-1/2}} dt.$$

By (C.4), $\operatorname{sign} \partial_\mu G = -\operatorname{sign} K_{m-1}(\mu x) < 0$, since $K_\nu(x) > 0$ for $x > 0$ (compare [14, 10.32.8]). Thus $G(\mu, x) < G(1, x) = 0$, and the desired result follows from (C.5). ∎

REFERENCES

[1] M. Abramowitz and I. A. Stegun, Handbook of mathematical functions with formulas, graphs, and mathematical tables, vol. 55 of National Bureau of Standards Applied Mathematics Series, 1964.

[2] A. Bamberger and T. H. Duong, Formulation variationnelle espace-temps pour le calcul par potentiel retardé de la diffraction d'une onde acoustique. I, Math. Methods Appl. Sci., 8 (1986), pp. 405–435.

[3] L. Banjai, C. Lubich, and F.-J. Sayas, Stable numerical coupling of exterior and interior problems for the wave equation, Numerische Mathematik, 129 (2015), pp. 611–646.

[4] H. Barucq, J. Diaz, V. Mattesi, and S. Tordeux, Asymptotic behavior of acoustic waves scattered by very small obstacles, ESAIM Math. Model. Numer. Anal., 55 (2021), pp. S705–S731.

[5] E. Bécache and M. Kachanovska, Stability and convergence analysis of time-domain perfectly matched layers for the wave equation in waveguides, SIAM J. Numer. Anal., 59 (2021), pp. 2004–2039.

[6] A. Bendali, P.-H. Cocquet, and S. Tordeux, Scattering of a scalar time-harmonic wave by n small spheres by the method of matched asymptotic expansions, Numerical Analysis and Applications, 5 (2012), pp. 116–123.

[7] A. Bendali, P.-H. Cocquet, and S. Tordeux, Approximation by multipoles of the multiple acoustic scattering by small obstacles in three dimensions and application to the Foldy theory of isotropic scattering, Arch. Ration. Mech. Anal., 219 (2016), pp. 1017–1059.

[8] T. Betcke, J. Phillips, and E. A. Spence, Spectral decompositions and nonnormality of boundary integral operators in acoustic scattering, IMA J. Numer. Anal., 34 (2014), pp. 700–731.

[9] M. Cassier and C. Hazard, Multiple scattering of acoustic waves by small sound-soft obstacles in two dimensions: mathematical justification of the Foldy-Lax model, Wave Motion, 50 (2013), pp. 18–28.

[10] D. P. Challa and M. Sini, On the justification of the Foldy-Lax approximation for the acoustic scattering by small rigid bodies of arbitrary shapes, Multiscale Model. Simul., 12 (2014), pp. 55–108.

[11] ———, The Foldy-Lax approximation of the scattered waves by many small bodies for the Lamé system, Math. Nachr., 288 (2015), pp. 1834–1872.

[12] J. B. Conway, Functions of one complex variable, Springer-Verlag, New York-Heidelberg, 1973. Graduate Texts in Mathematics, 11.

[13] R. Dautray and J.-L. Lions, Mathematical analysis and numerical methods for science and technology. Vol. 5, Springer-Verlag, Berlin, 1992. Evolution problems. I, With the collaboration of Michel Artola, Michel Cessenat and Hélène Lanchon, Translated from the French by Alan Craig.

[14] *NIST Digital Library of Mathematical Functions*. http://dlmf.nist.gov/, Release 1.1.1 of 2021-03-15. F. W. J. Olver, A. B. Olde Daalhuis, D. W. Lozier, B. I. Schneider, R. F. Boisvert, C. W. Clark, B. R. Miller, B. V. Saunders, H. S. Cohl, and M. A. McClain, eds.

[15] L. L. Foldy, The multiple scattering of waves. I. General theory of isotropic scattering by randomly distributed scatterers, Phys. Rev. (2), 67 (1945), pp. 107–119.

[16] P. Grisvard, Elliptic problems in nonsmooth domains, vol. 69 of Classics in Applied Mathematics, Society for Industrial and Applied Mathematics (SIAM), Philadelphia, PA, 2011. Reprint of the 1985 original [MR0775683], With a foreword by Susanne C. Brenner.

[17] M. Hassan and B. Stamm, An integral equation formulation of the N-body dielectric spheres problem. Part I: Numerical analysis, ESAIM Math. Model. Numer. Anal., 55 (2021), pp. S65–S102.

[18] G. C. Hsiao and W. L. Wendland, Boundary integral equations, vol. 164 of Applied Mathematical Sciences, Springer-Verlag, Berlin, 2008.

[19] D. V. Korikov, Asymptotic behavior of solutions of the wave equation in a domain with a small hole, Algebra i Analiz, 26 (2014), pp. 164–199.

[20] D. V. Korikov and B. A. Plamenevskiĭ, Asymptotics of solutions for stationary and nonstationary Maxwell systems in a domain with small holes, Algebra i Analiz, 28 (2016), pp. 102–170.

[21] R. Kress, Minimizing the condition number of boundary integral operators in acoustic and electromagnetic scattering, Quart. J. Mech. Appl. Math., 38 (1985), pp. 323–341.

[22] R. Kress and W. T. Spassov, On the condition number of boundary integral operators for the exterior Dirichlet problem for the Helmholtz equation, Numer. Math., 42 (1983), pp. 77–95.

[23] J. Labat, V. Péron, and S. Tordeux, Equivalent multipolar point-source modeling of small spheres for fast and accurate electromagnetic wave scattering computations, Wave Motion, 92 (2020), pp. 102409, 21.

[24] M. Lax, Multiple scattering of waves, Rev. Modern Physics, 23 (1951), pp. 287–310.

[25] J. Liao, Foldy-Lax approximation on multiple scattering by many small scatterers, Appl. Anal., 92 (2013), pp. 2547–2560.

[26] J. Liao and C. Ji, Extended Foldy-Lax approximation on multiple scattering, Math. Model. Anal., 19 (2014), pp. 85–98.
[27] C. Lubich, Convolution quadrature and discretized operational calculus. I, Numer. Math., 52 (1988), pp. 129–145.
[28] ———, Convolution quadrature and discretized operational calculus. II, Numer. Math., 52 (1988), pp. 413–425.
[29] C. Lubich, On the multistep time discretization of linear initial-boundary value problems and their boundary integral equations, Numer. Math., 67 (1994), pp. 365–389.
[30] S. Marmorat, Modèles asymptotiques et simulation numérique pour la diffraction d'ondes par des petites hétérogénéités, PhD thesis, Université Paris-Saclay, 11 2015.
[31] P. A. Martin, Multiple scattering, vol. 107 of Encyclopedia of Mathematics and its Applications, Cambridge University Press, Cambridge, 2006. Interaction of time-harmonic waves with N obstacles.
[32] ———, Time-domain scattering, vol. 180 of Encyclopedia of Mathematics and its Applications, Cambridge University Press, Cambridge, 2021.
[33] V. Mattesi, Propagation des ondes dans un domaine comportant des petites hétérogénéités : modélisation asymptotique et calcul numérique, theses, Université de Pau et des pays de l'Adour, Dec. 2014.
[34] W. McLean, Strongly elliptic systems and boundary integral equations, Cambridge University Press, Cambridge, 2000.
[35] M. I. Mishchenko, Electromagnetic scattering by particles and particle groups: an introduction, Cambridge University Press, 2014.
[36] F. W. J. Olver, Asymptotics and special functions, AKP Classics, A K Peters, Ltd., Wellesley, MA, 1997. Reprint of the 1974 original [Academic Press, New York; MR0435697 (55 #8655)].
[37] A. G. Ramm, Wave scattering by small bodies, Rep. Math. Phys., 21 (1985), pp. 69–77.
[38] F.-J. Sayas, Retarded potentials and time domain boundary integral equations, vol. 50 of Springer Series in Computational Mathematics, Springer, [Cham], 2016. A road map.
[39] M. Sini, H. Wang, and Q. Yao, Analysis of the acoustic waves reflected by a cluster of small holes in the time-domain and the equivalent mass density, Multiscale Model. Simul., 19 (2021), pp. 1083–1114.
[40] A. Tourin, M. Fink, and A. Derode, Multiple scattering of sound, Waves in random media, 10 (2000), p. R31.